UNIVERSITA' DEGLI STUDI DI PARMA

DIPARTIMENTO FARMACEUTICO

DOTTORATO DI RICERCA IN BIOFARMACEUTICA-FARMACOCINETICA

RESPIRABLE MICROPARTICLES OF AMINOGLYCOSIDE ANTIBIOTICS FOR PULMONARY ADMINISTRATION

Tutor:
Chiar.mo Prof.P.Colombo

Co-tutor:
Dr.D.Traini

Coordinator:
Chiar.mo Prof.P.Colombo

PhD Candidate
Chiara Parlati

XXI° ciclo (2006-2008)

To my parents
Nando e Lory

INDEX

I. INTRODUCTION

Inhalation drug therapy, in which drugs are delivered to the lungs in the form of aerosol or particles, is the main method for the treatment of diseases affecting the respiratory system: bronchial asthma, chronic obstructive pulmonary disease (COPD), pneumonia, bacterial infections in CF and bronchiectasis [1]. Small molecules such as glucocorticoids, e.g. budesonide (Pulmicort®), fluticasone (Flutide®); β_2-agonists e.g. terbutaline (Bricanyl®), salbutamol (Ventoline®), salmeterol (Serevent®) and formetorol (Oxis®) or antibiotics e.g. tobramycin (TOBI®) for local administration in the lungs, are successfully used for the treatment of respiratory disease.

In this way the drug directly reaches the desired site, where much lower doses can be used, compared to oral or injected route [2]. It can get faster action of the active in the lungs and at the same time reduce the possible side effects associated with the systemic distribution. Moreover, the low metabolic activity in the lungs allows systemic delivery without liver passage and avoids the effects of gastric stasis and pH. Furthermore, the pulmonary route provides a large well-perfused surface area (~100 m^2) that permits a higher absorption rate with respect to the gastrointestinal tract. Administration of drug directly to the lungs by use of various aerosol delivery systems results in rapid absorption across bronchopulmonary mucosal membranes.[3]

This administration route is widely used for the treatment of diseases such as asthma and COPD and could be employed for the treatment of pulmonary bacterial infections and to reduce the toxicity of certains drugs (eg. aminoglycoside antibiotics may cause ear and kidney toxicity by orally and iv administration) [4].

The lungs, structured in such a way as to allow the passage of gas, prevent the entry of foreign bodies. To overcome these physiological barriers, sophisticated methods of administration are required; namely, systems that aerosolize in the form of cloud, droplets or solid particles of drug during the breathing [5].

The effectiveness of treatment is related to the real possibility that a substantial proportion of drug (bronchodilator, anti-inflammatory or antibiotic) reaches the proximal airways, where it can make its therapeutic action. This quantity is also dependent on the physiology of respiration and the mucociliary clearance; the inhaler efficiency and the characteristics of the formulation, such as the aerodynamic properties. Since the physiologic status of the lungs are linked to oneself and then inconstant, scientific investigations are aimed at standardizing delivery systems and formulations.

The product formulated for the inhalatory route has to be considered one of the more complex, because it's formed by an active, appropriately formulated, and a special device.

Schematically it's possible to say that the effectiveness of an inhalation therapy, especially for a drug powder formulation, is dependent on factors that are related to the **patient**, the **device** and the characteristics of the **formulation**. Afterwards, the principal variables affecting this factors will be exposed.

I.1 Anatomy and physiology of the respiratory tract

The lungs are physiologically responsible for the gases exchange and not for absorption, their anatomical and functional characteristics differ from those of bodies to

absorption, and therefore inhalation administration's priorities must be the preservation of the integrity of the respiratory mucosa and its features.[6]

Understanding inhalation aerosol therapy requires a knowledge of lung function, particularly as it relates to the mechanical properties of the lung during the process of ventilation. The airways of the lungs provide a pathway of normally low resistance to the flow of air into and out of the lung, where the alveoli perform the essential function of gas exchange.

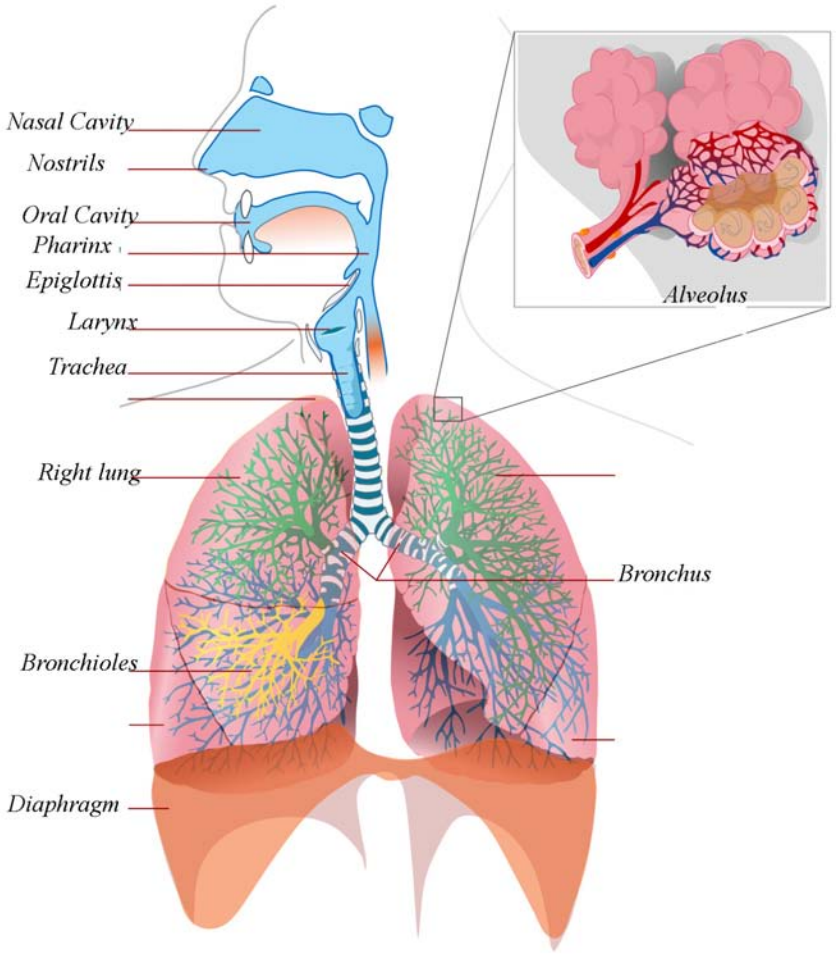

Figure 1: Schema of the respiratory system.

The lungs are spongy, sac-like organs. They are stretchy, which allows them to expand during the inspiration. They are also very elastic, so they return to their original shape with the expiration.

This apparatus is increasingly compared to the structure of a tree, where the portion tracheo-bronchial and bronchiolitis are compared to branches, with the alveoli representing foliage.

The respiratory system can be divided into *three portions*: nose-pharyngeal (from nostrils to the larynx); tracheo-bronchial tract (from trachea by up to bronchiolitis terminals) and pulmonary tract (alveolar ducts and sacs).

The trachea is a flexible, tube-like structure. Its upper end is connected to the larynx, and its lower end splits to become the right and left main bronchi. The bronchi begin outside the lung as extra-pulmonary bronchi and then enter the lung and become intrapulmonary bronchi [7].

Inside the lung, the bronchi branch repeatedly, just like the branches of a tree. These branches become smaller and smaller and eventually form bronchioles. All this branching structure represent the tracheo-bronchial tree. The bronchioles are the smallest air-conducting passages in the lung, their diameter being less than 1mm. They connect the larger airways to the alveoli, where gas exchange takes place. Like the larger airways, the bronchioles branch and split into smaller and smaller bronchioles. The alveoli are the respiratory structures of the lung. They are found at the tips of the branching bronchioles. Heading to the alveoli, located at the end of more than 17 bifurcations of the airways, reduces the thickness of the walls lung.[8]

Furthermore, it is possible to subdivide the respiratory system in *two functional zones*: conducting and respiratory zone.

The conducting zone consists of the first 16 generations of airways forming of the trachea (generation 0), which bifurcates into the two mainstem bronchi, which further subdivide into bronchi than enter two left and three right lung lobes. The intrapulmonary bronchi continue to subdivide into progressively smaller-diameter bronchi and bronchioles [9]. This zone ends with terminal bronchioles. Accordingly, the function of the conducting zone is to move air by bulk flow into and out of the lungs during the breath.

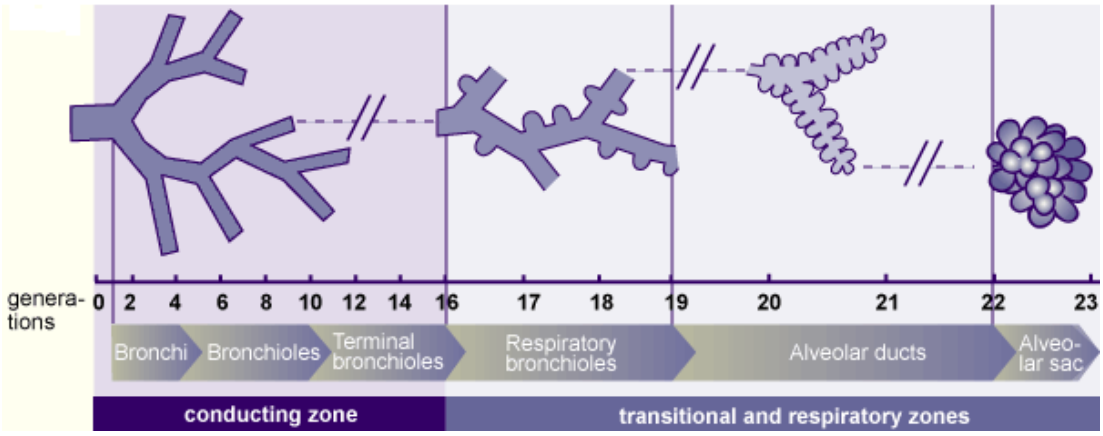

Figure 2: Schema of the generations of airways and division in conducting and respiratory zones.

The respiratory zone (consisting of respiratory bronchiolitis, alveolar ducts and alveolar sacks) has a huge surface compared to the areas of transition and of tenure. This zone consists of all structures that participate in gas exchange and begins with respiratory bronchioles containing alveoli. These bronchioles subdivide into additional respiratory bronchioles, eventually giving rise to alveolar ducts and finally to alveolar sacs. The acinus is defined as the unit comprised of a primary respiratory bronchiole, alveolar ducts and sacs.

The epithelium of the airways includes various cell types that play different functions according to the particular site of location.

- Ciliated cells are extended on the luminal surface of the airway from the trachea to the terminal bronchus and are the most numerous cells. From their apical surface protrude the cilia, that provide a sweeping motion of the mucus coat and play a crucial role in removing of small inhaled particles from the lungs.

- Mucus cells are interspersed among the ciliated cells and also extend through the full thickness of the epithelium. Their principal function is the secretion of the mucus, which is a viscous fluid containing proteoglycans and glycoproteins. They cover the luminal surface of the epithelium and fulfil four important functions:

- Protection of the epithelium from the dehydration;
- Promotion of saturation of inhaled air by the water in the mucus;
- Repression of microbial colonization of the airways for the presence in the mucus of antibacterial proteins and peptides such as defensins and lysozyme;
- Protection from inhaled xenobiotics or chemicals.

Failure to clear mucus from the airways as a result of ciliary disfunction or mucus hypersecretion (as may occur in cystic fibrosis or chronic bronchitis) can result in airway obstruction and infection. Such a situation may adversely affect the therapeutic activity of an inhaled drug by increasing the thickness of the mucus layer through which the drug must diffuse to reach its site of action.[10]

- Clare cells are non ciliated cells that have a spheric-shaped apical surface founded among ciliated cells. They are secretory cells and prevent the luminal adhesion, particularly during expiration by secretion of a surface-active agent (a lipoprotein).

- Type I pneumocytes and **type II pneumocytes** constitute the alveolar epithelium. The first one cover about the 95% of the alveolar surface area and are squamous; type II are cuboidal secretory cells expressed among type I but most of these are concentrate at septal junctions. Type II cells are as numerous as type I cells but line only the remaining 5% of the alveolar surface. They are stam cells which differentiate and replace the type I cells after injury. Both cells type are joined between them and with occasional brush cells , by zonulae occludentes. This peculiar organization enable the cells to form an effective barrier between the air space and the components of the septal wall [11].

The alveolar epithelial type II cell is the only pulmonary cell that is able to produce all the **surfactant** component. This surface-active agent was characterised and is now know to be composed of ≈90% (w/w) *lipids* (with ≈80-90% phospholipids) and of ≈10% proteins. Its composition may deviate greatly in pathologic states [12].
Unlike most other lipid-rich components of cells and organs, the surfactant lipids are characterised by an unusually high level of saturated fatty acid chains, such as the predominant dipalmtoylphosphatidylcholines (DPPC), which contribute substantially to the unique properties of pulmonary surfactant [13]. Lung surfactant contains unsaturated phosphatidylcholines (≈35%), phosphatidylglycerol (≈10%), phosphatidylinositol (≈2%), phosphatidylethanolamine (≈3%) and sphingomyelin (≈2.5%). The protein fraction contains a highly variable amount of serum proteins and four apoproteins that are associated with surfactant and contribute to its specific function [13-14-15].

I.2 Pulmonary deposition

The respiratory system in itself restricts the entrance of particulate matter by various means: geometry of the airways and clearance mechanism of the lungs [16].

Five mechanisms govern particle deposition in lung airways, namely: *inertial impaction, gravitational sedimentation, diffusion, interception and electrostatic attraction* [17].

These mechanisms could be affected by three variables: *aerosol characteristic, ventilatory parameters and respiratory tract morphologies.*

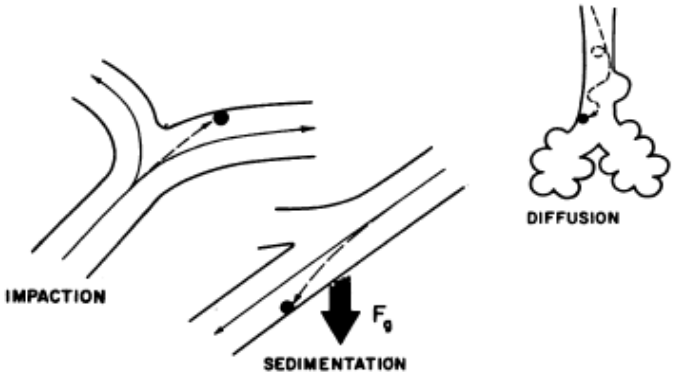

Figure 3: Three particle deposition mechanisms occurring within the respiratory tract. [20]

- Inertial impaction: defined as inertial deposition of a particle onto an airway surface. It happens principally close to the airway bifurcations of the large conducting airways. Here flow velocities are high and there are rapid changes in the direction of the airflow.

- Gravitational sedimentation: occurs in the small conducting airways where the velocity of the air is low and for particle below 5μm in size.

- Diffusion: occurs in small airways and alveoli where the airflow is very low and for submicrometer-sized particles (below 0.5) and are subject at Brownian motion.

- Interception: is important only for fibres (asbhestos) and aggregates. For such particles, deposition may occur when a particle contacts an airway wall, even though its centre of mass might remain on a fluid streamline [19-20-21].

- Electrostatic attraction: electrostatic charges enhance deposition by increasing attractive forces to airway surfaces, in particular for fresh generated particles.

As pointed out before the efficiencies of this different deposition mechanism could be formulated in terms of three classes of variable:

I.2.1 Ventilatory parameters

For patient with fixed morphology and set drug the breathing is the only parameter that can be regulated. Several studies have proved that total lung deposition can be influenced by breathing profile and physiologic condition of the lungs. In particular has been shown that quite breathing is appropriate for an inhalation therapy aimed to target aerosol in a deep region of the lung. The turbulence into the ducts can be increase by a rise in inhalation velocity. This can modify the deposition into the lungs, in particular it can enhance the impaction deposition mechanism in the upper respiratory tract but decrease sedimentation and diffusion by decreasing residence time [24]. The air distribution velocity within the lung is determined also by the tidal volume, for this reason the mass delivery to the deeper airways may also enhanced by increasing of tidal volume, by holding the breath for few seconds after inspiration [23]. Particles with a high density and a small geometric diameter had slightly greater deposition fractions than particles that were aerodynamically similar, but had lower density and larger

geometric size (typical of manufactured porous particles) [24]. This can be explained by the fact that particles with a small geometric diameter deposit primarily by diffusion, which is a function of geometric size but is independent of density.

I.2.2 Respiratory tract morphology

Individual variations in airway anatomy affect particle deposition in several ways: the diameter of the airway influences the motion required by the particle before it contacts the airway surface; the cross section of the airway determines the flow velocity for a given volumetric flow rate and the variations in diameter and branching patterns along the bronchial tree affect the mixing characteristics between the tidal and reserve air in the lungs [25]. For particles with aerodynamic diameters below 2μm, convective mixing can be the most important factor determining deposition efficiency. There are also significant individual differences in respiratory tract anatomy. The surface of the mucous layer defines the effective diameters of the conducting airways for airflow. In normal subjects the mucous layer on the larger conductive airways is believed to be only about 5μm and to decrease with airway size. In terminal bronchioles it may be only 0-1μm thick hence, the reduction in air path cross section by the mucus is negligible. On the other hand, in bronchitis, the mucous layer may be much thicker and in some places may accumulate and partially or completely occlude the airway. Air flowing through partially occluded airways will form jets, which will probably cause increased small airway particle deposition by impaction and turbulent diffusion [26].

Furthermore, some diseases such as asthma, chronic obstructive respiratory disease (COPD), cystic fibrosis (CF) and lung cancer may causes changes in the pulmonary tract by obstruction or constriction of the airways.

I.2.3 Aerosol characteristic

An aerosol can be defined as a system of solid or liquid particles which are dispersed in a gaseous medium able to remain suspended in this medium for a long time relative to the time scale of interest.

For a spherical particle, particle size is defined as the *geometrical* (real) diameter. For non spherical particles, particle size may be defined with the *projected area* diameter commonly used as the *geometrical (equivalent)* diameter.

Another important convention for describing particle sizes is frequently used in aerosol science namely *aerodynamic (equivalent)* diameter. It is defined as follows:

the aerodynamic (equivalent) diameter is the diameter of a unit density (1 g/cm3) sphere that has the same terminal settling velocity as the subject particle[17]. This parameter is calculated using the following formula:

Equation 1
$$d_{ae} = d_v \sqrt{\left(\frac{\rho_{part}}{\chi \rho_0} \right)}$$

where d_v is the geometric diameter of a sphere of volume equivalent ρ_{part} is the particle density, ρ_0 is a reference density of 1g/cm^3 and χ a dynamic form parameter that is equal to 1 for a perfect sphere. This factor describes the moving of the particles inside the air flow based not only on their diameter volume but also according to their shape and density. For poly-disperse aerosol, that are aerosol particles formed by different size,

size distribution is usually characterized by mean medium aerodynamic diameter (MMAD, mass mean aerodynamic diameter) (See section III.2.9).

Actually, particles come in a range of sizes and an aerosol is described by a size distribution. Usually, such a distribution can be satisfactorily represented by a lognormal function and described by the geometric mean and geometric standard deviation. Depending on application, one of these parameters with associated geometric standard deviation can be used to describe the aerosol. We can roughly say that the particles larger than 5μm tend to stop at the level of oro-pharynx and do not determine clinical effects if swallowed and absorbed in the gastrointestinal tract could give rise to possible side effects.

The drug particles in the range between 2 and 5μm reach proximal district of lungs, that is the primary inflammation site and the attack by pathogenic bacteria is most probable, which can carry the therapeutic application.

The finer particles (less than 2μm) reach the alveoli, where they are absorbed by the systemic circulation. This point has opened up new chances of administration, assuming the exploitation of the lungs as a "door" to get a systemic action.

The advantages of this administration to get systemic effect are: raising of the surface area that exposes the alveoli and a rich vascularisation, giving a rapid absorption of deposited drugs; it is also avoided the risk of degradation, which often afflicts oral administration in the gastrointestinal tract, and the metabolism of hepatic first pass, making it a suitable way to the administration of peptides.

Aerodynamic diameter is the most appropriate parameter in terms of particle deposition by impaction and sedimentation. Diffusional displacement, which is the dominant mechanism for particles < 0 5μm, depends only on particle size and not on

density or shape. Interception also depends on the linear dimensions of the particle, including its shape, since aerodynamic drag can affect orientation within the airway.

In addition to size, the profile of a deposition is best governed by other characteristics of the powder, such as:

- characteristic of the solid state;
- hygroscopicity;
- interparticellar-forces;
- chemical composition.

The crystallinity index defines the solid state nature of the powder. This index will provide information on the presence of crystalline or amorphous structures in the powder moreover useful information can be inferred about the dynamics of production processes for inhalation powder [26].

The hygroscopicity index indicates the trend that has a powder to form aggregates during the time. A complicating factor for water-soluble particles is the change in size that occurs in humid atmospheres. Furthermore, dry aerosols of materials, such as sodium chloride, sulphuric acid, and glycerol, will take up water vapour and grow in size within the warm and nearly saturated atmosphere in the lungs. Such changes in size may cause significant changes in deposition pattern and efficiency. It is essential to ensure the same efficiency of administration for all the shelf life of the product, that does not change the humidity of the powder in terms of conservation and that this value will remain the lowest possible. This value is influenced by the method of preparation of the powder and the nature of the components [27].

The presence of interparticellar forces that are opposed to the breakdown of the powder is perhaps the most critical aspect to be considered in studies on the

aerodynamic behaviour of a powder. The attractive forces that lead to the formation of agglomerations can be grouped into three categories:

- Van der Waals forces;
- capillaries forces;
- electrostatic forces.

The first ones will generate between permanent or induced dipoles and act within a very short distance. The second are due to the formation of liquid bridges stemming from condensation of water on the surface of particles. These will attract because of tensions to the surface of liquids. Their magnitude may undermine the ability to manipulate the powder, where the vapour pressure of the surrounding gas is close to saturation pressure.

In operational terms, this force on the powder is kept low, for this reason it can be considered negligible. The third are determined by the exchange of electrons between the surfaces of non-conductors. These forces can establish when, during the aerosolization process, the powder friction on the device walls facilitates the loading of electrostatic particles, so this leads to the repulsion between them. The electrostatic charges on drug particles influence the deposition of the drug in the respiratory once inhaled.

I.3 Delivery devices

To be acceptable for clinical use an inhalation delivery system must meet certain criteria:

- it must generate an aerosol with most of the drug carrying particles less than 10μm in size (ideally in the range 0.5-5μm), the exact size depending on the intended application;
- it must produce reproducible drug dosing;
- it must protect the physical and chemical stability of the drug;
- it must be relatively portable and inconspicuous during use;
- it must be readily used by a patient with minimal training.

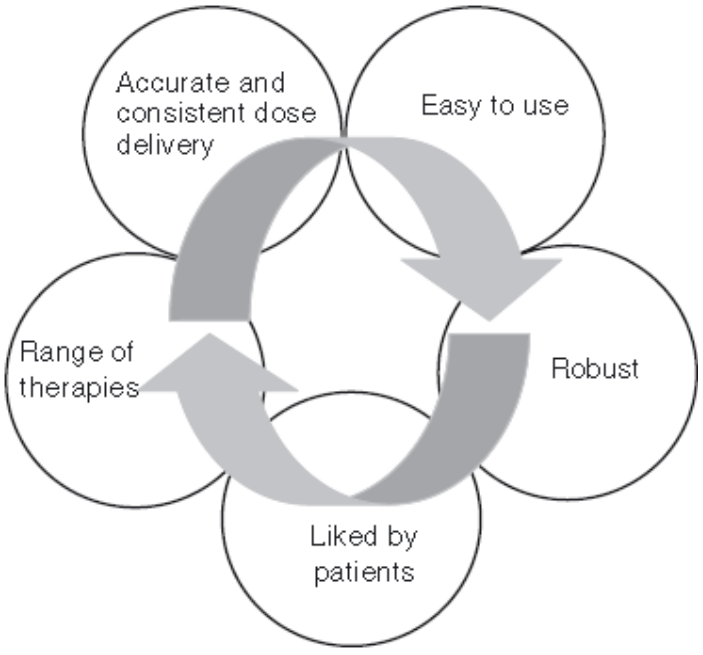

Figure 4: Criteria for an ideal inhaler [28]

The ideal inhalation system must be a simple to use, inexpensive and portable device to improve the patient's compliance. It must also protect the physical and chemical stability of the drug formulation. Moreover, the delivery device has to generate an aerosol of suitable size and a reproducible drug dosing. Equipment currently used to obtain a deposition of the drug suitable for pulmonary administration are of three types:

- Nebulizers;
- Metered Dose Inhaler (MDI);
- Dry Powder Inhaler (DPI).

I.3.1 Nebulizers

Nebulizer has been the first used in therapy since the early 19th century. These systems generate aerosols from suspension or solution of drug in an appropriate solvent [29]. In the solution the active ingredient is dissolved in a solvent to form a homogeneous phase while, for some drugs, insoluble or unstable in solution, it is possible to produce suspensions, namely heterogeneous systems where you can distinguish a phase of solid particles dispersed and a continuous phase solvent. This formulations may contain preservatives to reduce microbial growth[30].

The currently most used equipment of this type are:

- *Air-jet nebulizers*: the aerosol is formed by a high-velocity airstream from a pressurized source directed against a thin layer of liquid solution.

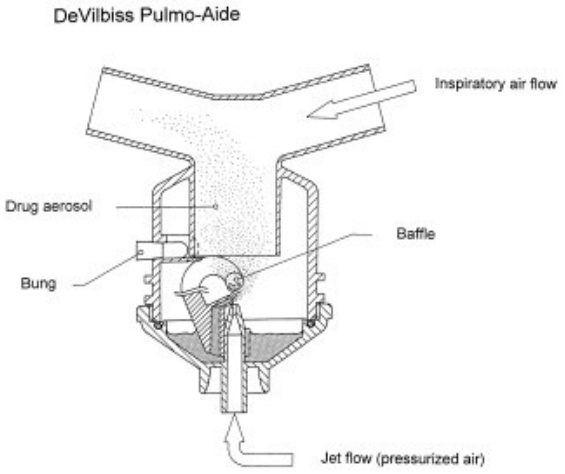

Figure 5: The working principleof the jet nebulizer is explained using a schematic presentation of the Hudson T Updraft nebulizer. [29].

Different designs of the same basic principle are used. For a typical nebulizer, the gas flow from the compressor passes through a narrow hole, impinges on the entrained drug solution and droplets are formed. Larger droplets are trapped by the baffle. Small particles pass the baffle and are available for inhalation by the inspiratory flow.

- *Ultrasonic nebulizers*: use the vibration of a piezoelectric crystal to aerosolize the solution. Droplets are produced by a rapidly vibrating piezoelectric crystal. The frequency of the vibrating crystal determines the droplet size for a given solution. In most ultrasonic nebulizers the vibrations are transferred directly to the surface of the drug solution in a drug reservoir.

New developments in liquid spray delivery devices include the use of piezo-electric atomization, high pressure micro-spray nozzle system and electrostatic generation of aerosol clouds.

Despite being a component that does not require too much cooperation from the patient and also allows you to deliver high doses of medication, nonetheless it has some drawbacks such as dependence on power supply a long duration of administration, a weak control over dosage and high cost. For the nebulizers the amount of drug inspired is approximately equivalent to half the delivered amount but the amount of drug in the

"respiratory range" obtained using a nebulizer is about 10% of the labelled dose [25]. Furthermore, in some cases, the use of preservatives such as sodium metabisulphite, benzalkonium chloride and ethylene diamine tetraacetic acid (EDTA) has caused coughing and broncho-constriction.

Currently, aerosol formulations of tobramycin (Tobi®) are normally administered with these kind of inhalers [31].

I.3.2 Pressurized Metered-Dose Inhalers (MDI)

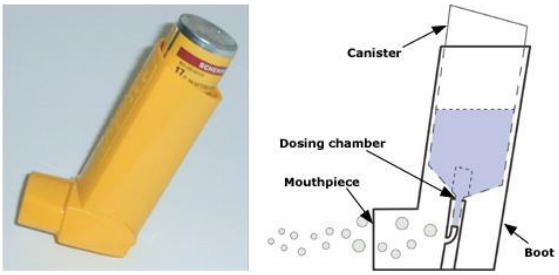

Figure 6 Typical MDI system on the left and shematic rapresentation of canister and dosing chamber

Currently, the metered-dose inhalers are the most popular devices for the inhalation administration. They are commercially available as a pressurized cans handy and ready to use. With this device a medication is mixed into the canister with a propellant and the performed mixture is expelled in precise measured amounts upon actuation of the device [32].

The technique adopted for the inhalation and the formulation affect the therapeutic response. The drug is either suspended or dissolved in a suitable propellant, pessurized until it liquefies in the canister. The liquefied propellant serves as source of energy to expel the formulation from the valve and as dispersion medium for the drug and other excipients [33].

The principal components of a typical MDI are the container, the metering valve and the actuator.

The basic ingredient of a MDI are: drug, one or more propellants, a **surfactant** such as *oleic acid*, lecithins or sorbitan trioleate (SPAN 85) (at percentages between 0.1 and 2 w/w) is typically present to aid the dispersion of suspended drug particles or dissolution of a partially soluble drug and to lubricate the metering valve mechanism. Drug can be dissolved in the liquefied propellant/surfactant combination or suspended in the form of micronized particles; **antioxidants** such as ascorbic acid or **chelating agent** like EDTA to enhance chemical stability and, in most cases, a **flavour** or suspended **sweeteners** to hinder the disagreeable taste [32].

A liquefied propellant serves both as an energy source to expel the formulation from the valve in the form of rapidly evaporating droplets and as a dispersion medium for the drug and other excipients [33].

After the drawing up of "Montreal protocol on Substances that Deplete the Ozone Layer" that decreed the ban of chlorofluorocarbon (CFC), the (CFC)-based MDIs were replaced with non-CFC propellant and, in particular, with hydrofluoroalkanes (HFA) such as HFA 134a (1,1,1,2-tetrafluoroethane) or HFA 227 (heptafluoropropane)[35].

In order to obtain a good deposition of the drug in the lung simultaneous coordination between activation and inhalation device is required. Proper use of MDIs requires that patients learn how to coordinate exhalation and inhalation with actuation of the device. This may be very difficult particularly for very young and old patients [34].

To improve inhalant technique and drug delivery spacer devices were introduced in therapy. The concept of how spacers work is simple: after actuation the drug is suspended within a tube or spacer device for a few seconds prior to inhalation. The use of a spacer reduces the need for patient coordination of actuation and inhalation.

An additional problem in MDIs use is the unstable physical nature of the suspended drug particles in propellant; this fact, combined with suboptimal valve design, has led to reports of irreproducible dose metering following a period of rest. Moreover, the dose is emitted at high velocity and could make premature deposition in the oropharynx, thus only a small fraction of drug (10-20%) reaches the deposition region into the lung. Part of this problem could be overcame with the use of system to decelerate the cloud flow.

In the Gentlehaler, a modification of the actuator with a vortex chamber led to a substantial reduction of the spray velocity [36].

I.3.3 Dry Powder Inhalers (DPI)

The dry powders inhalers have been developed since the fifties and have several advantages: the absence of propellants and the unnecessary coordination or activation and inhalation because are activated by the inspiratory flow of the patient [37].

Since the benefits of DPI are closely linked to the inspiratory flow generated by the patient effort, because the diseases treated using this route of administration generally shown a worsening of the respiratory function and consequently the patients do not have an optimal FEV (forced expiratory volume) [38].

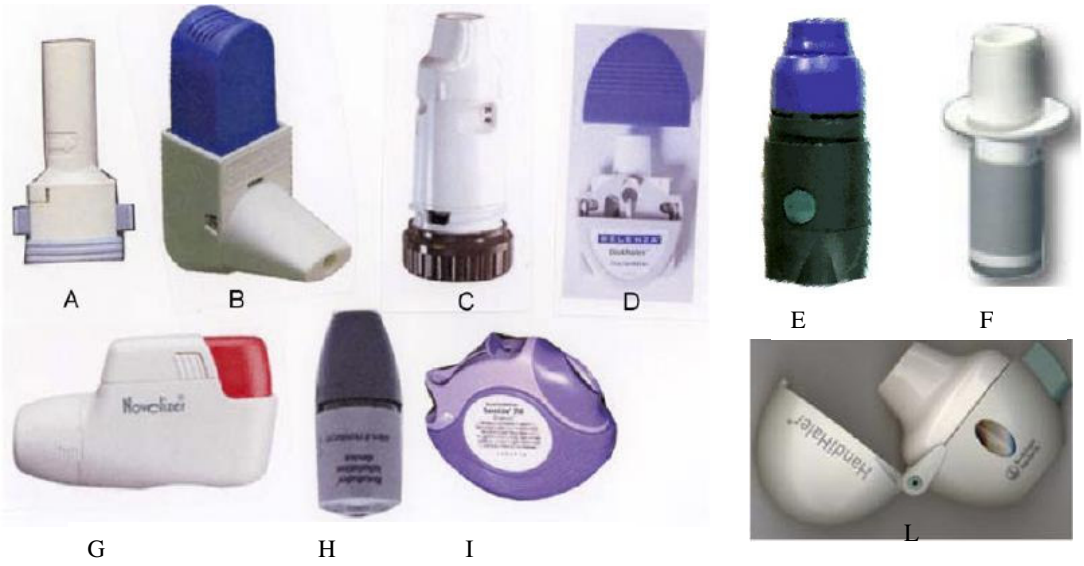

Figure 7: Photographs of some currently available DPI devices: (A) AerolizerTM, (B)EasyhalerTM, (C) TurbohalerTM, (D) DiskhalerTM, (G) NovolizerTM, (H) RotahalerTM,(I) ClickhalerTM, (E) MAGhalerTM, (F) SpinhalerTM, (L) HandihalerTM (*Source*:Photograph from the web:http://images.google.com.au/inages).

This goal is attainable only if the turbulence created in the chamber after delivery is able to aerosolize a bed of powder at best. For this reason DPI requiring an air flow equivalent to 30 L / min have been designed: such a flow can be more easily obtainable from patients with compromised lung capacity (asthmatics, elderly, children) [39].

Delivery of medication with a DPI requires minimal patient cooperation and coordination of breathing with actuation of the device. The DPIs are designed to rapidly deliver the drug powder once it is released, using the patient's inspiratory efforts to inhale drug containing particles[40-41].

There are essentially two types of DPIs:

- Single-dose devices

The first dry powder device described has been the Spinhaler ® (Aventis). The basic mechanism is the piercing of the capsule that contain the drug formulation.

Inspiration by the patient generates an airflow that rotates the capsule and projects the powder into the airstream [42].

In the Aerolizer (Novartis), a device used in this study, the capsule is pierced too.

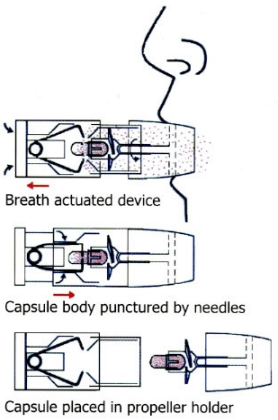

Figure 8: Mechanism of use of a monodose DPI with piercing capsules

Upon inhalation, the flowfield generated within the DPI makes the capsule rotate at high speed. This ejects the powder contained in the capsule through the holes into the surrounding flowfield. It is believed that break-up could occur through a number of capsules by induced deagglomeration mechanisms: powder agglomerates could impact with the internal walls of the capsule, when it rotates before ejection: forcing powder agglomerates through the small holes in the capsule could induce break-up, preventing slugs of powder from exiting the capsule. High speed impactions with the surrounding walls of the device could occur as the particles are ejected from the capsule, and the spinning capsule could act as a rotor to deagglomerate the ejected particles through mechanical impaction with the external walls [43].

Also the Turbospin® is a breath-activated, reusable DPI that works with a single unit capsule (containing powders), which needs to be loaded into the device each time prior to use.

- Multi-dose devices

Multi-dose DPIs contain more than one dose of drug. There are two types of multi-dose DPI:

-- reservoir that contains a bulk supply of drug from which individual doses are released with each actuation. The first such inhaler to be developed was the TurbuhalerTM [43] which is used to deliver β_2-agonists and corticosteroids separately and in combination. The drug located within this inhaler is formulated as a pellet of a soft aggregate of micronized drug which may be formulated with or without any additional lactose excipient. To administrate the dose, the patient twists the base of the device resulting in a dose of drug being shaved off the formulation while holding the inhaler in a vertical position. It is essential that this orientation is used when dose metering all reservoir DPIs, because they rely on gravity to fill the dose metering cup. The dose is then dispersed by turbulent airflow as the patient inhales through the device. Also, attention has been directed to the protection of the formulation from moisture ingress during routine storage and patient use. The majority of this type of DPIs are disposable and cannot be refilled with additional drug.

-- multi-unit dose devices that use individually prepared and sealed doses of drug. The first of such DPI was the Aerohaler^{TM} which contained six unit dose capsules as a storage medium, each delivering one dose of drug. The device was used to deliver fenoterol and ipratropium bromide and was very similar in design to single-unit dose inhalers. The sealed blisters offer a high degree of protection against environmental factors such as humidity and because the pre-metered doses of drug are factory prepared and separately packaged to assure dose uniformity.

Table I: DPI devices currently available on the market [43]

Device	DPI type	Company	Delivery method	Drug(s)
Breath-actuated single unit dose				
Spinhaler®	Single dose	Aventis	Capsule	Sodium cromoglycate
Rotahaler®	Single dose	GlaxoSmithKline	Capsule	Salbutamol sulphate
				Beclomethasone dipropionate
Inhalator®	Single dose	Boeringher-Ingelheim	Capsule	Fenoterol
Handihaler®	Single dose	Boeringher-Ingelheim	Capsule	Tiotropium
Aerolizer®	Single dose	Novartis	Capsule	Formoterol
FlowCaps®	Single dose	Hovione	Capsule	/
TwinCaps®	Single dose	Hovione	Capsule	Zanamivir
Breath-actuated multiple dose				
Turbuhaler®	Multi-dose	Astra Zeneca	Reservoir	Salbutamol sulphate
				Terbutaline sulphate
				Budesonide
Diskhaler®	Multi-unit	GlaxoSmithKline	Blister	Salmeterol xinafoate
				Beclomethasone dipropionate
				Fluticasone propionate
				Zanamivir
Diskus®	Multi-unit	GlaxoSmithKline	Strip pack	Salbutamol sulphate
				Salmeterol xinafoate
				Fluticasone propionate
Aerohaler®	Multi-unit	Boeringher-Ingelheim		Ipratopium bromide
Easyhaler®	Multi-dose	Orion Pharma	Reservoir	Salbutamol sulphate
				Beclomethasone dipropionate
Ultrahaler®	Multi-dose	Aventis	Reservoir	
Pulvinal®	Multi-dose	Chiesi	Reservoir	Salbutamol sulphate
				Beclomethasone dipropionate
Novolizer®	Multi-dose	ASTA	Reservoir	Budesonide
MAGhaler®	Multi-dose	Boeringher-Ingelheim	Reservoir	Salbutamol sulphate
Taifun®	Multi-unit	LAB Pharma	Reservoir	Salbutamol sulphate
Eclipse®	Multi-unit	Aventis	Capsule	Sodium cromoglycate
Clickhaler®	Multi-dose	Innoveta Biomed	Reservoir	Salbutamol sulphate
				Beclomethasone dipropionate
Twisthaler®	Multi-dose	Schering-Plough	Reservoir	Mometasone furoate
Active device				
Airmax®	Multi-dose	Norton Healthcare	Reservoir	Formoterol
				Budesonide
Inhance®	Single dose	Pfizer	Blister	Insulin

Table II: Next generations DPIs (approved or in development stage) [43]

Device	DPI type	Company	Delivery method	Drug(s)
Aspirair	Multi-dose	Vectura	Powder/Active	Apomorphine hydrochloride
Omnihaler	Single dose	Innoveta Biomeds Ltd	Powder/Active	/
Actispire	Single dose	Britania	Powder/Active	/
NEXT DPI	Multi-unit	Chiesi	Reservoir	/
DirectHaler	Multi-unit	Direct-Haler	Pre-metered	/
JAGO	Multi-dose	SkyPharma	Reservoir	Salbutamol sulphate
Airmax	Multi-dose	Norton Healthcare	Reservoir	Formoterol Budesonide
Turbospin	Single dose	PH&T	Capsule	/
AIR	Single dose	Alkermes	Capsule	/
MicroDose	Multi-unit	MicroDose/ 3M	Powder/ Electronic activated	Insulin
Cyclovent	Multi-dose	Pharmachemie	Reservoir	Morphine
Dispohaler	Multi-dose	AC Pharma	/	/
Conix One	Single dose	Cambridge Consultant	Foil seal	Vaccines
Microhaler	Single dose	Harris Pharmaceutical	Capsule	Sodium cromoglycate
Technohaler	Multi-unit	Innoveta Biomeds Ltd	Blister	/
Spiros	Multi-unit	Dura	Blister/Active	Albuterol sulphate
Bulkhaler	Multi-unit	Asta Madica	Reservoir	/
Miat-Haler	Multi-unit	MiatSpA	Reservoir	Formoterol Fluticasone propionate Budesonide
Prohaler	Multi-unit	Valois	Blister	/
Otsuka DPI		Otsuka Pharmaceutical	Compact cake	/
Acu-Breath	Multi-dose	Respirics	Powder	Fluticasone propionate
MF-DPI	Multi-unit	/	Reservoir	Mometasone furoate
Swinhaler	Multi-dose	Otsuka Pharmaceutical	Powder	Budesonide
Pfeiffer	Single dose	Pfeiffer GmbH	Active	/
Certihaler	Multi-dose	Novartis	Powder	Formoterol

I.4 Formulation of dry powder inhalers

The behaviour of powder particles during inhalation is highly dependent on the characteristics of the formulation and therefore, of the powder itself for this reason, the physical properties inherent to the active and final formulation must be well assessed. It would be theoretically possible to direct an aerosol in the deepest portion of the respiratory system, only by strict size control of the particles making up the drug [44].

As described above (See section I.2.3), the most widely used factor to define particle size and that mostly affects the deposition in the respiratory tract is the

aerodynamic diameter (d_{ae}) particle. It is defined as the diameter of a sphere of uniform density with the same velocity sedimentation of the particle considered.

Conventional aerodynamic optimization involves the reduction of the particle size to less than 5µm. Such particles are able to deposit in the respiratory tract but methods for size reduction, such as jet-milling can affect drugs and introduce changes in the physical properties of the particles [45-46]. To overcome the detrimental effect of milling, spray drying can be an alternative (See section III.2.1), since particles in the appropriate size range can be directly produced [47].

An attractive strategy in the preparation of inhalation particles is to manipulate both size and density of inhalation particles. Particles larger than 5µm are still able to penetrate into the alveolar region, provided that the density of the particles is scaled down to obtain a mean aerodynamic diameter of 1-3µm, which corresponds to a density of <0.4 g/cm^3 [48].

Its possible to use different production techniques to obtain micronized powder suitable for pulmonary delivery. These techniques include the classics, such as grinding jet fluid, and other more advanced of considerable interest for many applications, not only in pharmaceuticals: the "spray drying", the "spray freeze drying" and the extraction with supercritical fluids. The use of these advanced techniques of "particle engineering" to achieve optimization of fine particle fraction has led to increased capacity of aerosolizing or dissolving the drug[49-50].

As explained above, the fraction of a respirable inhalation powder depends not only on the volume diameter of particles but also by their size and density the ultimate goal of these techniques is to change these parameters to improve the respirability of the drug [51].

The particles are composed mainly from drug and other ingredients that have been approved by the regulatory authorities for their use in inhalation formulations. The main carrier used in this technology is phosphatidylcholine, naturally found in the lung surfactant.

Some particles (PulmoSphere®), produced by the "spray drying", have characteristics of low density and porosity. These features give the aerosol particles constituted the value of aerodynamic diameter less than 5μm, although the volume diameter is greater. This technology can be applied to effectively administer a large number of molecules to the lung [48].

I.5 Pulmonary infections: Bronchiectasis and Cystic Fibrosis

In some relatively rare conditions affecting the lungs, repeated and aggressive attacks from pathogenic bacteria occur, with which the immune system cannot cope.

Among them a certain frequency is encountered with bronchiectasis; this condition is characterized by an irreversible bronchial focal dilation (widening), accompanied by chronic infection.

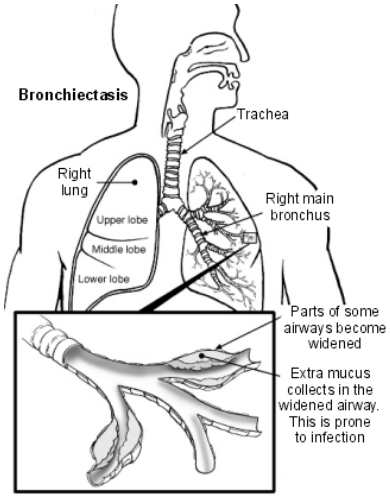

Figure 9:Schema of the widening of the airways and extra mucus

In bronchiectasics the surface of the bronchial wall is partially destroyed and chronically inflamed, the ciliate cells are progressively damaged and the mucous secretions accumulated. The bronchial wall becomes less elastic, the airways enlarge get flaccid and can develop swelling or pouches resembling small balls. The increased production of mucus promotes the growth of bacteria and often leads also the bronchus obstruction. This induces the gathering and accumulation of infected secretion that may cause further damage to the bronchial wall. The bronchiectasis is caused by various conditions: congenital or acquired [52].

Among the congenital conditions that can develop into bronchiectasis note that more than 50% of those who have this complication is affected by cystic fibrosis (CF), other conditions are represented by: primary ciliary dyskinesia (including Kartagener syndrome) and Marfan syndrome. Other causes may be represented by immunological abnormalities such as immunoglobulin deficiency syndrome, abnormal white blood cell

count, lack of complement, some autoimmune disorders or hyperimmune (such as rheumatoid arthritis and ulcerative colitis).

The acquired conditions can be several:

- respiratory infection: bacterial infections (such as pertussis or infections caused by Klebsiella, Staphylococcus and Pseudomonas), fungal infections (such as aspergillosis), infections incurred by mycobacteria (such as tuberculosis), viral infections (influenza, adenovirus infections (HIV), upper respiratory syncytial virus or measles);
- bronchial obstructions: lung cancer, swelling of lymph glands, inhalation of articles or excess mucus;
- "inhalation injuries" of smoke, gas or noxious particles or stomach acid or food particles;
- other conditions such as abuse of drugs, particularly heroin, the Young syndrome and the yellow nail syndrome.

The bronchiettasis spreads further to the emergence of a vicious cycle of inflammation, bronchial damage, iperproduction and stagnation of mucus and chronic microbial infection. It is therefore important to prevent and eradicate microbial colonization in the patients predisposed to lung damage.

As the CF is the main cause of bronchiectasis, we should provide some hints on this disease. The CF is the most common lethal autosomal recessive hereditary disorder, worst in the European origin populations, affecting an average one out of 2500 live births. However, this frequency varies according to geographic and ethnic origin of the patients. The gene encoding the CFTR protein has been identified and cloned in 1989 by Francis S. Collins, University of Michigan and Lap-Chee Tsui and John R. Riordan, the University of Toronto, is on the long arm of chromosome 7 and consists of 27

exons[53]. Since then, more than 1,000 mutations in the CFTR gene were identified and the identification of new ones is constantly growing. The first mutation, that is still the most frequently occurring results from the deletion of three base pairs on exons 10 and represents the deletion of a phenylalanine residue at position 508 (ΔF508). Currently, mutations in the CFTR gene are classified according to the biomolecular mechanisms, which cause the functional deficiency of the protein CFTR (Table III).

This membrane protein works like a channel for the passage of chlorine in cell membranes within the lungs and other organ systems. The absence or the defect (for the slight form of CF) of CFTR in the lungs leads to decreased chloride secretion and increased reabsorption of sodium. The consequent thick mucus produced in the dehydrated epithelium predisposes the patient to develop impaired mucociliary clearance and bacterial infections. Moreover, the transepithelial potential difference becomes hyperpolarized: the inability of Cl^- ions to follow Na^+ results in a more negatively charged mucosal surface [54].

The clinical presentation varies with age. In 10% of the affected newborns, it presents as meconium ileus (intestinal obstruction due to abnormally thick meconium). Later the symptomatology involves two major organ systems, respiratory and digestive, manifesting as repetitive respiratory infections and signs of malabsorption.

The respiratory involvement predominates and it is related to an obstruction of bronchioles by thick and viscous mucous favouring the growth of microorganisms. This explains the repeated respiratory infections by the opportunistic germs.

This disease involves some other organs, particularly the reproductive system and the liver. Atrophy and absence of vas deferens caused by obstructive azoospermia renders 98% of men sterile, on the other hand 80% of affected females are fertile.

The primary cause of morbidity and mortality in patients with cystic fibrosis is pulmonary disease [55].

The defective chlorine transmembrane transport is due to five different classes of mutations of the cystic fibrosis transmembrane conductance regulator (CFTR), as shown in Table III.

Table III: Classification of mutation of CFTR

Class I- *Lack of synthesis:* mutations altering the production of the protein. These mutations result in the total or partial absence of the protein. This class includes the nonsense mutations and those that produce a premature stop codon (anomalies of splicing and frameshift mutations). In certain cases the mutated mRNA is unstable and doesnít produce the protein. In other cases, the abnormal protein produced will probably be unstable and degrade rapidly. This is what produces the truncated protein or the protein containing the aberrant sequence (anomalies of splicing or the frame shift). Functionally, these mutants are characterized by a loss of conductance of Cl- channel in the affected epithelia.
Class II- *Lack of maturation:* mutations altering the cellular maturation of the protein. A number of mutations alter the maturation of the protein and thus the transport of these proteins to the plasma membrane. In this way, the protein is either absent from the plasma membrane or present in a very small quantity. The mutations of this class represent the majority of CF alleles (DF508).
Class III- *Lack of activation:* mutations disturbing the regulation of Cl- channel. These mutations are frequently situated in the ATP binding domain (NBF1 and 2).
Class IV- *Lack of conductance:* mutations altering the conduction of Cl- channel. Certain segments of membrane spanning domains participate in the formation of an ionic pore. The missense mutations situated in these regions produce a correctly positioned protein that has a cAMP dependant Cl- channel activity. But the characteristic of these channels is different from those of endogenous CFTR channel with a diminution of ion flux and a modified selectivity.
Class V- *Slowed down synthesis:* mutations altering the stability of mRNA or mutations altering the stability of mature CFTR protein.

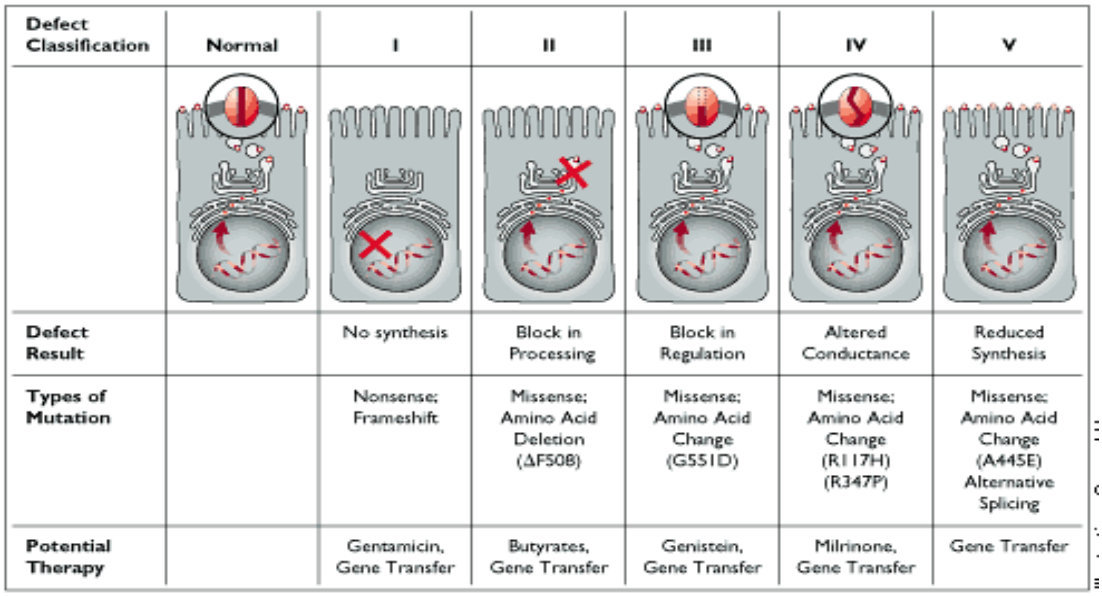

Figure 10: Schematic representation of mutation and functional results.

The understanding of the molecular mechanism of CFTR dysfunction provides the scientific basis for the development of drugs for a CF therapy. Pharmaceutical research is currently proceeding on three fronts:

- Correction of CFTR defects with a gene replacement theory;
- Pharmacological correction of CFTR function;
- Improvement of the symptoms affecting CF patients.

Gene replacement therapy offers an intriguing approach to the problem acting directly on the genetic defect responsible of the disease. However, gene therapy is still hindered by the difficulties in accomplishing the attainment of an efficient delivery of the genetic material and a lasting, therapeutically relevant transfection of the target cells [56].

I.5.1 Therapy

There is no effective treatment of CF, but the timely diagnosis and symptomatic treatment has made it possible to increase the mean survival up to 35 years.

The symptomatic treatment is available in the form of respiratory physiotherapy, antibiotic therapy, nebulisation with bronchodilators and mucolytics, administration of proteases inhibitors for pulmonary symptoms and administration of substitute pancreatic enzymes and vitamins for pancreatic insufficiency [57].

In advanced stages, the triple (heart-lung-liver) transplant has shown promising results but the major hindrance is the availability of donor organs.

Among the latest therapeutic advances, the gene therapy of CF has met a number of obstacles. Other promising strategies are under study with the objective of compensating

for the defect in the production and/or function of the CFTR protein depending on the type of mutation.

Massive use of antipseudomonal antibiotics and physical therapy have been primarily responsible for the increase in the median age of death. Antibiotics reduce the influx of neutrophils to the lungs, which slows the rate of progression of proteolytic lung destruction.

Treatment of pulmonary infections: antibiotic therapy

The aim of antibiotic therapy in chronically-infected CF patients is to stabilise lung function and, if possible, to restore some of the lost lung function. Intravenous antibiotics active against *Pseudomonas Aeruginosa* are used early on, when symptom of an impending exacerbation first appears. Suggested antibiotic regimen include an aminoglycoside (e.g. tobramycin sulphate (Nebcin) or amikacin sulphate (Amikin)) administered with an extended-spectrum penicillin. The bactericidal activity of tobramycin (O-3-Amino-3-deoxy-α-D-glucopyranosyl-(1-6)-O-[2,6 diamino-2,3,6-trideoxy- α -D-ribohexopyranosyl-(1-4)]-2-deoxy-D-streptamine) is accomplished by binding irreversibly to 30S and 50S ribosomal subunits resulting in a defective protein [58-59].

Established Pseudomonas infections are rarely eradicated by antibiotics but chronic infection can usually be well controlled. Problems arise when pseudomonal strains become resistant to the antibiotics.

Aminoglycosides are highly polar and a poor drug penetration into the endobronchial space is generally observed when the parenteral route of administration is used. The mean peak sputum concentration after parenteral administration is only 12-20% of the

peak serum concentration. Like other aminoglycoside antibiotics, tobramycin has a narrow safety margin. The therapeutic plasma concentration of tobramycin is in the range of 4-8 mg/l and may cause severe ear toxicity and kidney toxicity in a long-term therapy [60].

The popularity of aerosol administration of antibiotics is increasing: this route offers several advantages over the intravenous route: the direct application of antibiotics to sites of action in the lung is very efficient and systemic adverse reactions of aminoglycoside antibiotics are avoided [61].

In 1981 the first controlled trial of inhaled antibiotics showing effectiveness and safety was published. In this study gentamycin an carbenicillin were administered by nebulisation.

Two aminoglycosides, tobramycin and amikacin, are recommended in patients with CF for inhalation and are also the drug of choice for intravenous administration. Inhaled colistin sulphate is also used. Other antibiotic investigated for the inhalation route in patient with CF include neomycin and ceftazidime [62].

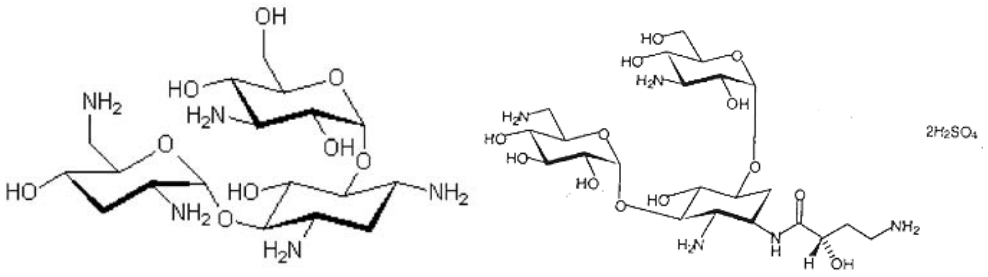

Figure 11: Chemical structures of tobramycin (left) and amikacin (right).

The use of aerosolized antibiotics has been proven to ameliorate lung function, reduce systemic long-term toxicity as well as decrease hospitalization [63-64-65]. Furthermore, when considering drugs such as aminoglycoside antibiotics administered

parenterally, high doses [66] are required to overcome poor lung distribution [67], due to their high polarity and poor drug penetration into the endobronchial space [68]. Consequently, these classes of antibiotics exhibit a narrow safety margin [69] since they may cause severe ototoxicity and nephrotoxicity in long-term therapy.

Table IV: Recommended dosages for antibacterial agents in the treatment of P. aeruginosa lung infections in cystic fibrosis patients [66].

Antibiotics	Route of administration	Dose $mg \cdot kg^{-1} \cdot day^{-1}$	Administrations per day n	Maximum daily dose g
Amikacin*	*i.v.*	30	2	-
Aztreonam	*i.v.*	150	4	8
	i.v.	100	continuously	8
Cefepime	*i.v.*	100 150	2 3	6
Ceftazidime	*i.v.*	150 250	3 4	12
Ceftazidime	*i.v.*	100 150	continuously	12
Ciprofloxacin	*p.o.*	30	2 3	1.5 2.25
Colistin	Inhaled	80 160#	1 2	0.320#
Sulphomethate	*i.v.*	160#	3	0.48
Imipenem/cilastatin	*i.v.*	50 100	3 4	4
Meropenem	*i.v.*	60 120	3	6
	i.v.	60	continuously	3
Netilmicin*	*i.v.*	10	2	-
Ticarcillin	*i.v.*	500 750	4	30
Tobramycin*	*i.v.*	10	2	-
	Inhaled	150 300#	1 2	0.6

*: dose based on measurements of serum concentrations; #: absolute dose (dependent on age and situation). These recommendations may not be the approved dosing recommendations by regulatory authorities in different countries.

The administration of aminoglycoside antibiotics by inhalation offers an attractive alternative due to the delivery of lower amount of antibiotic directly to the site of infection (600 mg per 5 ml; TOBI®) while minimizing bioavailability [70] so reducing systemic side effects. Tobramycin solution for inhalation [TOBI®] is the only antibiotic product approved by the Food and Drug Administration for respiratory delivery [71]. Although the administration of tobramycin by nebulisation has many advantages for the treatment of lung infections, the formulation requires to be given via nebulisation over an extended administration time (approx 20 minutes) [72]. The nebulisation approach has limited versatility and low efficiency, poor reproducibility and potential risk of bacterial contamination [73].

As mentioned below dry powder inhalers have many advantages over liquid nebuliser systems i.e., breath-actuated, low patient coordination, propellant free and a short treatment time.

In literature some attempts have been done in order to have a respirable tobramycin powder to be used in a dry powder inhalation devices. The solutions adopted involved the use of lipophilic adjuncts as mixture of cholesterol and phospholipids capable to hydrophobize the micronized drug particles, or the use of high-pressure homogenization and spray drying techniques to develop a formulation composed of a mixture of micro and nanoparticles. [74-75-76].

II. AIM OF THE WORK

In this work aminogycoside antibiotics, with a special focus on tobramycin, for DPI products were formulated with the following aims:

-to minimize the adjunct amount used in formulation development, in view to obtain a formulation carrier free with a high amount of drug. This is particularly useful for the aminogycoside antibiotics as a result of the high dose requested in order to obtain a therapeutic effect, especially compared to other class of drug commonly administrated by pulmonary route;

-to modify the surface properties of aminogycoside microparticles in order to improve drug deposition in the lung. A high amount of drug directly on the site of action increases the efficacy of the therapy and reduces the dose administrated. In this manner it is possible to reduce the systemic side effects associated with the use of aminogycoside antibiotic, that are concentration dependent (kidney toxicity and ear toxicity);

-to reduce the agglomeration tendency and to protect the formulations from the environmental humidity. This problem is particularly important for tobramycin due to the high hygroscopicity of the drug that could increase with a micronization process.

Therefore, the aim of this work was to develop a high respirable and stable tobramycin powder for pulmonary administration, in order to offer a novel alternative to

the product for nebulization TOBI®, at present the only aminoglycoside antibiotic available on the market, which is a tobramycin-solution for inhalation.

The spray drying process was selected for the production of tobramycin micro-particulate powders. The first step of the research was the production via spray drying of micronized dry powders of aminoglycoside to obtain the reduction of particle size and make it respirable.

Afterwards, the focus of this study was to prepare a series of tobramycin microparticles, with a high aerosolisation efficiency and resistance to environmental humidity, using small amounts of lipophilic adjunct (≤2 %w/w). These systems were evaluated in terms of the aerosol performance, morphology and structure, surface composition, physical state and in vitro cell toxicity.

III. MATERIALS AND METHODS

III.1 Materials

Tobramycin base (T) was supplied by Lisapharma (Italy). Acetic Acid, Phenilbutyrric Acid (PBA), Naringin (Nar), Lauric acid, Myristic acid, Palmitic acid, Oleic acid, Sodium stearate, Stearic acid, Arachidic acid and Behenic acid were purchased by Sigma-Aldrich. All solvents and chemical were of analytical grade. Water was purified by reverse osmosis (MilliQ, Millipore, France).

III.2 Methods

III.2.1 Spray Drying

Spray drying is by definition the transformation of feed from a fluid state into a dried particulate form by spraying the feed into a hot drying medium [77]. Spray drying provides the possibility of formulating particles suitable for inhalation in one step. Right formulations for spray drying are solutions, suspension or emulsion. In a typical spray dryer the formulation is atomized into millions of small droplets, which are dried in a heated stream of gas into millions of small particles. Laboratory spray dryers, such as the widely used “Mini Buchi” use pneumatic nozzle, such as a two-fluid nozzle for atomization of the feed solution. Commonly used drying media are air; the spray-dried particles are separated from the drying gas by a cyclone or a bag filter.

Spray drying consist of four process stages:

a) Atomization of feed into a spray;

b) Spray-air contact (mixing and flow);

c) Drying of spray (moisture/volatiles evaporation);

d) Separation of dried product from the air.

Each stage is carried out according to dryer design and operation and, together with the physical and chemical properties of the feed, determines the characteristics of the dried product.

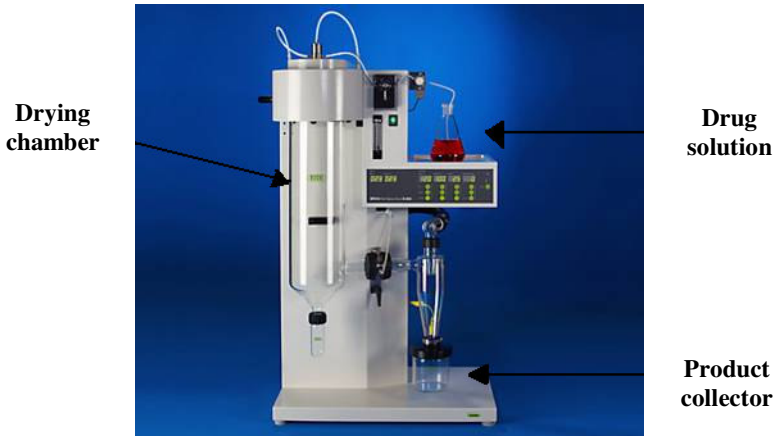

Figure 12: Schematic representation of a Spray-Drier and it's principal stages.

Droplet drying (solvent evaporation) starts instantaneously after atomization as the droplets meet the hot gas flowing through the dryer. Drying will proceed at a constant rate as long as the droplet surface is saturated. During this short period (~10^{-4}s), the temperature at the droplet surface will be equal to the wet bulb temperature T_{wb} (depending on the inlet and outlet temperatures). Simultaneously, dissolved material is transported through diffusion and convection to the surface of the droplet [78].

After drying the product was collected on wax paper, the yield was calculated with the following formula:

$$Yield\% = \frac{Mass_F}{Mass_S} \times 100$$

Equation 2

where $Mass_F$ is the weight of the product from the spray-drying process $Mass_S$ is the solid content of the initial solution to be spray-dried.

All the solutions were spray-dried using a Buchi B-192 (Buchi, Flawil, Switzerland) and Mini Spray Dryer B-191 (Buchi, Flawil, Switzerland).

III.2.2 Scanning Electron Microscopy (SEM)

The morphology of the surface of each micro-particle formulation was investigated using Scanning Electron Microscopy (SEM): (JSM 6000F JEOL, Japan and Scanning Microscope JSM 6400 Jeol, Japan), high resolution field emission microscope (0.6nm at 30kV) and (SEM – Scanning Microscope JSM 6400, Japan). The electron beam is produced by heating a metallic filament that function as cathode, generally a loop of tungsten. An anode placed right below the cathode forms powerful attractive forces for the electrons, causing them to accelerate down the microscope column towards the sample to be analysed. Before reaching the sample, the electron beam is condensed and focused as a very fine point on the material to be analysed. Once the electron beam hits the sample, there is production of secondary electrons, which are collected, converted to voltage and amplified. The image viewed consist of thousands of spots of varying intensity, which are dependent on the topography of the sample. The SEM column must always be in vacuum in order to prevent electron beam instability.

Since the SEM uses electrons to produce image, it requires samples be electrically conductive. In order to view non-conductive samples, such as most organic drugs, these must be covered with a thin layer of conductive material (carbon, gold, platinum, etc.) using a sputter coater.

Samples were mounted on adhesive black carbon tabs, (pre-mounted on aluminium stubs), and sputter-coated with platinum or gold (Sputter coater S150B, Edwards High Vacuum, Sussex, UK) at 40 nm thickness prior to analysis.

III.2.3 Energy dispersive spectroscopy-Scanning electron microscopy (EDS-SEM)

The lipophilic adjunct distribution on the surface of the tobramycin microparticles were analyzed using SEM-EDS (Scanning Electron Microscopy-Energy Dispersive Spectroscopy, JSM 6000F JEOL, Japan). High resolution field emission microscope (0.6nm at 30kV), Windowless EDS microanalysis. All samples were mounted on adhesive black carbon tabs, (premounted on aluminium stubs), and sputter-coated with platinum (Sputter coater S150B, Edwards High Vacuum, Sussex, UK) at 40 nm thickness prior to analysis.

Energy dispersive X-ray analysis, also known as EDS, EDX or EDAX, is a technique used to identify the elemental composition of a sample or small area of interest on the sample. During EDS, a sample is exposed to an electron beam inside a scanning electron microscope (SEM). These electrons collide with the electrons within the sample, causing some of them to be knocked out of their orbits. The vacated positions are filled by higher energy electrons which emit x-rays in the process. By

analyzing the emitted x-rays, the elemental composition of the sample can be determined. EDS is a powerful tool for microanalysis of elemental constituents [80-81].

These studies were conducted in order to try to identify any differences between the particles surface composition. It would be difficult to evaluate the topography and composition of a particulate material by analysing a relatively small number of samples, however, these techniques may afford some information concerning the chemical composition of any particle surface features.

III.2.4 Focused ion beam-Energy dispersive spectrometry-Scanning electron microscopy (FIB-EDS-SEM)

High resolution investigation of the microstructure of materials is very often restricted to the study of the very surface of the sample. This is because most high resolution analytical and imaging techniques like scanning electron microscopy (SEM), atomic force microscopy (AFM) or scanning tunnelling microscopy (STM) only provide information about the surface microstructure of the sample. To locally investigate the internal microstructure of the sample at high resolution, the sample has to be opened up. This can be done very precisely by the use of a focused ion beam (FIB) for cutting into the sample and the use of a field emission SEM for high resolution imaging of the internal structure. It is possible to use the FIB for cutting, polishing or pattering while one can observe the process live in high resolution SEM imaging [81-82-83-84]. In addiction, the specimen chamber is equipped with an analytical attachment like x-ray detectors for EDS. Gallium ions (Ga^+) are extracted from a high brightness liquid metal ion source and then accelerate to an energy of 20 ke.

To monitor the ion milling process in real time at high resolution in the SEM the Cross Beam operation is used. Both beams are turned on and while the ion bam is milling a defined area, the SEM is used to image the milling process at high resolution in real time. This enables the operator to control the milling process and to perform extremely accurate cross sections and device modifications. Moreover, after the cutting, the EDS analysis was performed to evaluate the lipophilic adjunct distribution on the inner structure of microparticles [84]. The instrument in this work was a FEI Quanta 200 3D.

III.2.5 X-ray powder diffraction

X-Ray powder diffraction (XRD) is a powerful and widely-used tool for crystalline state evaluation. X-rays are the part of the electromagnetic spectrum lying between ultraviolet and gamma rays. When X-rays are incident on a crystalline sample, they are scattered in all directions; in some of these directions the scattered beams are completely in phase and reinforce one another to form the diffracted beams. As defined by Bragg's law, diffraction will occur if a perfectly parallel and monochromatic X-ray beam, of wavelength λ, is incident on a crystalline sample at an angle θ that satisfies the Bragg equation:

Equation 3
$$n\lambda = 2d\sin\theta$$

where n is the order of reflection and d the distance between planes in crystals.

The XRD pattern consist of a series of peaks collected at different scattering angles. If the sample is amorphous X-rays are not coherently scattered and no peaks can

be observed.

The crystallinity of all formulations was characterised using X-ray powder diffraction (XRD- S6000 Shimadzu Corporation, Japan) with the following settings: 5-45° 2θ, step time 2° min^{-1}, 25° C.

III.2.6 Differential scanning calorimetry (DSC)

Differential scanning calorimetry (DSC) can be used to measure any kind of phase transition, for a given compound, that is associated with heat transfer. The principle behind DSC is that two cups, placed in a oven, one containing the sample and the other nothing (or an inert material), are heated and kept at the same temperature. Once an endothermic or an exothermic phase transition occurs within the sample, the heat flow provided to keep the two cups at the same temperature needs to be respectively increased or decreased thus giving rise to an endotherm or exotherm. DSC is a technique that is frequently used in preformulation studies in order to evaluate the crystalline state, the presence of polymorphs or the existence or an amorphous form of a given drug. In this study a DSC 821^e STARe (METTLER Toledo, USA) driven by STARe software has been used.

III.2.7 Measures of density

The *true density* of the spray-dried powders was measured by an Multivolume Pycnometer 1305. The samples were weight in a cup. Per each batch of the spray-dried powders were analysed 3 samples.

Helium Pycnometer Operative Conditions:

Minutes Purge: 3 min

Minutes Vacuum: 3 min

V_{CELL}: 8.479

V_{EXP}: 6.217

V_{SAMP} can be calculated with the following formula (equation 3), which was used to calculate the true density with another formula (equation 4).

Pressure P1, P2

Equation 4
$$V_{SAMP} = V_{CELL} - \frac{V_{EXP}}{[(P_1 / P_2) - 1]}$$

Equation 5
$$Density = \frac{NetWeight}{V_{SAMP}\,Average}$$

where P_1 and P_2 are pressures.

The density of a material is defined as its mass divided by its volume.

Equation 6
$$\rho = \frac{Ms}{V}$$

The bulk density is a property of powders, granules and “divided” solids. The bulk density could be defined as the mass of many particles divided by the total volume they occupy and is often measured by the "tap" density method. A material's tap density is obtained by filling a container of known volume with a known mass of sample and

vibrating it. This value is commonly referred to as "tap" density because it is typically obtained using a mechanical device that alternately lifts and drops the container a specified number of times, producing a loud tapping noise. Because this measurement varies depending on the vigor and number of taps, tap density is not an inherent property of a material. It is nevertheless a measurement of considerable interest in packaging, handling, and shipping bulk granular products.

Bulk and tapped density were measured using a tap density tester (JEL Stampfvolumeter STAV 2003). Bulk density was determined by filling about 1g of the various powders produced into a 10ml measuring cylinder and tapped density was measured by tap density measurement following 1000 taps, which allowed the density plateau [85].

Bulk and tapped density values allow the determination of the Carr's compressibility index by the formula

Equation 7

$$Carr's\_Index(\%) = 100\frac{(V_B - V_T)}{V_B}$$

where V_B is the bulk volume and V_T is the tapped volume.

Carr's Index values of less than 25 are usually taken to indicate good flow characteristics, values above 40 indicate poor powder flowability.

Another parameter correlated with the flowability of the powders is the Hausner Ratio.

A value greater than 1.25 is considered to be an indicator of poor flowability [86]

Equation 8

$$H = \frac{\rho_T}{\rho_B}$$

III.2.8 Determination of water content

The water content of the dry powders was assessed by two different methods.

III.2.8.a Karl Fisher titration

Measurements were performed by the Karl Fisher (KF) volumetric titration method with a Crison Titromatic 1S.

This method is designed to determine the water content in substances, utilizing the quantitative reaction of water with iodine and sulphur dioxide in the presence of a lower alcohol, such as methanol, and an organic base (B), such as imidazole or pyridine, as shown in the following equations:

$$CH_3OH + SO_2 + B \rightarrow [BH]^+ + SO_3CH_3^-$$
$$H_2O + I_2 + SO_3CH_3^- + 2B \rightarrow SO_4CH_3^- + 2[BH]^+ + 2I^-$$
$$SO_2 + CH_3OH + H_2O + I_2 + 3B \rightarrow 3HB^+ + SO_4CH_3^- + 2I^-$$

In the coulometric titration method iodine is produced by electrolysis of the reagent containing iodide ions. The water content in a sample is determined by measuring the quantity of electricity which is required for the electrolysis based on the quantitative reaction of the generated iodine with water[87]. The water content was measured in triplicate. The determination limits were set between 100 mg and 200 mg of sample.

III.2.8.b Termogravimetric analysis (TGA)

Termogravimetric analysis (TGA) was done with a TG50 (METTLER Toledo, USA) driven by STARe software. TGA measures the amount and rate of weight change in a material, either as a function of increasing temperature, or isothermally as a function of time, in a controlled atmosphere. It can be used to characterize any material that exhibits a weight change due to decomposition, oxidation or dehydration. Runs were set from 25°C to 270°C at 0°C/min with samples of between 5 and 0 mg in a platinum pan.

III.2.9 Laser diffraction

Laser diffraction is probably the most widely used technique for particle-size analysis in the pharmaceutical industry. Laser diffraction measurements are based on the phenomenon that particles scatter light in all direction with an intensity pattern dependent on particle size. The principle behind laser diffraction measurements is that a representative sample, dispersed at an adequate concentration in a suitable liquid or gas, is passed through the beam of a monochromatic light source followed by subsequent recording of the light scattered at various angle by a multi-element detector. These numerical scattering values are then transformed, using an appropriate optical model, to yield the proportion of total volume to a discrete number of size classes forming a volumetric particle size distribution.

Mean particle size and particle size distribution (PSD) are thus obtained through a matrix conversion of the scattered intensity measurements as a function of the

scattering angle and the wavelength of the light on applicable scattering theory. For particles larger than ~50μm, the Fraunhofer approximation can be used to calculate particle-size distributions from light scattering data without knowledge of the optical properties. For particle sizes smaller than 50μm, analysts must use Mie theory, which requires the specification of the particle RI and absorption (imaginary refractive index) together with the dispersant RI to obtain accurate results. The refractive index of pharmaceuticals is generally in the 1.38-1.65 range and is required only to an accuracy of ±0.2 to achieve reliable results. In the Mie theory (used by Malvern, U.K.), the scattered light intensity of a particle is a function of different variables: particle size, particle refractive index, medium refractive index, light wavelength, scattering angle.

Laser diffraction reports the volume of material of a given size because the light energy reported by the detector system is proportional to the volume of the measured particle. Volume-based distributions will always shift to larger particle sizes in comparison with number distributions. In fact, it is mathematically impossible for the volume distribution reported by counting methods, unless measurements are made at the limits resolution of the counting method. Particles are three-dimensional objects and therefore cannot be described by one number that equates to the particle size. For this reason, all techniques measure some property of a particle and provide the diameter of the equivalent sphere as the particle size. It is this approximation that is the source of differences between sizing techniques when non-spherical objects are measured.

Calculations are based on the theory of “equivalent spherical diameter” in order to determine particle sizes; that is to consider the diameter of theoretical sphere that

would produce the same signal as the studied particles. Using this theory, numerous equivalent diameters, including other parameters, such as surface, volume or weight, can be calculated.

The characterization parameters used were:

$\mathbf{D_{v(0.1)}}$, 10% of the volume distribution is below this value,

$\mathbf{D_{v(0.5)}}$ is the *volume median diameter*, is the diameter where 50% of the distribution is above and 50% is below,

$\mathbf{D_{v(0.9)}}$, 90% of the volume distribution is below this value

D[4,3] is the equivalent volume mean diameter or De Broucker mean diameter,

Equation 9
$$D[4,3] = \frac{\Sigma d^4}{\Sigma d^3}$$

D[3,2] is the equivalent surface area mean diameter or Sauter mean diameter,

The **Span** is the width of the distribution based on the 10%, 50% and 90% quantile.

Equation 10
$$Span = \frac{Dv(0.9) - Dv(0.1)}{Dv(0.5)}$$

Values presented are the average of at least 3 determinations.

Particle size was measured by laser light scattering Mastersize X (Malvern Instruments Ltd., UK) and Mastersizer 2000 (Malvern Instruments Ltd, UK). Approximately 5-10 mg of each sample were dispersed in chloroform, sonicated for 10 min in a water bath (FXP12M Unisonics, Australia) and added to a small volume sample dispersion unit for analysis.

Detection limits for the equipment range from 0.02-2000 μm.

III.2.10 In-vitro assessment of lung deposition

Impactors are the most widely used means for determining in vitro the particle size distribution of aerosols generated from medical inhalers and nebulizers. They measure aerodynamic particle size directly, this being the most relevant parameter for predicting particle transport within the respiratory tract. At the same time, they provide the only way of quantifying the mass of active pharmaceutical agents as well as other non-physiologically active components of the formulation in different size ranges.

Methods of aerosol particle sampling are execute by passing the airflow and suspended aerosol through one or more orifices of know dimensions and impinging it onto a collection surface at fixed distances from the orifice. Particles with an inertial force high are unable to follow the streamlines and collide on the firsts plates. Smaller particles are enable to remain airborne, follow the streamlines and avoid hitting the impaction plate. The velocity of the particles increases from one stage to another and the particles are impacted at the lower stages as they present smaller and smaller sizes.

Its use is recommended by United States Pharmacopoeia, European Pharmacopoeia. The orifice diameter and orifice to surface distance is setted, the only variable influencing the collection of the powder of an impactor is the flow rate. Normally, the impactors are designed to operate in a widely range of flow rate (15 to 100 l/min)but this require the re-computing of the cut-off values of the instrument and the changing of the inspiration time (between 8 to 2.4 sec) so that a volume of 4 litres of air is drawn through the inhaler.

Three apparatus are used for this work.

- Glass impinger or twin stage impinger (TSI)

- Andersen cascade impactor (ACI)
- Next generation impactor (NGI)

III.2.10.a Glass impinger or Twin Stage impinger (TSI)

This apparatus is the easier for establish the lung deposition of formulations. The impinger consist in two interconnecting glass flask and the samples are collected into a suitable liquid for the analysis. The apparatus is designed to be operated at 60 l/min and consists of a stage with an operational cut-off diameter of 6.4 μm. As this apparatus results in a relatively inefficient size-selective sampling has been used in the first phases of development because of its simplicity and the short time required for carrying out a test.

III.2.10.b Andersen Cascade Impactor (ACI)

This impactor consists of 8 aluminium stages together with a final filter. The stages are clamped together and sealed with O-rings. This allows a more detailed particle size distribution and can be operated at various flow rates.

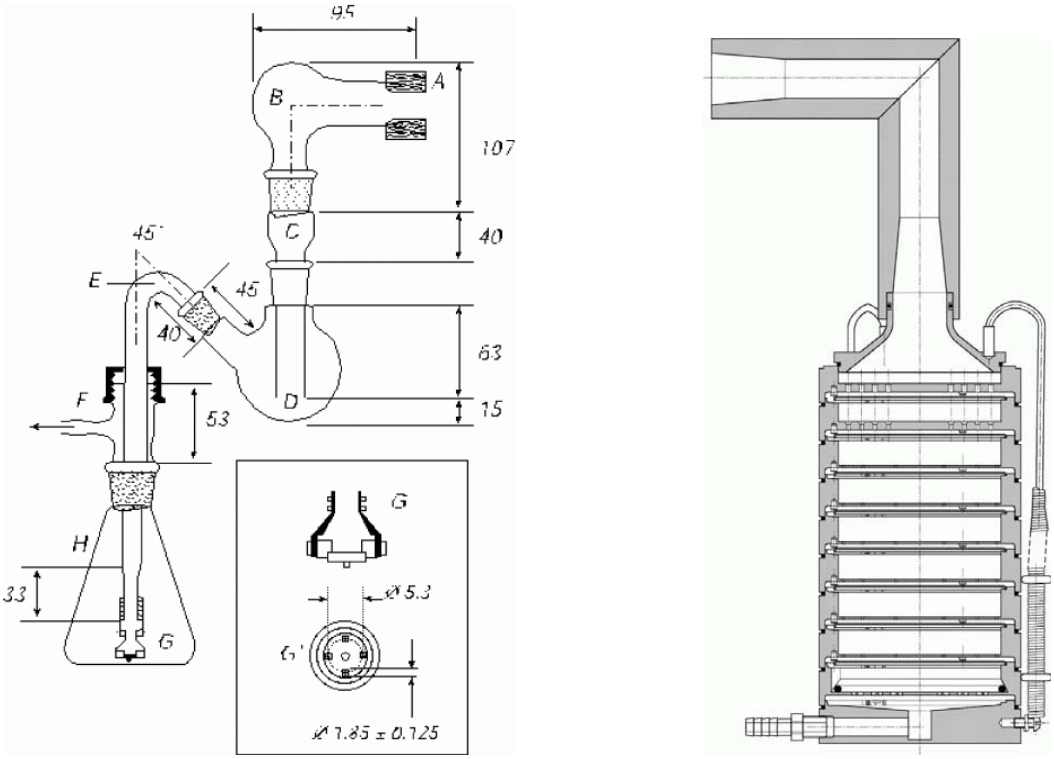

Figure 13: Schema of a glass impinger (left) and ACI (right) (Eur.Ph.6).

III.2.10.c Next Generation Impactor

The NGI is an horizontal cascade impactor designed with 7 stages and a micro-orifice collector (MOC). This impactor is also composed like the ACI by a throat and a preseperator and connected at a vacuum pump due to generate the air flow inside the system. The impactor layout has removable impaction cups with all the cups in one plane. There are three main sections to the impactor: the bottom frame that holds the impaction cups, the seal body that holds the jets, and the lid that contains the interstage passageways. Multiple nozzles are used at all but the first stage. The flow passes through the impactor in a saw-tooth pattern.

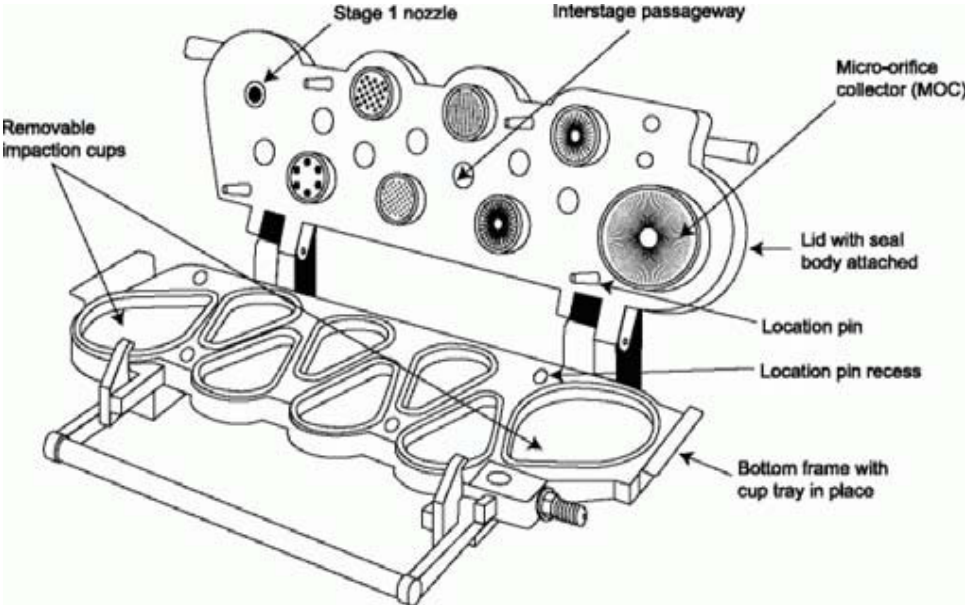

Figure 14: Schema of NGI (Eur.Ph.6)

NGI has a volumetric airflow rate of 60 l/min in order to have a correct activation of the device Aerolizer®. The time activation pump is 4 seconds (USP 31) [28].

Over the flow rate range of 30-100 l/min the cut-off diameters range between 0.24 µm and 11.7 µm, evenly spaced on a logarithmic scale. In this flow range, there are always at least 5 stages with cut-off values between 0.5 µm and 6.5 µm. The collection efficiency curves for each stage are sharp and minimise overlap between stages, unlike the ACI. The horizontal conformation of the NGI make it easier to use than the ACI.

III.2.10.d Interpretation of results

Data interpretation is done by plotting the percentages cumulative undersize samled at each stage of the impactor against cut-off diameter of the stages, resulting in

a collection efficiency curve.

The experimental mass median aerodynamic diameter (MMAD) and the geometric standard deviation (GSD) can be delivered from the log-probability scale plot. The MMAD of the particles is defined from this graph as the particle size at which the line crosses the 50% mark.

The MMAD corresponds to the diameter of the particles deposited in the impactor for which 50% w/w of particles have a lower diameter and 50% w/w have a higher diameter. This parameter better reflects the possible aerosolization of particles as aggregates and not only as individual particles.

The following parameters were calculated according to the USP 31:

- Recovery: percentage of the active compound fraction recovered from the device regarding to the mass of powder emitted from the device. The Eur Pharm determines the values have to be between 75-125 % in order to be considered as valid.

- FPD (Fine Particle Dose): the mass in mg of the active compound powder with dimensions equal or lower to 5µm. Fractions with such dimensions, that allows a pulmonary deposition, are calculated by the equation 11:

Equation 11 $$FPD = \frac{R}{n}$$

where R corresponds to the total drug mass lower to 5µm and n is the number of doses discharged during the test.

- FPF (Fine Particle Fraction): percentage of drug mass lower than 5 μm regarding to the total quantity of drug collected in the device. The fraction that would be delivered from the inhaler is then calculated by the equation 12:

Equation 12 $$FPF = \frac{R}{\Sigma A} * 100$$

where ΣA is the total mass of the active compound collected from the device.

- MMAD (Mass Median Aerodynamic Diameter): is the dimension (μm) which splits the dimensional distribution in two parts with same weight. It's calculated in diagram the undersized cumulative fraction of the active compound in Log Probit scale versus aerodynamic diameter in Log scale. With data interpolation it is possible to verify the MMAD like the corresponding diameter to 50% of the cumulative fraction.

- Delivered or Emitted Dose: the dose (mg) which leaves the device and it is calculated by weight differences of the inhaler device before and after drug delivery.

III.2.10.e Aerodynamic particle size analysis

The aerodynamic particle size distribution was evaluated using the ACI and the NGI (both Copley Instruments, U.K.) operated under pharmacopoeial conditions. Dry powder inhalation devices (Turbospin® , PH&T, Milan, Italy and Aerolizer®) were filled respectively with gelatine and hydropropylmethylcellulose (HPMC) capsules size 2 and HPLC capsules size 3 (Capsugel, Colmar, France). The flow rate was adjusted to a pressure drop of a 4kPa, as is typical for inspiration by a patient. Apparatuses was operated at airflow rate of 60 l/min for 4 sec so that a volume of 4 litres of air was drawn through the inhaler as recommended by the pharmacopoeias (Eur. Ph.. 6 and USP 31). Drug deposition in the device, throat and all stages was determined by HPLC analysis. For accuracy each test was conducted in triplicate.

III.2.11 Derivatization procedure of tobramycin

The chemical structure indicates that tobramycin has five primary amines, one primary hydroxyl group and four secondary hydroxyl groups. Due to the absence of a chromophore, direct high performance liquid chromatography (HPLC) method for tobramycin are not straightforward [92]. To increase the UV absorptivity of the molecule, a derivatization method is often applied [93].

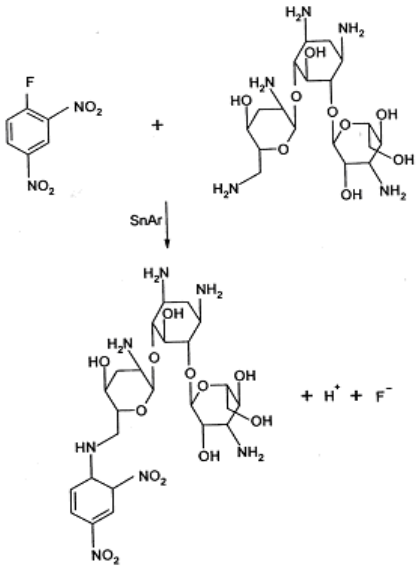

Figure 15: Reaction of the derivatization procedure (SnAr).

Nucleophilic Aromatic Substitution (S_NAr) reactions are essential tools for the analytical detection and quantification of tobramycin. The essential advantage of DMSO in these reactions is that due to the lack of solvation of anions in this solvent. These naked species are extremely reactive in DMSO. Thus, rate enhancements of S_NAr reactions in DMSO of the order of 106 x have been reported. Consequently, S_NAr reactions in DMSO can be performed at lower temperatures than in conventional solvents, including other dipolar aprotic solvents. Inasmuch as side-reactions in DMSO are minimized, this translates to selectivity advantages in DMSO relative to conventional solvents. It is clear from the graph below that reactions in DMSO are faster than the comparable reactions run with other solvents. Increasing the temperature to accelerate the rate of product formation in other solvents often results in the formation of unwanted side reactions.

III.2.12 Derivatization procedure of amikacin

At present, amikacin analytical determination is made using microbiological, immunological (RIA, radiochemical, EIA) and chromatographic methods [94]. Due to lack of volatility and chromophore of aminoglycosides, most chromatographic methods use derivatization to produce volatile, UV/vis absorbing [95] or fluorescent derivatives [96]; a cleanup procedure is often required prior to or after derivatization to eliminate interfering products. Pre-column derivatization is usually preferred, over post-column, because it does not require special equipment [97].

Amikacin was derivatized using the method described in a work of Santi-Nicoli [98] and in particular the amikacin was derivatized by mixing 100 µl of aqueous solution of the drug with 300 µl of methanol, 40 µl of NaOH 0.05M and 50 µl of a methanolic solution of the derivatizing agent (FDNB) 180 mg/ml (modified from Refs. [95,99]). The presence of a high proportion of methanol is necessary to maintain FDNB in solution, while NaOH serves to have un-protoned AK amino groups, thus allowing the derivatization reaction to take place. When AK was dissolved in vehicles different from water, the derivatization volumes were changed according to Table V in order to maintain the same solvents proportion and to avoid unnecessary dilution. The obtained mixture was heated at 90 ◦C in an air circulating oven for 10 min, then cooled and injected in HPLC. Each solution was separately derivatized prior to injection.

TableV: Details on derivatization volumes [98]

Details on derivatization volumes

AK vehicle	Volume derivatized (µl)	MeOH added (µl)	NaOH 0.05M added (µl)	FDNB[a] added (µl)
H_2O	100	300	40	50
MeOH:H_2O (50:50)	200	200	40	50
MeOH:H_2O:NaOH 0.05 M (5:5:2)	240	200	–	50

[a] 80 mg/ml solution in MeOH.

III.2.13 HPLC system

The suitable and validated quantification method is described in the USP 31. For this specific analysis the HPLC system consisted of a HPLC system Waters717+ with auto sampler, a 600 pump, 486 variable wavelengths UV detector set at 365nm and a 600 controller with Millennium V.32 software (all Waters Ltd., Sydney, Australia). The HPLC system was equipped with a 30 cm, 3.9 mm stainless steel (5 mm particle size) reversed-phase C18 column (Waters, Ireland) and Shimadzu LC-10AS liquid chromatography, Shimadzu SPD-10° UV-Vis detector.

III.2.14 Statistical analysis

The Student's *t* test was used to compare the lung deposition pattern between the different formulations. For all test the significance level was set at p=0.05.

III.2.15 In vitro cell toxicity

The toxicity of the tobramycin formulations and the Sodium Stearate on lung epithelial cells was investigated using a human alveolar basal epithelium A549 cell line, from the American Type Culture Collection (Manassas, VA) were cultured in Dulbecco's Modified Eagles'Medium (DMEM) supplemented with 10% heat-inactivated foetal bovine serum, 2mM L-glutamine (ThermoTrace, Melbourne, VIC, Australia), 100 U/ml penicillin, 100 μg/ml streptomycin and 0.25 μg/ml amphotericin B (Invitrogen, Carlsbad, CA). Cell cultures were grown in 10 cm plates, in an atmosphere

of 5% CO_2 in air in a humidified incubator at 37°C. The medium was exchanged every 2-3 days and cells were sub-cultured twice wekly.

For toxicity analysis the A549 cells were seeded in 96-well plates at a density of 3200 cells/well. Each well contained 100µl of the same medium used for culture cell. The cells were grown at 37°C in a 5% CO_2 atmosphere for 24 hours before use in cell viability assays.

Prior to analysis microparticles powders were subjected to gamma irradiation to ensure bacterial contamination of the powder did not influence toxicity (conducted by Steritech, Sydney, Australia). Briefly, cobalt 60 was used for irradiation (25kGy) and radiated samples were confirmed via the use of a gamma indicator dot placed on the outer of sterilisation bag. Exposure time was calculated according to the density of the samples and the received dose monitored via a dosimeter.

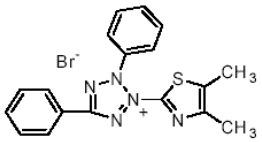

Figure 16: Chemical structure of MTT.

Cytotoxicity of each batches of tobramycin microparticles formulations, micronized sodium stearate and tobramycin raw material were investigated by replacing the cell culture medium he test powder in 100 µl of pre-warmed cell culture medium. Toxicity was measured after 24 hours exposure by measuring cell respiration, an indicator of cell viability, utilizing the mitochondrial-dependent reduction of 3-(3,4-dimethylthiazol-2-yl)-2,5-diphenyltetrazolium bromide (MTT) to formazan. This test assesses energy production by the mitochondria, viable cells will therefore be purple and non-viable will have no colour. After 4 hours of cell incubation with MTT formazan crystals develop in living and early apoptotic cells , dead cells don't produce formazan crystals.[100]

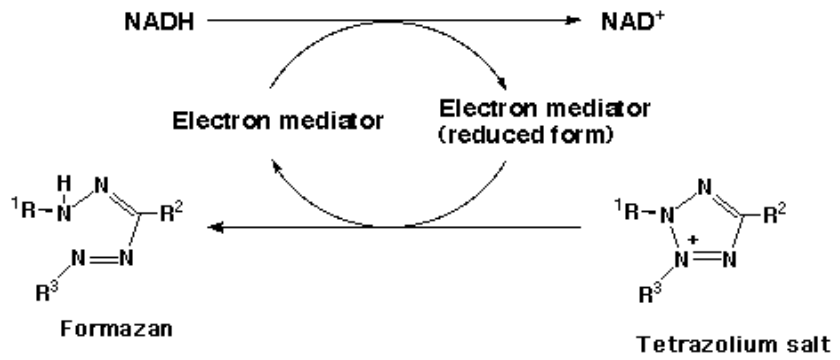

Figure 17: Reduction reaction for the tetrazolium salt.

In addition, a positive control test formulation was prepared by dissolving Triton X-100 in PBS to create a 0.5 $mg.ml^{-1}$ solution. Likewise, a negative control test formulation was also used in the form of the same medium used for culture in cell culture plates. Only the 60 internal wells were used for result collection purposes. The remaining 36 wells contained only culture medium.

After 24h of cell incubation, 50µl of the MTT solution (0.5 mg.ml-1 in PBS) was added to each well. After 4h the medium was removed and any formazan crystals generated were solubilised with 100 µl DMSO. The absorbance of each well was measured by spectrophotometry (SpectraMax 190, Molecular Devices, USA) at 550 nm after complete solubilisation of the crystals. [101-102]. The relative cell viability (%) was calculated as follows:

Equation 13

$$Viability\% = {}^{A}\!/_{C} \times 100$$

Where A is the absorbance obtained for each of the concentrations of the test substance and C is the average absorbance obtained for each of the negative controls.

III.2.16 In vitro release profile

Currently, there is no pharmacopoeia method suitable for the study of in vitro release profile of the drug for pulmonary administration (FDA) [103].

The dissolutions studies on amikacin micropowders has been performed with a traditional dissolution system with paddle (ERWEKA DT6R, Dusseldorf, Germany).

But the use of the traditional dissolution system where 1L of media is used for testing, as used for solid dosage forms, is not representative of the lung environment. In actual fact, the lung contains approximately 1 ml of fluid in the lower bronchial tree [104]. Subsequently, it is likely that the release mechanism of drug from the micro-particles, upon impaction in the lung, will be by passive diffusion, instead of by dissolution. A recent study by Salama et al. [105] has shown that for inhalation powders a modified Franz cell is the system that is more suited to accurately investigate drug diffusion in the lung flow through Franz cell was utilised as the core component to allow larger sink volumes and ensure reproducibility between multiple apparatus.

Briefly, Franz flow cells (Type-2, internal volume 20 ml, with heated water jackets, PermeGear, Inc. Bethlehem, PA, USA) were mounted in a six-station stirrer (V6B, PermeGear Inc. Bethlehem, PA, USA). Each Franz cell had a medium reservoir, containing 0.05M Phosphate Buffer (pH=7.4) at 37±0.5°C, using a temperature controlled water bath (which also maintained the Franz water jacket temperature via a

recirculating pump). Each medium reservoir was passed through its respective Franz cell using a peristaltic pump (Carter-Manostat) at flow rate of 5 $ml.min^{-1}$ (with two channel used for each cell). A 0.45μm nitrocellulose membrane (MF^{TM} Membrane Filters, Millipore, Bedford, MA, USA) was used to evaluate drug diffusion. The membrane diameter available for diffusion was 2.5 cm. When the system was equilibrated and stable, after approximately 1 hour, a 50 mg of powder was evenly spread on the previously buffer-soaked and fixed membrane filter in the Franz cell. Samples were taken at predetermined time intervals (3, 5 minutes and every 5 minutes up to 30 and every 15 minutes up to 120) from the dissolution medium reservoir (sample sink) and assayed using the HPLC method described previously. Prior to analysis, all samples were filtred through a 0.2 μm PTFE disposable filter to be sure not to have residues (Whatman® plc, Kent, UK) to make sure have not NaSt residual. All samples were analysed in triplicate. Was performed a statistical analysis of the dissolution curves from different powders.

The drug release/diffusion profiles of tobramycin microparticles containing different concentrations of sodium stearate were presented as percentages of transported drug plotted as function of time[106].

Moreover, the data was analyzed using the Weibull distribution equation and the relationship between sodium stearate concentration and time for 63.2% of tobramycin to be dissolved was analysed [107-108].

III.2.17 Surface Energy

The powders are complex systems and it is reasonable to assume that each crystal will have different surface properties due to the different proportions of various functional groups that are present. Its unreasoning to seek the surface energy of a powder, as simply there can never be a single surface energy. The actual trend is to simplify complex behaviour such that it is described by a single number.

With vapour probes it is the affinity for different vapours with a solid surface that is used to assess the solid surface properties. The complexity comes from the fact that powder surfaces are not homogeneous, hence the multitude of different binding sites can be expected to give rise to different surface energy values. The fact that there are many surface energies to be determined gives rise to the chance to study the surface with great detail and understanding, but equally may present problems if the measured energy is not the one that dominates the process of interest. Powder vapour interactions can be studied either gravimetrically, calorimetrically or chromatographically.[109-110]

III.2.17.a Inverse gas chromatography (IGC)

Chromatographic approaches are the ones that have been seen an increase in use. The concept of Inverse gas chromathography (IGC) is a simple one and that is to take a standard gas chromatographic (GC) experiment and invert the known and unknown, such that the unknown is the column packed with the powder to test, and the known are the vapours that are injected.

In order to calculate surface energies the method prescribe to plot $RT\ln V_n$ as a

function of $a(\gamma_L{}^D)^{1/2}$, where R is the gas constant, T is the absolute temperature, V_n is the retention volume, a is the surface area of the probe molecule, and $\gamma_L{}^D$ is the dispersive component of surface energy of the probe molecule. If data for non-polar probes (a series of alkanes) are plotted a straight line is produced from which the dispersive component of solid surface energy is obtained.[109] If retention data for probes with polar contributions to their surface energy are plotted, this results in responses that are located above the line drawn through the alkane probe results, and the vertical distance between the data points of polar probes and the alkane line gives the specific energy of adsorption of a polar probe with a solid material (ΔG^{AB}). The value of ΔG^{AB} is related to the acidic or electron accepting parameter (K_A) and the basic or electron donating parameter (K_D) as described in Equation 14:

Equation 14 $$DG^{AB} \quad K_A DN + K_D AN^*$$

where DN is an electron donor or base number characterised according to Gutmann, and AN* is an electron acceptor or acid number[109]. By measuring the value of ΔG^{AB} for polar probes, a linear plot of $\Delta G^{AB}/AN^*$ versus DN/AN* is obtained. The values of K_A and K_D of sample powders can then be determined from the gradient and intercept of the line, respectively [110-111]. Whilst this is the most frequently used approach, there are issues. Firstly, some workers prefer not to use surface area of probes due to orientation effects and instead may use enthalpy of vapourisation. Secondly, the units obtained for the dispersive component are in line with the surface energy data from contact angles, whereas the polar contributions end up as dimensionless numbers, making it hard to use such data in any meaningful calculations. For this reason it is sometimes preferred that

the free energy of adsorption of the polar probes are used as is, rather than being converted to an acid and base dimensionless term.[110-111-112]

III.17.b Contact angle (CA)

As mentioned above surface energies of drug substances and excipients provide a means of predicting the interaction between different solid materials. Another method to obtain surface energy data is the contact angle. This method has been used to predict various physico-chemical interactions, such as that between a drug and a dry powder inhaler carrier, and binder–drug interactions, which yielded good correlations with properties of granules and tablets.

It is possible to use several different approaches to obtain a surface energies value. The approach used in this thesis coming from the van Oss theory, an alternative approach to the DLVO theory.[115-116] This approach decomposes the surface energies, obtained from contact angle values into single contribution, independent each other. In particular van Oss introduced a polar acid-base (AB) component. In the method of Good and van Oss the contact angle of three separate liquids with known nonpolar (γ^{LW}), acid (electron acceptor-γ^{+}) and base (electron donor-γ^{-}) components have to be measured (Van Oss et al., 1988). The solid surface free energy is the sum of nonpolar (LW, Lifshitz-van der Waals) and polar (AB, acid-base) components given by Equation (15) and Equation. (16) [116]:

Equation 15 $$\gamma_i^{AB} = 2\sqrt{\gamma_i^{+}\gamma_i^{-}}\,(1+\cos\theta)\gamma_i^{TOT}$$

Equation 16 $$\gamma_i^{AB} = 2\left(\sqrt{\gamma_s^{LW}\gamma_i^{LW}} + \sqrt{\gamma_s^{+}\gamma_i^{-}} + \sqrt{\gamma_s^{-}\gamma_i^{+}}\right)$$

From the theoretical point of view the solid surface free energy is not dependent on the liquids used for its calculation. In practice this is not the case. Further, IGC at infinite dilution measures only a small portion of the powder surface; with a heterogeneous surface, adsorbates would tend to interact first of all with the more energetic surface sites.

III.2.18 Micro Fourier Transform Infrared Spectrometry (m-FTIR)

This study was carried out in an effort to obtain direct structural information about the structure of the spray dried tobramycin micropowders. The structure of a molecule is determined by the spatial orientation of the amide backbone and the presence of hydrogen bonds. IR spectra in the mid-infrared spectral range were recorded in the transmission mode on a Digilab FTS 40A spectrometer attached to a UMA 500 microscope, at the resolution of 8 cm1. Each spectrum represented a collection of 256 scans. Samples of inks placed on KBr plates (windows) were put in the infrared beam on the microscopic stage of the spectrometer.

III.2.19 Time-of-flight secondary-ion mass spectrometry (Tof SIMS)

Time-of-flight secondary-ion mass spectrometry (ToF-SIMS) is a highly surface sensitive analytical method for surface chemical identification and surface chemical distribution analysis (mapping). In the ToF-SIMS experiment, a pulsed primary ion

beam is incident on the sample surface and time-of-flight (ToF) secondary ion mass analysis is performed on the ejected positive or negative secondary ions. With the use of multi-stop timing electronics, ToF mass analysis enables the entire mass spectrum derived from each pulse to be collected. [117] The analysis has been performed by aTime-of-flight secondary ion mass spectrometer (TOF-SIMS) - Physical Electronics TRIFT II to the Ian Wark Research Institute (Adelaide, University of South Australia).

III.2.20 Dynamic vapour sorption (DVS)

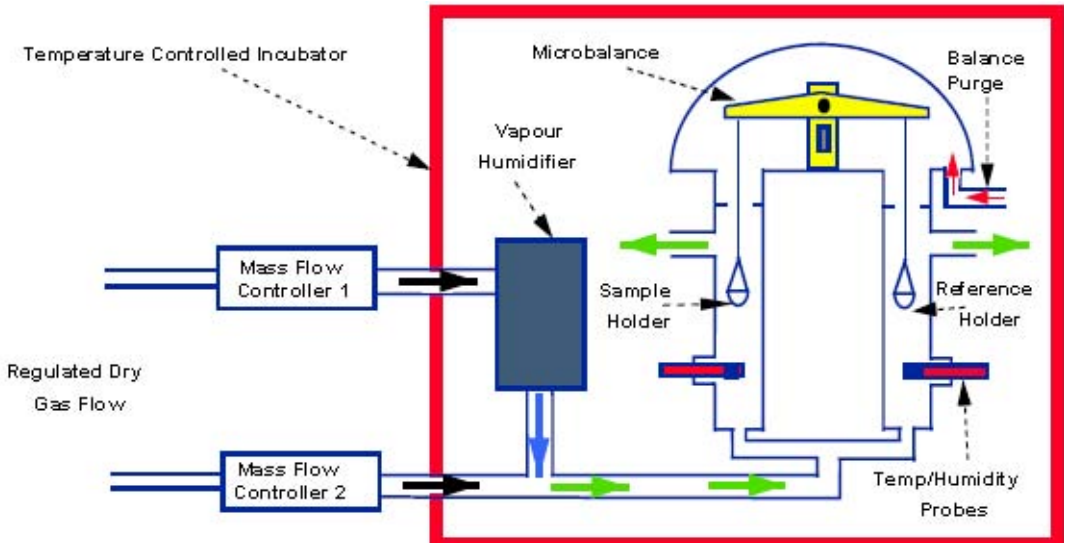

Figure 18: Schematic representation of a DVS system.

The DVS system consist in an ultra-sensitive recording microbalance capable of measuring changes in sample mass lower than 1 part in 10 milion. The main instrument is housed in a precisely controlled constant temperature incubator. This ensures very high instrument baseline stability as well as accurate control of the relative humidity generation. The required humidity are generated by mixing dry and saturated vapour gas flows in the correct proportions using mass flow controllers. Humidity and temperatures probes are situated just below the sample and and reference holder to give independent verification of system performance. The DVS records the uptake (adsorption) and release (desorption) of water from or onto a sample gravimetrically. In the first step of an experimental run, the sample was dried at 25°C and 0% RH for at least 600 min to bring the sample to near zero wt % H2O. Following the drying step, the instrument was programmed to increase the RH to target values in a stepwise fashion. The target RH

was the RH setpoint targeted by the mass-flow controllers; the sample RH was the actual RH measured by a fixed probe adjacent to the sample. For the experiment, the equilibrium water content was measured at target RH values from 0% RH to 90% RH in increments of 5% RH, and from 90% to 0% RH in increments of 10% RH. A weight change of less than 0.005% per min was chosen as the criterion for reaching equilibrium at each RH step before proceeding to the next RH step.[118-119-120].

The hygroscopicity of powders were tested using a dynamic vapour sorption (DVS) analyser (Surface Measurement Systems, UK) equipped with a Cahn D-200 microbalance (ATI Instruments, USA). All experimentswere conducted at 25 ºC. The flow of dry nitrogen bubbling through deionised water was controlled to obtain the various RHs. Samples (30-40 mg) of powder tapped out from the drug holder were loaded directly into the DVS sample pan. The powders were subjected to two sorption-desorption cycles from 0 to 90% RH in 10% RH steps. The step-change criterion was the rate of mass change (dm/dt) 0.0002 % of the initial mass per minute over five minutes. The data were analysed with the DVS Analysis Suite Version 3.6 (Advanced) (Surface Measurement Systems, UK).

IV. RESULTS AND DISCUSSION

IV.1 Part 1 FORMULATION AND CHARACTERIZATION OF SPRAY DRIED TOBRAMYCIN MICROPARTICLES FOR INHALATION

The major obstacle of DPI technology is the availability of a drug powder having an aerodynamic favourable size and behaviour. The attainment of a respirable powder of aminoglycoside antibiotic and in particularly tobramycin, is a difficult task due to the unsuitable size and shape of the original drug particles and to the hygroscopicity of the powder. As previously mentioned, spray drying provides the possibility of manufacturing particles suitable for inhalation since controlling the apparatus parameters it can control in one step the crucial characteristics of aerosol particles i.e., size, shape and density.

The first step of the study was focused on the research of the correct setting condition for the spray drying and to the choice of a set of adjuncts able to produce respirable and stable aminoglycoside antibiotics micropowders suitable for pulmonary administration. We focused our attention on the antibiotic tobramycin. In particular, have been product several batches of tobramycin microparticles from different starting solutions and different operative conditions. The first powders were produced by acidification of starting aqueous solution with acetic acid and phenylbutirric acid. A formulation was produced with naringin, a flavonoid [121-122-123-124].

We made different tobramycin solution to be spray-dried. The primary tobramycin aqueous solutions (pH 10.9) was acidificated by addition of acetic acid 1M, bringing the pH value at 7.4 and 6; the values of the physiological pH and the tobramycin inhalation solution (Tobi®, Chiron Corporation, USA), currently used in medical practice, respectively.

Others starting solution of tobramycin was acidificated also with phenylbutyric acid (PBA). The relative amount by weight of tobramycin and PBA was 40:60 and the solid concentration in the solution to be spray-dried was 2% (w/w); this has allowed to obtain a pH value of 7.04, close to physiological pH value.

In a second solution with PBA was added also 1%w/w of Naringin.

The solutions, kept under magnetic stirring, were spray-dried using a Buchi B-191 (Buchi, Flawil, Switzerland) spray-drier at different inlet temperature (T_{inlet}) shown in Table VI and at the following conditions: feed rate 3 ml min^{-1}, aspiration rate 100% and air flow rate 600 l h^{-1}.

Afterwards, it was decided to produce dry powder of tobramycin without acidify solutions to be spray-dried and the pH of the solutions was 10.9. The first powder was made from an aqueous solution of tobramycin base. The subsequent powders were produced from hydroalcoholic solutions to different concentration of ethanol from 15 to 60 with an increase of 15% for each solution. The solutions, kept under magnetic stirring, were spray-dried using a Buchi B-191 (Buchi, Flawil, Switzerland) spray-drier at the following conditions: feed rate 3 ml min^{-1}, aspiration rate 100% and air flow rate 600 l h^{-1}.

Table VI: Quantitative composition of the prepared powder by spray drying technique

	T % p/p	PBA % p/p	Nar % p/p	EtOH % v/v	Conc.Solution % p/v	Tinlet °C	Toutlet °C
Tobramycin raw	-	-	-	-	-	-	
T-CH_3COOH pH6	100	-	-	-	2	140	85-87
T-CH_3COOH pH6	100	-	-	-	4	140	83-85
T-CH_3COOH pH7.4	100	-	-	-	2	140	85-87
T-CH_3COOH pH7.4	100	-	-	-	4	140	83-85
T-PBA	40	60	-	-	2	125	75-78
T-PBA-Nar	50	49	1	-	2	125	75-78
Tb	100	-	-	-	1	125	75-78
T15	100	-	-	15	1	125	75-78
T30	100	-	-	30	1	125	75-78
T45	100	-	-	45	1	125	75-78
T60	100	-	-	60	1	125	75-78

The particle size distribution of the powders was determined using laser diffraction. As you can see in the Table VII the spray-drying process was able to micronize the tobramycin, but all the batches produced with acetic acid shown a $d_{v0.5}$ higher than 5μm; the powders with PBA and PBA-Nar had $d_{v0.5}$ around 4μm, but for both the set of powders the high hygroscopicity were a crucial problem for the aerosolisation and stability.

The microparticles produced without acidification, with the only EtOH as solution modifier, fall in the size range useful for pulmonary delivery and shown a better stability as it possible to see from the micrographs.

Table VII: Yield of SD process, water content and dimensional analysis of the raw material and SD microparticles.

	Yield % p/p	Water%	d_v 0.1	d_v 0.5	d_v 0.9
Tobramycin raw	-	4.55±0.17	0.89±0.02	**4.01±0.12**	16.02±0.51
T-CH_3COOH pH6	73.7	7.62±0.14	1.20±0,37	**5.34±1.74**	12.88±0.93
T-CH_3COOH pH6	46.5	6.74±0.77	1.33±0.29	**6.18±0.13**	16.52±1.21
T-CH_3COOH pH7.4	45.3	6.56±0.21	1.32±0,25	**6.61±0.34**	15.08±0.36
T-CH_3COOH pH7.4	63.4	6.77±0.35	1.45±1,50	**7.89±1.12**	18.93±0.73
T-PBA	54.8	5,43±1.02	1.33±0,03	**3.98±0.005**	8.20±0.02
T-PBA-Nar	73.2	4.27±1.32	0.89±0.01	**4.01±0.07**	16.02±0.13
Tb	74.5	8.19±0.10	0.97±0.03	**3.54±1.02**	7.47±1.43
T15	79.8	11.86±0.21	1.03±0.06	**3.64±0.96**	8.78±1.32
T30	82.5	11.80±1.96	1.03±0.04	**3.48±1.02**	8.07±1.04
T45	74.5	7.85±0.42	0.96±1.02	**2.56±0.99**	5.88±1.12
T60	82.0	6.84±0.42	1.01±0.02	**3.73±0.11**	7.67±1.12

The microparticles produced by acidification of initial solution was analysed only with the optical microscope because showed a deliquescent behaviour when exposed to the environment without protection (Figure 19) that opposed to the aerodynamic performance during aerosolisation. Then, when ethanol was added in the solution to decrease the powder residual water content after the spray drying, these tobramycin powder batches had a better stability compared to the acetic batches as shown in Figures 19-22 .

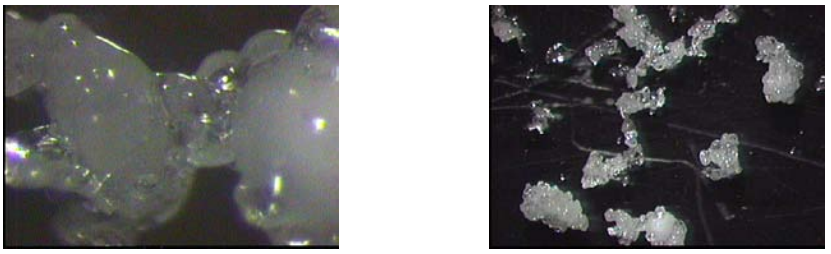

Figure 19: Optical microscope images of Tobramycin-Acetic Acid (pH7.4) after few minutes on slide.

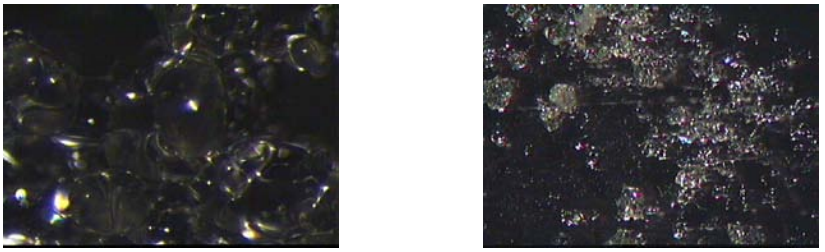

Figure 20:Optical microscope images of Tobramycin-PBA-Nar after one hour on slide.

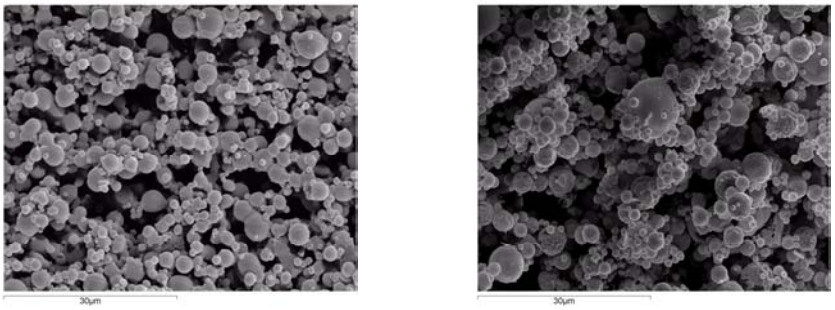

Figure 21: Scanning electron microphotographs: T15 (on the left) and T30 (on the right).

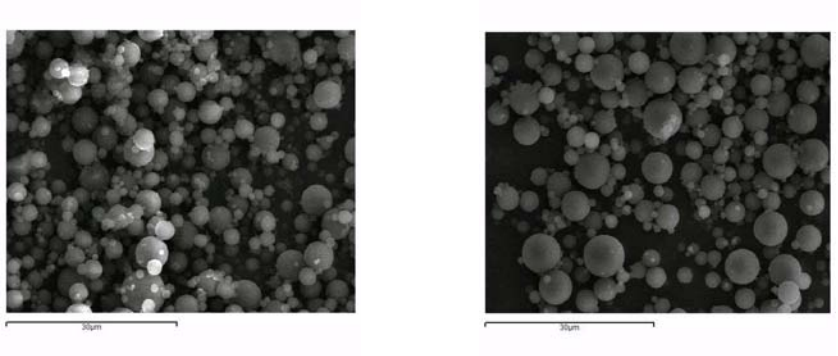

Figure 22: scanning electron microphotographs: T45 (on the left) and T60 (on the right).

Tobramycin is a very hygroscopic and the Karl Fischer titration was used in order to quantify the water content of the powders. Three samples for each batches were measured and the results are show in Table VII. The raw material had a water content of 4.55±0.17. This value increased with the SD micronization of the powder.

The calorimetric analysis was conducted on the raw material and micronized powders obtained following the process of spray drying.

As it is possible to see for all the SD formulations, the thermographs show a board endothermic plateau at 80-100°C, characteristic of a loss of water. There are no other thermic phenomena, in particular it is clear the absence of the endothermic peak of fusion characteristic of the crystalline raw material (Figure 23).

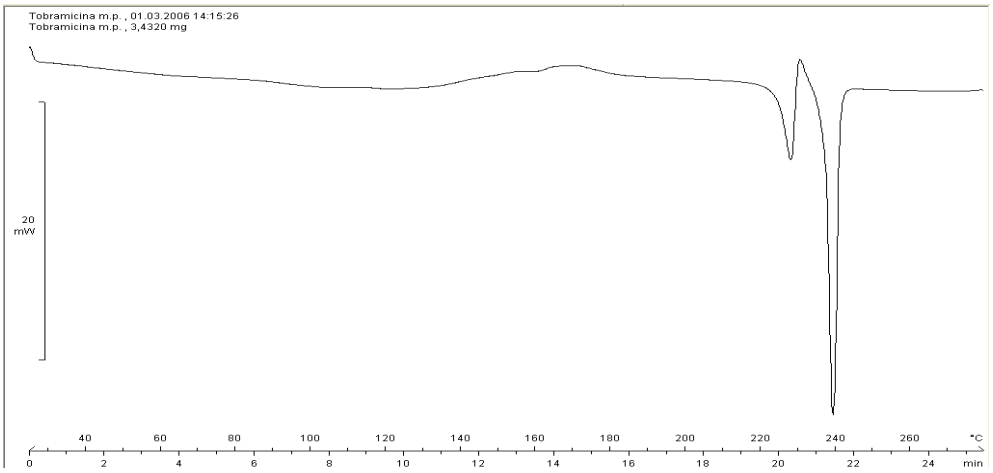

Figure 23: DSC-curve of tobramycin raw material.

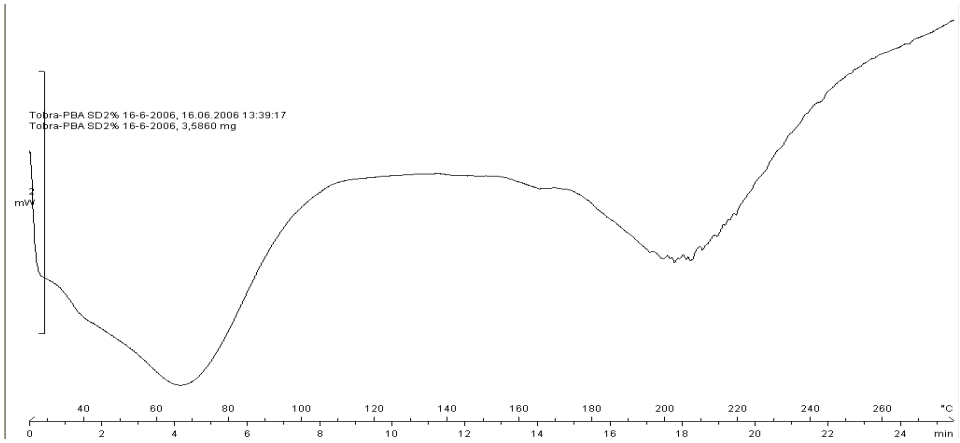

Figure 24:DSC-curve of the spray-dried powders (T-PBA)

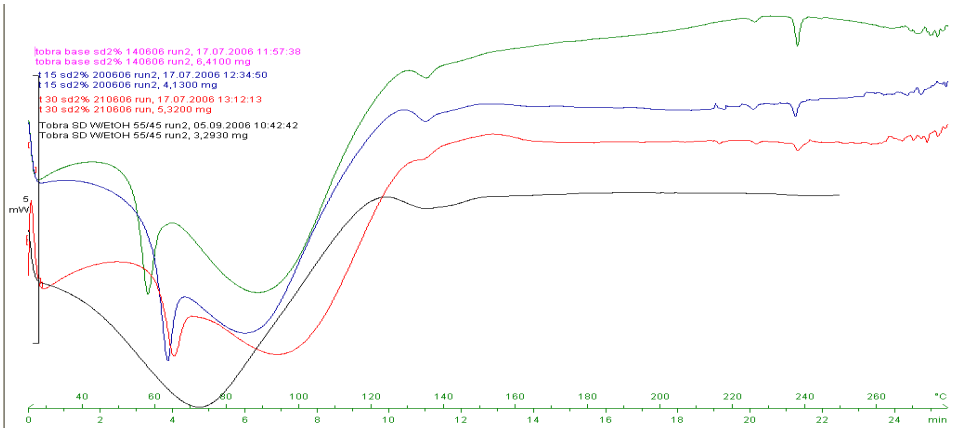

Figure 25: DSC-curves of the spray-dried powders (TpH6, T15, T30, T45).

The arosolization performance was determined using Twin Stage Impinger (TSI), the easier apparatus for a first study of the aerodynamic properties of the powders. With this apparatus is not possible to calculate the MMAD because it's separe the powders only in two populations as previously mentioned (See section III.2.10.a).

In the Figure 26 it is possible to see the deposition of the powders. S1 represent the non-respirable fraction and the S2 represent the respirable fraction, that is the fine particle fraction (FPF%).

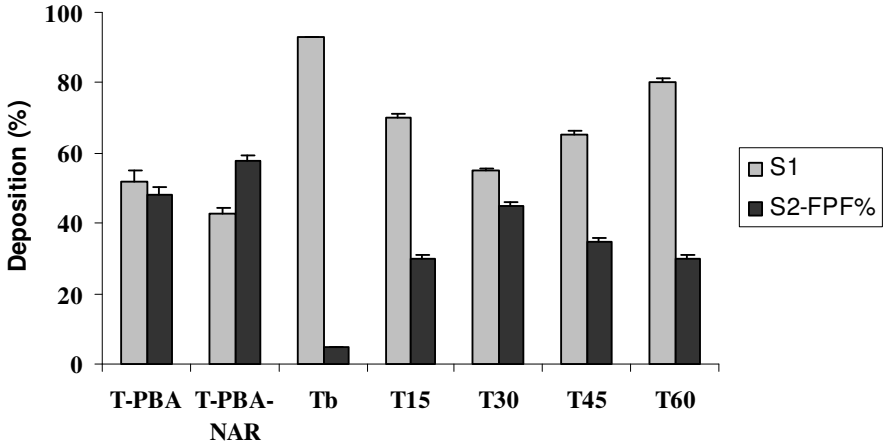

Figure 26: TSI deposition of the microparticles produced.

For the first two powders, with PBA and PBA-Nar the FPF% values were more than 40%. This could be interesting values but the deliquescent behaviour of these powders doesn't make possible further investigations.

Interesting appear the FPF% values of the powders from solutions with different % of EtOH made without acidification. The stability was increased for all the powders, but for the formulation without ethanol (Tb) most of the powders had the tendency to impact in the first stage (S1) of the impactor. This powder was more cohesive than the others formulations produced from hydroalcoholic solution.

IV.1 Conclusion

The spray drying of tobramycin solution without excipients both in neutral or acidic conditions gave rise to highly hygroscopic powder, deliquescent with a low flowability and not stable at normal storage conditions. Literature reports the use of lipophilic substances as adjuvant in tentative to reduce the water uptake of the micronized powders. Unfortunately, these substances are not miscible with water solution due to their nature, so requiring the invention of a procedure capable to homogeneously combine the adjuvant with the drug. For this reason, the first step of the investigation has been the evaluation of the properties of tobramycin spray dried powder with different amount of ethanol in the solution. The best performances was for the solution with the 30% of ethanol; this quantity is able to dissolve the lipophilic adjunct and gave us the basis for the next step of the research.

IV.2 Part 2 FORMULATION AND CHARACTERIZATION OF SPRAY-DRIED TOBRAMYCIN AND SODIUM STEARATE FOR INHALATION.

As previously mentioned, the major obstacle to the formulation of a stable and respirable dry powder of tobramycin is the hygroscopic behaviour of drug particles that would reduce their aerosolization and respirability. The solutions adopted involved the use of large amount lipophilic adjuncts such as mixture of cholesterol and phospholipids capable to hydrophobize the micronized drug particles, or the use of high-pressure homogenization and spray drying techniques to develop a formulation composed of a mixture of micro and nanoparticles.[74-75-76]

We studied the effect of low percentages of sodium stearate introduced in the formulation as lipophilic adjunct for obtaining spray-dried tobramycin microparticles having surface properties favourable for aerosolization and resistant to environmental humidity. The role of sodium stearate as aerodynamic modifier was assessed by studying the inhalation performance in dependence of the amount of adjunct introduced in the pulmonary powder.

Six batches of tobramycin powders containing different percentages of sodium stearate were manufactured by spray drying. Each formulation will be referred as the concentration of sodium stearate in the solid (w/w). Tobramycin microparticles were prepared by spray drying from (70/30) water/ethanol mixtures, with or without NaSt using a Buchi B-192 (Buchi, Switzerland) spray-drier at the following conditions: feed rate 3 ml min^{-1}, aspiration rate 100%, air flow rate 600 l h^{-1}, inlet and outlet measured temperatures of 125 and 75-78°C, respectively and feed concentration of 10 mg ml^{-1}. All powders were prepared under the same drying conditions with varying percentages of lipophilic adjunct. All powder batches prepared presented a spray drying yield of more than 60% and in particularly all powder batches prepared presented a yield ranging between 64±2.2% and 70 ± 5.7%

In order to understand the influence of hydrophobic adjunct on the aerosol performance of the microparticles, each formulation was evaluated in terms of physico-chemical properties.

Particle size distributions measured by laser diffraction of tobramycin microparticles containing different concentrations of sodium stearate are shown in Figure 27.

Analysis of the particle size distributions showed that the powders have similar mono-modal size distribution within a size range useful for respiratory delivery by powder aerosolization. However, variations in size were observed and their significance can be evaluated from the mean values and standard deviations as reported. For example, the 50^{th} percentile undersize ($d_{0.5}$) varied with respect to sodium stearate concentration. For example, $d_{0.5}$ values of 2.25 ± 0.03 μm, 2.28 ± 0.16 μm, 1.66 ± 0.002 μm, 1.49 ± 0.007

µm, 1.13 ± 0.001 µm and 1.48 ± 0.002 µm were observed for particles containing 0, 0.25, 0.5, 1, 1.5 and 2% w/w sodium stearate, respectively. Similarly, the 90th percentile undersize ($d_{0.9}$) values varied showing $d_{0.90}$ values of 8.19 ± 3.01 µm, 9.23 ± 0.62 µm, 4.24 ± 0.02 µm, 4.04 ± 0.02 µm, 3.94 ± 0.001 µm and 4.23 ± 0.04 µm for particles containing 0, 0.25, 0.5, 1, 1.5 and 2% w/w sodium stearate, respectively. However, regression analysis of $d_{0.5}$ or $d_{0.9}$ as a function of sodium stearate concentration indicated no linear relationship, since R^2 values of ≤ 0.680 were observed.

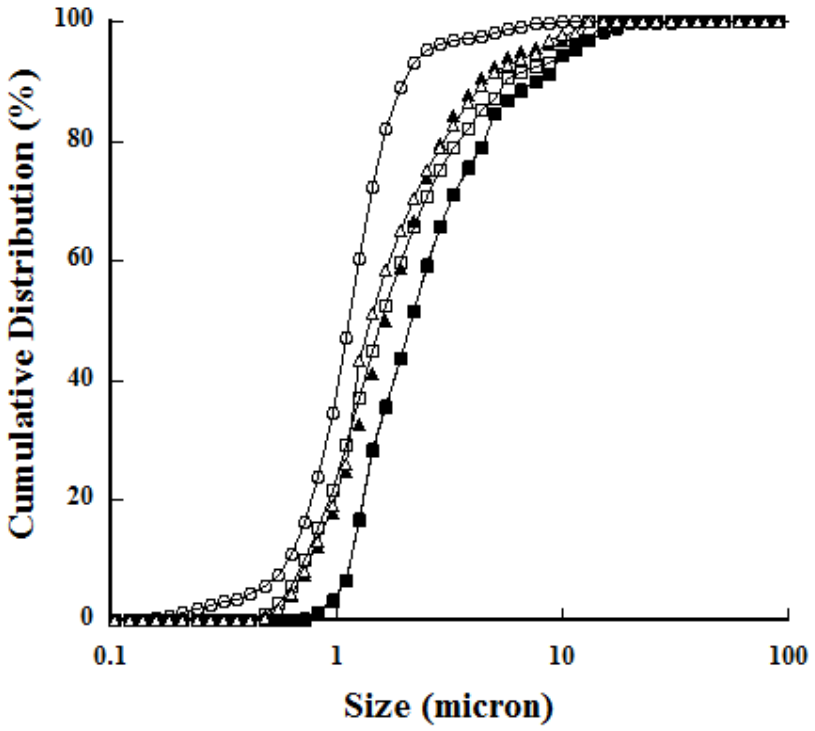

Figure 27: Particle size distributions of spray dried tobramycin microparticles containing different concentrations of sodium stearate adjunct (■ T0, ● T0.25, ▲ T0.5, □ T1, ○ T1.5, △ T2).

Scanning electron micrographs of tobramycin microparticles are shown in Figure 28, respectively. In general, the particles were spherical with smooth surfaces indicative of an amorphous spray dried material. No substantial differences were observed between the size of particles. Furthermore, micrographs of samples containing different concentrations of sodium stearate confirmed that adjunct concentration did not affect particle geometry or morphology.

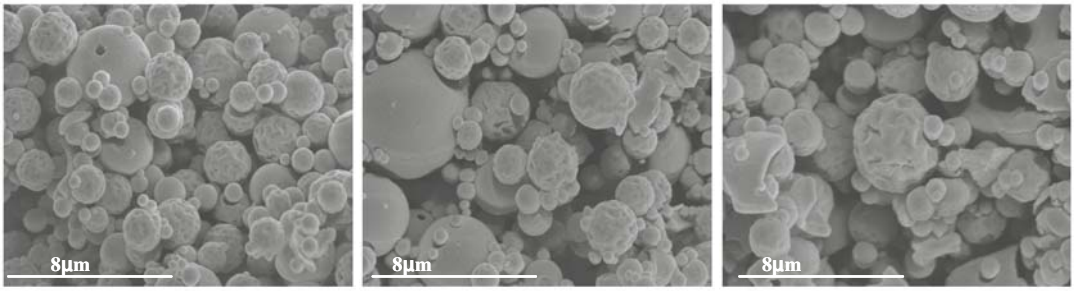

(a)

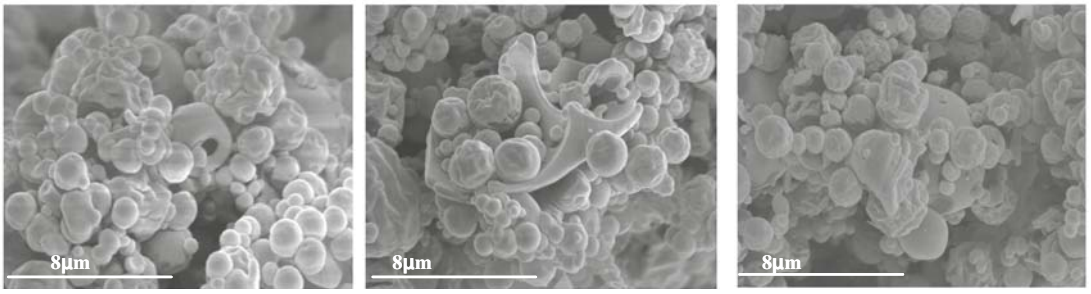

(b)

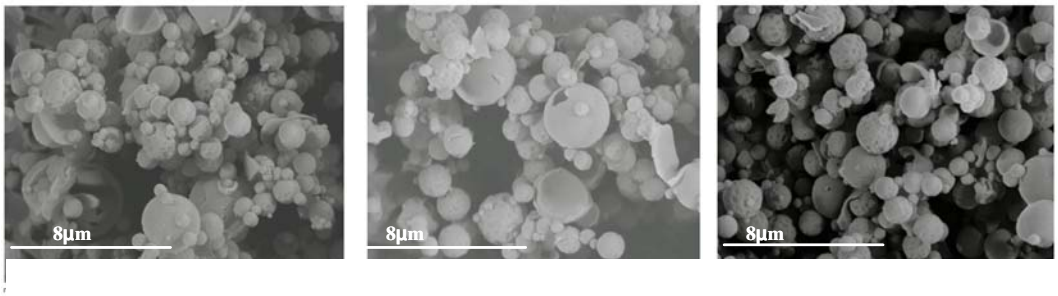

(c)

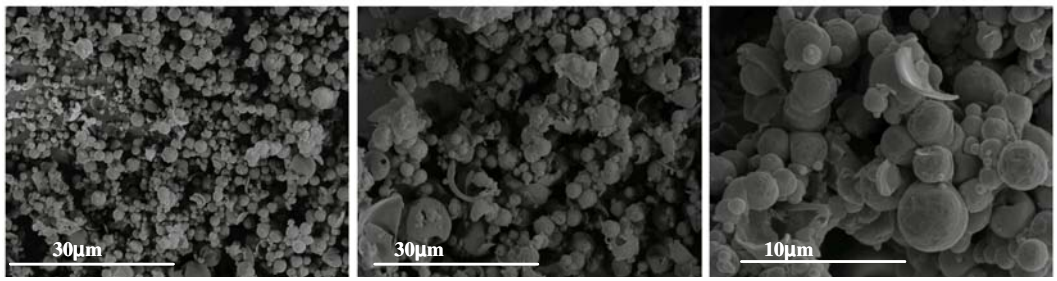

(d)

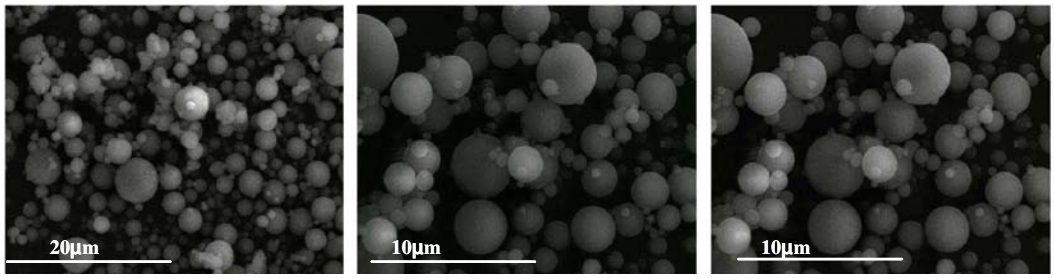

(e)

Figure 28: Scanning electron microphotographs: T0.25, (a), T0.5(b), T1(c), T1.5(d), T2(e).

The loss on weigh of the powders under heating was evaluated with the termogravimetric analysis. To some extent the loss on weight can be attributed to water content of the powder itself, although at temperatures above 100 °C could take over other phenomena. As shown in the graph there is a linear relationship between adjunct concentration and loss in weight % (R^2= 0.99) up to a concentration of 1%. After this point the value of loss on weight was stable around 7%.

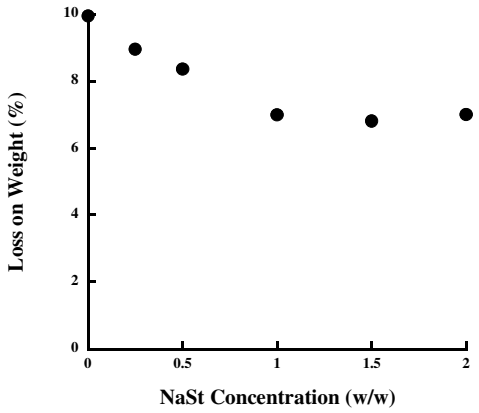

Figure 29: Loss on weight (%) values vs NaSt %.

X-Ray powder diffraction analysis of the spray dried samples presented a broad diffuse peak indicative of an amorphous material. Such observations are consistent with the spray drying of many organic materials, specifically those which are composed of binary components[125]. In addition, they are in good agreement with the SEM images which showed particles with smooth spherical structure.

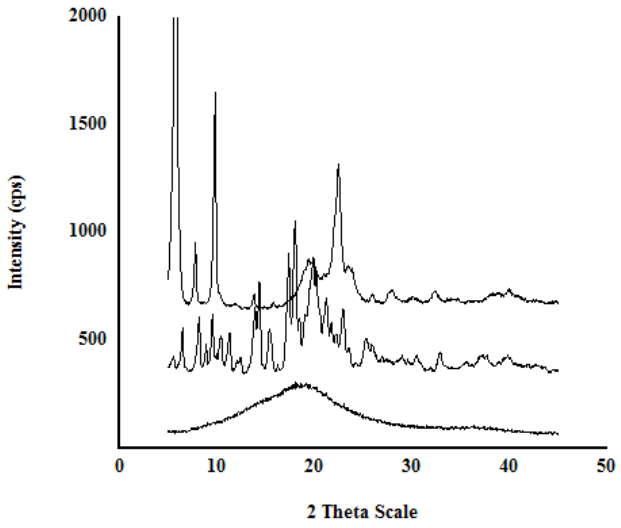

Figure 30: X-Ray powder diffraction patterns of tobramycin, sodium stearate raw material and T1 formulation.

The IR spectra obtained were compared with the spectrum of tobramycin raw material. The peak positions were searched for automatically by the computer. It was found that the spectra obtained in this way did not differ qualitatively from those recorded.

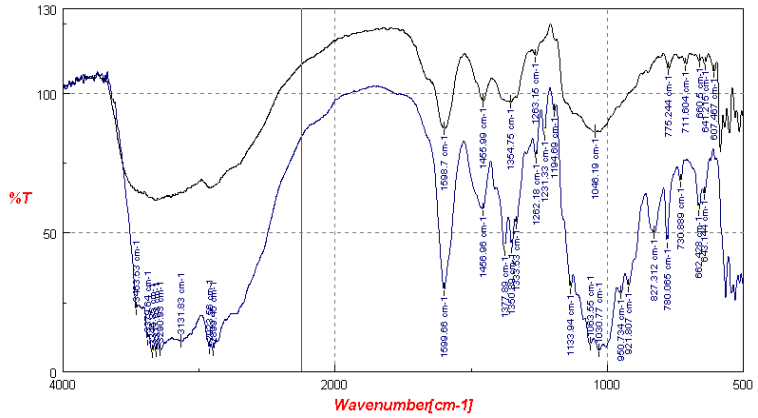

Figure 31: Micro FTIR raw material (black) T0.5 (blue).

The deposition (device/capsule, throat and NGI stages) of the microparticles after aerosolization is shown in Figures 32-37. The in vitro respirability parameters are reported in Table VIII. Mass median aerodynamic diameter values, compared with the volume diameter, indicates a possible agglomeration effect for tobramycin microparticles without and with 0.25% NaSt; the difference between the two equivalent diameters was significantly reduced by increasing the content of sodium stearate, with a minimum for the powders containing the adjunct between 1 and 1.5%. Analysis of drug deposition on each stage suggested sodium stearate concentration had a significant effect on the aerosolization performance. The aerosolization and deposition performance of tobramycin microparticles without lipophilic adjunct presented the poorest performance, since a FPF of 27.1 ± 1.9% was observed. This particle system

also had the highest device and capsule recovery (12.98±1.88 mg), indicating a highly cohesive powder.

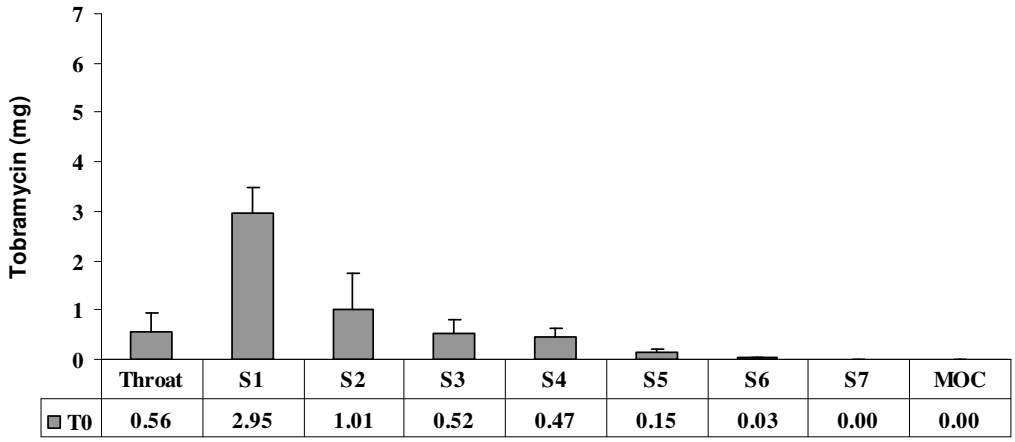

	Throat	S1	S2	S3	S4	S5	S6	S7	MOC
T0	0.56	2.95	1.01	0.52	0.47	0.15	0.03	0.00	0.00

Figure 32: Aerodynamic assessment by NGI of tobramycin 0 (T0).

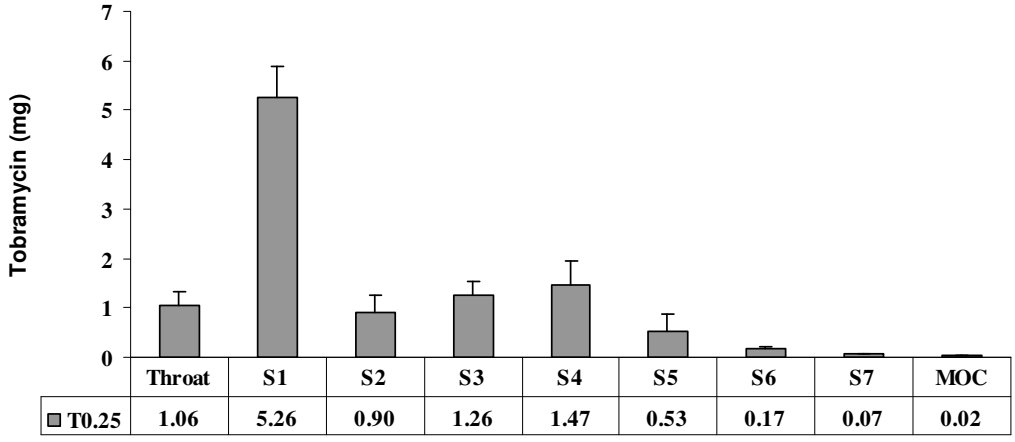

	Throat	S1	S2	S3	S4	S5	S6	S7	MOC
T0.25	1.06	5.26	0.90	1.26	1.47	0.53	0.17	0.07	0.02

Figure 33: Aerodynamic assessment by NGI of tobramycin 0.25 (T0.25).

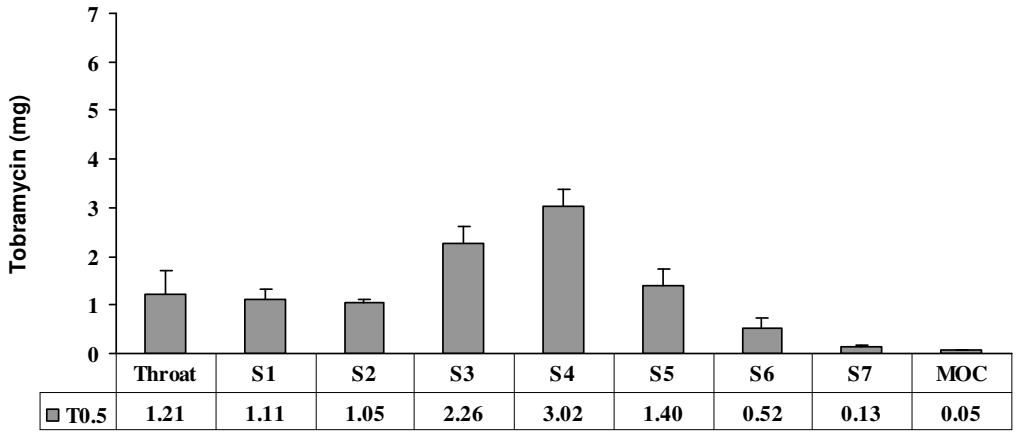

	Throat	S1	S2	S3	S4	S5	S6	S7	MOC
T0.5	1.21	1.11	1.05	2.26	3.02	1.40	0.52	0.13	0.05

Figure 34: Aerodynamic assessment by NGI of tobramycin 0.5 (T0.5).

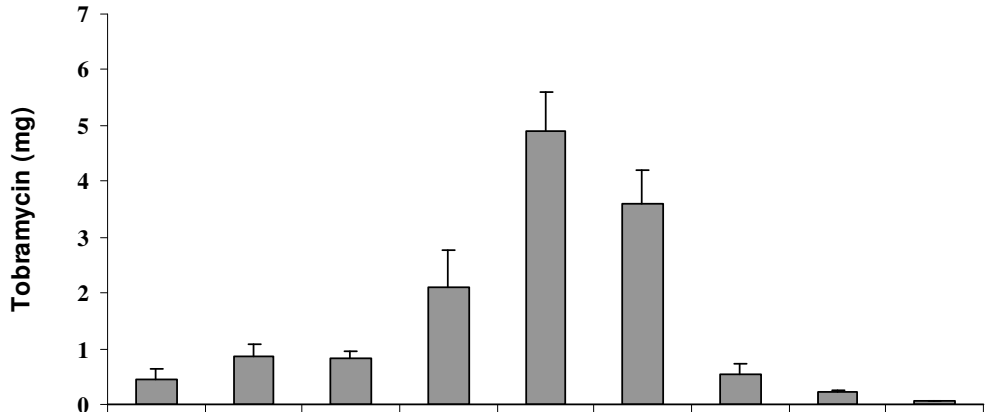

	Throat	S1	S2	S3	S4	S5	S6	S7	MOC
T1	0.44	0.85	0.82	2.10	4.89	3.59	0.53	0.22	0.06

Figure 35: Aerodynamic assessment by NGI of tobramycin 1 (T1).

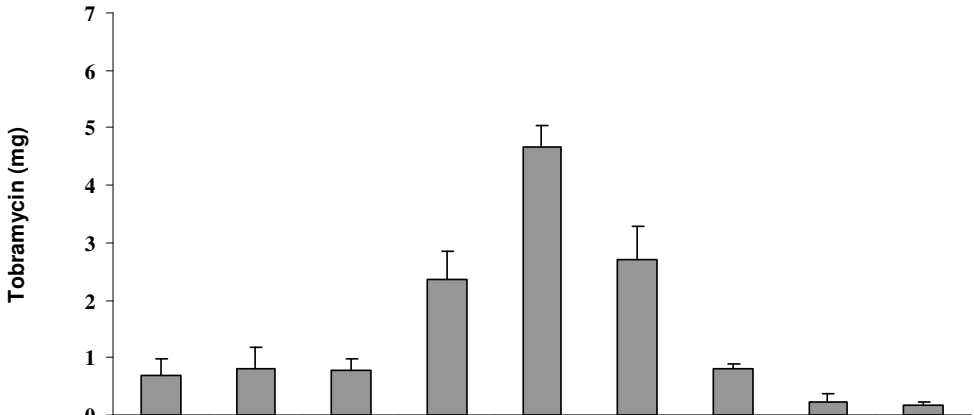

	Throat	S1	S2	S3	S4	S5	S6	S7	MOC
T1.5	0.70	0.81	0.77	2.36	4.67	2.71	0.80	0.23	0.18

Figure 36: Aerodynamic assessment by NGI of tobramycin 1.5 (T1.5).

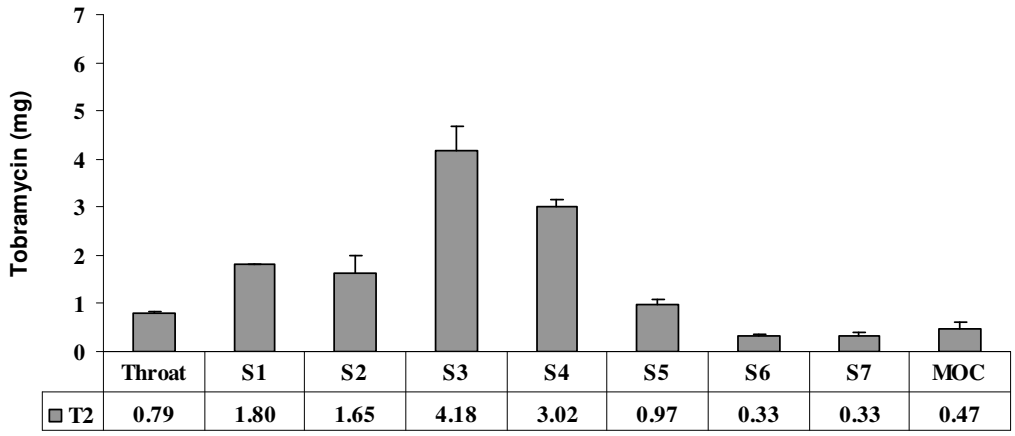

Figure 37: Aerodynamic assessment by NGI of tobramycin 2 (T2).

The addition of a small quantity of adjunct (0.25 % w/w) resulted in a significant decrease in capsule and device retention (8.65±0.45 mg), suggesting that the addition of adjunct aided powder flow by reducing interfacial interaction. Further addition of adjunct resulted in a small but significant decrease in device retention, considered that 2%w/w NaSt particles had 5.74 ± 0.62 mg deposited in the device and capsules. In comparison, analysis of stage-3 through to the micro-orifice collection plate (respirable size ranges) indicated that the addition of small quantities of NaSt between 0.25% w/w and 1% w/w resulted in high drug powder deposition. Furthermore, higher concentrations of sodium stearate between 1.5% w/w and 2% w/w resulted in a decrease of deposition on stages 4-6. The values of FPF were in good correlation with these findings, since FPF increased from 27.1 ± 1.9% with no adjunct, to a maximum of 84.3 ± 2.0% at 1% w/w adjunct, followed by a decrease to 66.4 ± 0.9% at 2% w/w when 2% w/w adjunct was added.

Table VIII: Deposition parameter (n=3; Mean ± standard deviation) of the different formulation measured by NGI

#	Metered Dose (mg)	Delivered Dose (mg)	FPD (mg)	FPF (%)	MMAD (µm)
T_0	18.67±0.95	5.69±1.01	1.55±0.39	27.18±1.9	7.49±1.19
$T_{0.25}$	19.39±1.31	10.74±1.25	3.52±0.69	32.80±1.49	7.63±1.02
$T_{0.5}$	18.52±0.19	10.74±0.97	7.32±0.39	68.17±1.65	2.79±0.10
T_1	18.99±0.19	13.52±1.37	11.41±1.64	84.35±2.0	2.29±0.14
$T_{1.5}$	19.18±0.41	13.25±1.00	10.77±0.57	81.26±1.70	2.17±0.25
T_2	19.28±0.33	13.54±0.59	9.00±0.45	66.45±0.9	2.95±0.14

The drug release/diffusion profiles of tobramycin microparticles containing different concentrations of sodium stearate were presented as percentages of transported drug plotted as function of time (Figure 38). The data was analyzed using the Weibull distribution equation and the relationship between sodium stearate concentration and time for 63.2% of tobramycin to be dissolved was analysed. The time for 63.2% of drug transported followed a parabolic profile with an increase observed with respect to sodium stearate concentration until 1%w/w. Further increase from 1% w/w to 2% w/w resulted in an increase in transport rate and thus a decrease of the time parameter.

Table IX: t63.2% values calculated from Weibull function.

#	t63.2%
T0	11.605±1.015
T0.25	12.839±1.328
T0.5	15.35±1.4
T1	23.757±2.541
T1.5	21.031±0.978
T2	16.24±0.83

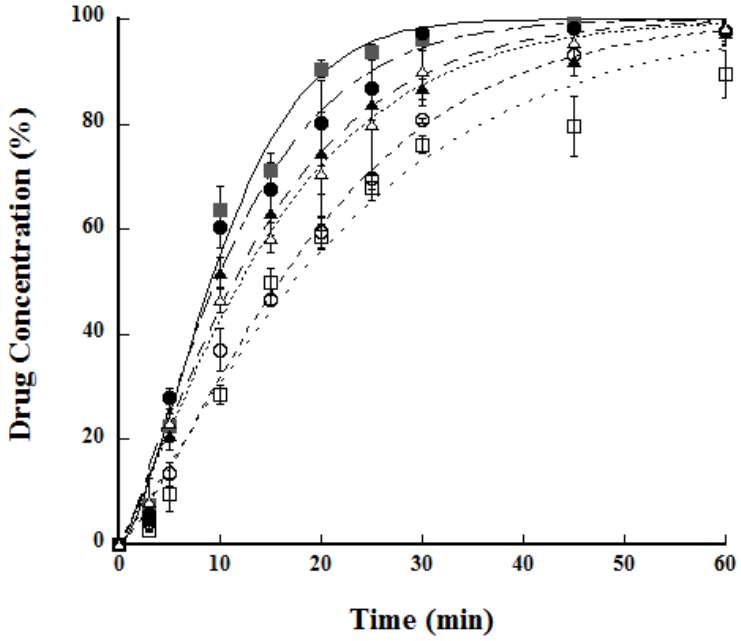

Figure 38: ***In vitro*** **transport profile of tobramycin from micro-particles containing different concentrations of sodium stearate fitted with Weibull distribution equation. (n=6; Mean and standard deviation). (T0, T0.25, T0.5, T1, T1.5, T2)**

To the author's knowledge, there have been limited studies into the relative toxicity of hydrophobic adjuncts delivered to the respiratory tract. Although more soluble than the acidic form (stearic acid), sodium stearate has relatively low aqueous solubility and thus potential toxicity during residence in the lung. Subsequently, the A549 lung epithelial cell viability after exposure to varied concentrations of different formulations of tobramycin-sodium stearate and of the stearate alone was investigated (Figure 39). In general, analysis of the data indicated that there was no significant relationship between either sodium stearate or total microparticles concentration and cell viability. Minimum cell viability was exhibited at 70% by the formulation

containing 0.5% of sodium stearate, a value non-significantly different from the one of pure tobramycin viability.

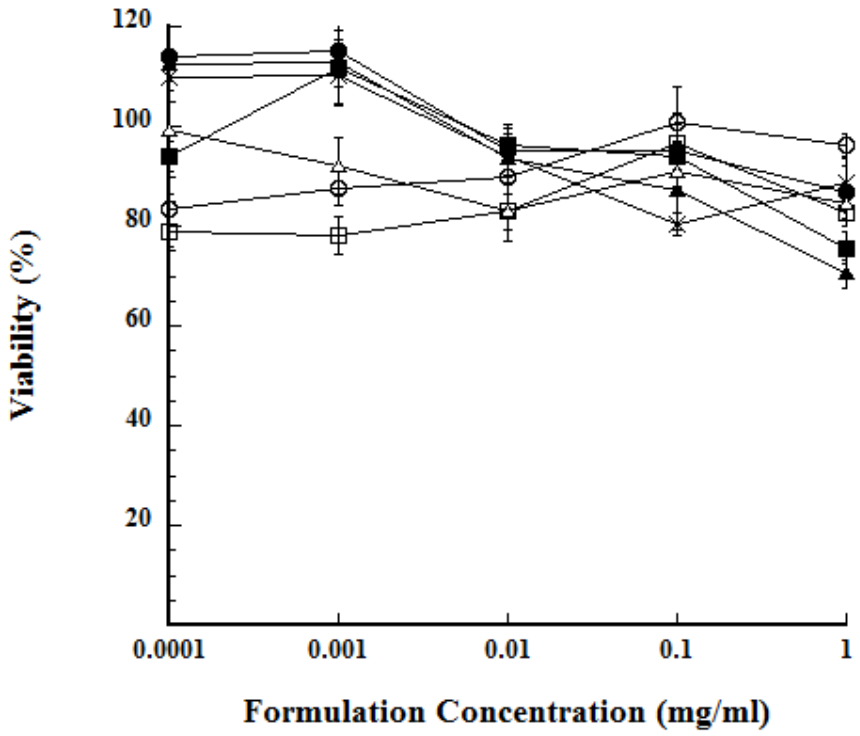

Figure 39: A549 epithelial cell viability measured by MTT cytotoxicity assay after 24 h exposure to different concentrations of formulation (n=5; Mean ± standard deviation). (x NaSt, ■ T0, ● T0.25, ▲ T0.5, □ T1, ○ T1.5, △ T2)

Furthermore, the inhibitory cell concentration (IC) indicated all samples were viable with no $IC_{50\%}$ value. Consequently, it may be concluded that tobramycin-sodium stearate powders were not toxic under the conditions or timescale studied.

Moreover, in Table X are reported the pH values for the tobramycin raw material and for the spray-dried formulation in DMEM. The tobramycin base had a basic pH and the sodium stearate does not affect the pH values of the formulations.

Table X: Values of pH for the tobramycin formulations in DMEM at conc. 1mg/ml.

pH values	*Conc. 1mg/ml DMEM*
7.40	DMEM alone
8.60	Tr.m.
8.60	T0
8.60	T0.25
8.60	T0.5
8.60	T1
8.60	T1.5
8.60	T2
8.40	NaSte

The EDS analysis was conducted in order to try to identify any differences between the particles surface composition. In particular we looking for the presence of sodium (Na) on the surface of the particle because this element is characteristic only of the adjunct and not of the tobramycin chemical structure.

The EDS analysis suggested a distribution of lipophilic adjunct on the surface of the microparticles. In general a linear relationship between adjunct concentration and sodium count was observed (R^2= 0.97) up to a concentration of 1%. Interestingly, after this point the count of sodium on the surface of the microparticles analysed significantly decreased. In particular the sodium counts increased from 7.24 ± 0.45 to 33.47 ± 1.97. The value of 7.24 obtained for pure tobramycin is the same of the blank constituted by the carbon tab coated with platinum used for mounting the sample. An increase in sodium stearate concentration over 1% resulted in a decrease in sodium counts to 13.64 ± 0.55 for the particles containing 1.5% w/w of adjunct and 11.54 ± 0.27 for particles at 2% w/w.

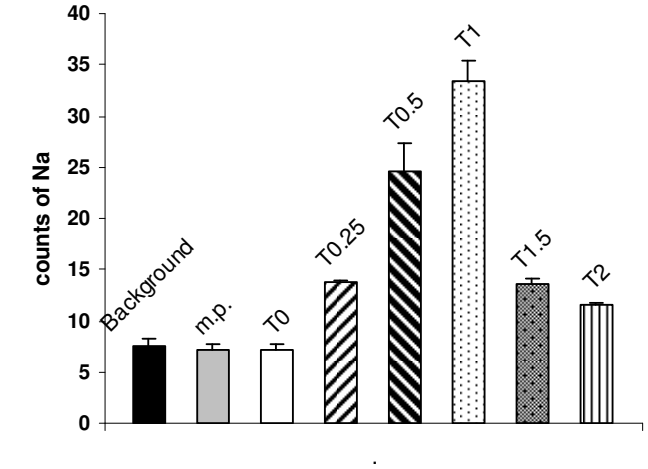

(a)

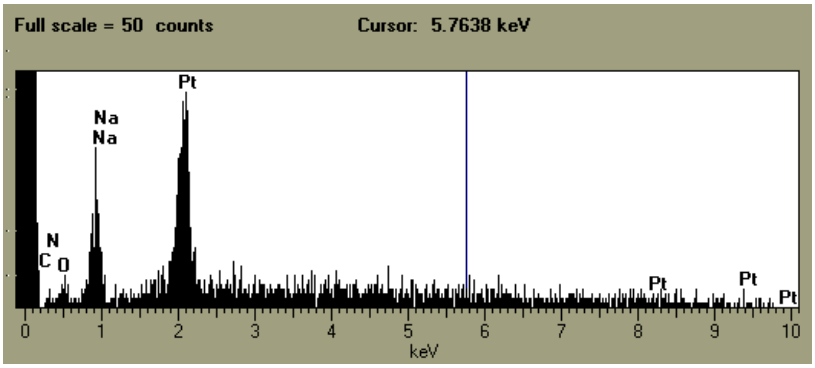

(b)

Figure 40: Sodium counts (a) and EDS spectrum (b).

Previous studies have shown that addition of small amount of various compounds such as trileucine, chitosan, leucine, phenylalanine, or cyclodextrin can improve particles dispersibility.[126-127-128-29]. Cholesterol and phospholipids (>5% w/w) have also been employed in tobramycin particle formations by spray drying [75]. The relationship between sodium stearate concentration, aerosolization and deposition performance was not linear over the adjunct concentration range studied. A parabolic dependence was observed with a peak around the 1% content of sodium stearate. In order to further understand the effect of this adjunct concentration on aerosol

performance, the relationships between fine particle fraction, particle surface sodium count, release rate and sodium stearate concentration were collectively analysed and shown in Figure 41A, 41B and 41C, respectively. Figures 41A and 41B, shown a positive relationship between the presence of adjunct on the particle surface, as measured with sodium count, and aerosol performance.

During the spray drying process, the solutes in the sprayed droplets will have a radial distribution as the droplet evaporates. In a binary system, the final distribution of each component in the dry solid will be due to the molecular structure of the individual components and their relative molecular mass. The molecular mass of tobramycin and sodium stearate is 467.5 g/mol and 306.46 g/mol, respectively, suggesting that they would have similar transport rate in a rapidly drying droplet and thus be evenly distributed throughout the solid. However, sodium stearate has a much lower aqueous solubility than tobramycin [130-131] and is a surface-active agent. It may be assumed therefore, that the hydrophobic adjunct would accumulate at the droplet liquid-air interface during the drying process and deposit on the dried particles surface. This surface accumulation would result in the increase in relative sodium counts and large reduction in interfacial tension between the contiguous microparticles. This would results in a significant improvement of the aerosolization efficiency . For sodium stearate concentrations over 1% w/w, a significant decrease in sodium counts (Figure 41B) was observed, suggesting a different mechanism of molecular re-distribution of the components during the drying process and internalisation of the lipophilic adjunct in the microparticles. Furthermore, comparing FPF and sodium counts for the 1.5% w/w adjunct microparticles, it is evident that the decrease in sodium count number was not immediately reflected by a lower respiratory performance. It is possible that the relative

decrease in particle size between 1% w/w and 1.5% w/w microparticles distribution, could have affected this results.

The *in vitro* drug transport (Figure 41C), the sodium counts (Figure 41B) and the *in vitro* deposition (Figure 41A) correlated with the NaSt content following a parabolic behaviour with the maximum values around 1% w/w of adjunct. No relationship was found between release rate and size distribution, suggesting that the decrease in dissolution/transport rate of powders containing sodium stearate between 0% w/w and 1% w/w was due to the increased concentration of the hydrophobic adjunct on the particle surface, affecting wetting and dissolution. A further increase from 1% w/w to 2% w/w of NaSt resulted in a faster dissolution/transport rate suggesting, as confirmed with EDS analysis, the internalisation of the adjunct in the solid particulate.

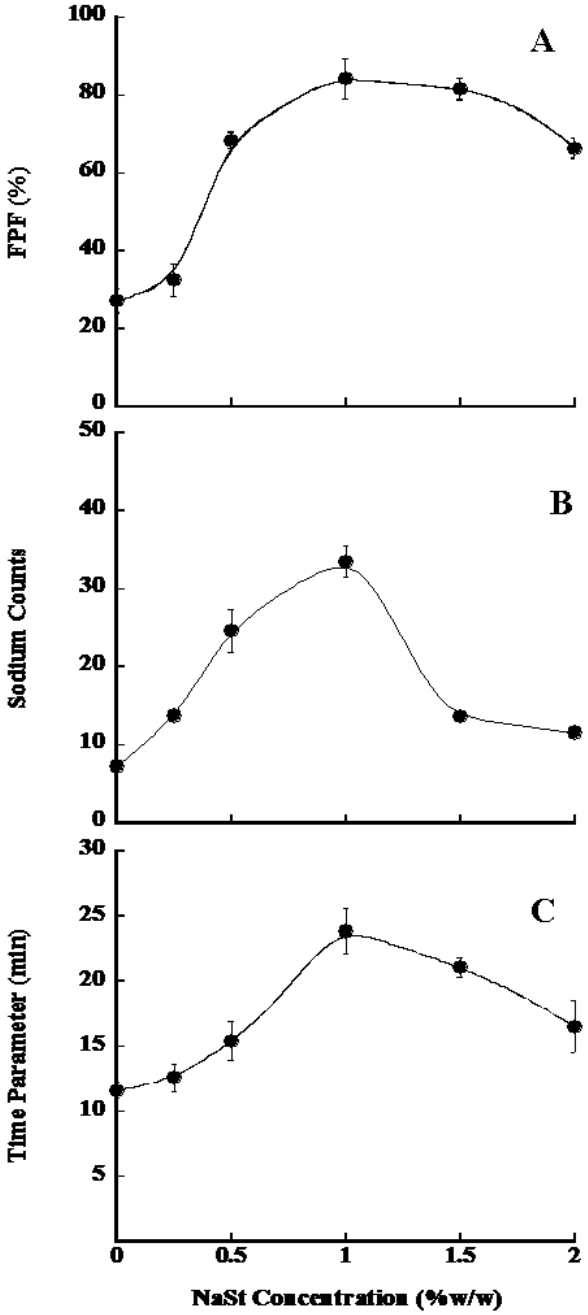

Figure 41: Relationship between initial sodium stearate concentration and (A) fine particle fraction, (B) sodium counts and (C) time parameter, time necessary for the 63.2% of drug dissolved.

The internalisation of the adjunct may be explained considering overall molecular structure of the components at different concentrations. The critical micelle concentration (CMC) for sodium stearate in aqueous solution has been reported between 4.0 x 10^{-4} and 5.6 x10^{-4} m, based on experimental and theoretical calculations [132-133-134]. Considering the molecular mass of 306.46 g/mol, the relative molar concentrations of sodium stearate in the spray dry solutions would be 3.3 x 10^{-4} m at a concentration of 0.01% w/v and 6.5 x 10^{-4} m at 0.02% w/v. These values correspond to final amount of 1% and 2% w/w sodium stearate within the microparticle formulation, which can be found at either side of the previously reported CMC range. Furthermore, the micelle structure in aqueous solution has been reported as containing 78 monomer groups [133]. Assuming, the CMC and micelle structure in this complex mixture would be in a similar range to that of a pure aqueous solution, the micelle mass would be approximately 23,904 g/mol compared with 306 g/mol for the individual stearate molecule. Essentially, in a micellular form the sodium stearate component would have more than fifty times the molecular mass of tobramycin and would have reduced molecular mobility during the drying stage. However, this system is dominated by the relative surface activities and ionic nature of the materials used. Sodium stearate is a surface-active agent and, at low concentrations (less than 1%), the hydrophobic chains will preferentially distribute at the air/water inter-phase, pointing away from the microparticle core. At high concentrations (more than 1%) a micellular system is formed, where the hydrophobic tails are shielded, and the ionic (and thus hydrophilic) nature of the sodium stearate micelles will result in higher internalization, promoting tobramycin partition at the inter-phase.

A schematic of this theoretical re-distribution of sodium stearate in the micro-droplets during the spray drying process is shown in Figure 42. This theoretical explanation took into account that during the evaporation process the concentration of sodium stearate will increase, suggesting that CMC will be reached during drying for all solutions. However, the drying process is very rapid and self-assembly of free sodium stearate will be hinderd by the concomitant presence of other molecules in the droplet and the rapid nature of this process. Indeed, spray drying is used to circumvent the self-assembling of molecules in producing amorphous over crystalline forms.

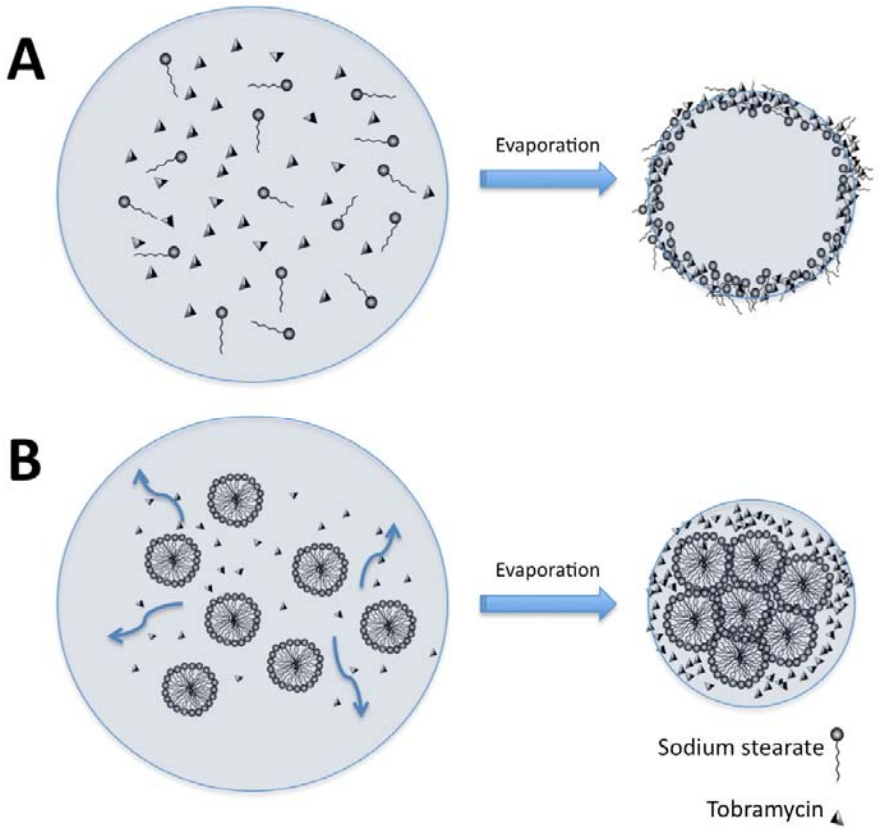

Figure 42: Schematic of the proposed particle formation process for binary mixtures of tobramycin and sodium stearate during spray drying where (A) low sodium stearate concentrations and (B) high sodium stearate concentrations.

Figure 43 presents the secondary ion image of a microparticle surface. The particle had an almost smooth but non-porous surface. Half of the microparticle was faced towards ion milling in a FIB machine. Just after peeling off a 2 layers, at a depth of c.ca 600nm from the surface of the microparticles, some holes started to appear on the surface. This happened for all the microparticles analysed (only one for each batch).

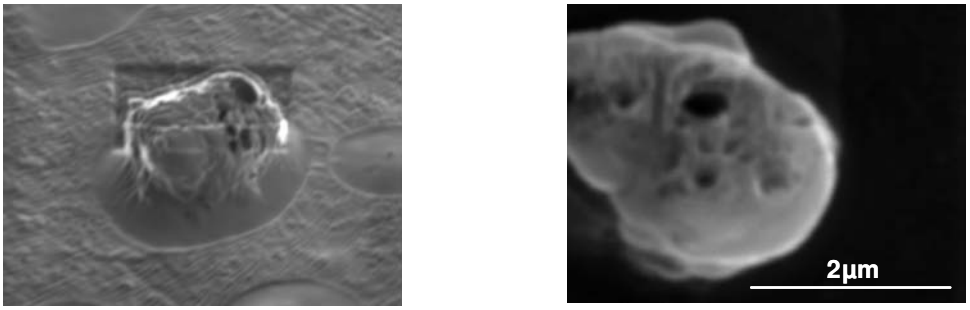

Figure 43: FIB image of a microparticle of T1 formulation.

This analysis gave us some indication about the internal structure of the microparticles that is important for density and respirability values.

After this we tried to execute a EDS analysis on the inner structure in order to evaluate the amount of sodium into the microparticles. We got some information but these are not significant because obtained on one particle for each batch. Moreover, the depletion of material of the particles could fall back on the internal surface now exposed and affect the elemental analysis. Further analysis, in order to better understand the inner particles composition, was conducted with the Tof-SIMS.

Three tobramycin/sodium stearate particles for each sodium stearate concentration were sectioned with FIB-SEM (Focused Ion-Beam Scanning Electron Microscopy) to expose their internal structure.

With a spatial resolution of 0.2µm, it was believed that ToF-SIMS imaging could allow the observation of sodium stearate distribution on the outer and inner surface of cut

tobramycin particles. However, given the particle size was in the vicinity of 5-10μm, the spatial resolution proved insufficient for the production of a clear image of the particle. Although some results were obtained, ultimately, the results could not show conclusively whether variation in sodium stearate concentration had any influence in the nature of its distribution across tobramycin particles.

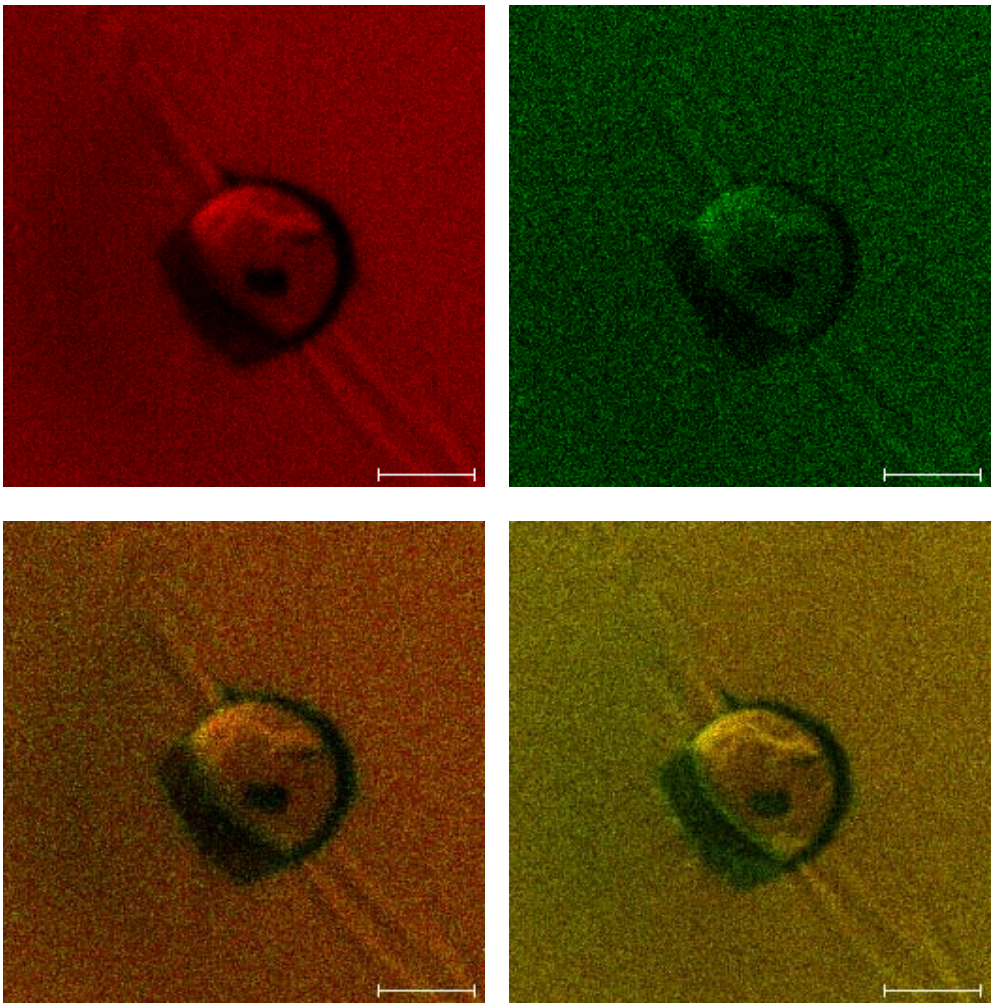

Figure 44: Tof-SIMS image of a microparticle of T1 formulation.

The true, bulk and tapped density was measured for all the tobramycin-sodium stearate powders. Moreover, for each batch the Carr's Index and the Hausner Ratio were calculated. Both parameter useful in the evaluation of the flowability of powders solids.

The tapped density of the spray-dried powders was similar for all powders; they ranged between 0.23 and 0.40. The highest values was obtained for tobramycin powder with 2%w/w of sodium stearate. Recently, study presented by Bosquillon et al shown that lower power tapped density is associated with better aerosolisation properties.[136]

Table XI: True and Tapped Density of Tobramycin and sodium stearate powders.

Batch	True Density (g/ml)	Bulk Density (g/ml)	Tapped density (1250 taps) (g/ml)	Carr's Index (%)	Flowability[135]*	Hausner Ratio
Tob r.m.	-	0.22	0.31	29.03	Poor, cohesive	1.40
T0	1.66 ± 0.08	0.25	0.40	37.5	Very poor	1.60
T0.25	1.52 ± 0.01	0.15	0.23	34.78	Very poor	1.53
T0.5	1.66 ± 0.09	0.17	0.26	34.61	Very poor	1.53
T1	1.37 ± 0.04	0.16	0.23	30.43	Poor, cohesive	1.43
T1.5	1.35 ± 0.09	0.16	0.25	36.00	Very poor	1.56
T2	1.58 ± 0.04	0.14	0.23	39.13	Very poor	1.64

The Carr's Index, as previously mentioned, gives an indication of powder flow properties; the values for the spray-dried powders are comprised between 30-39% indicate cohesive powder characteristic. As shown in Table XI for all powders, both parameters indicated the very poor flowability properties of the micronized powders.

The surface energy components and contact angle values with three liquids by Contact Angle method are presented in Table XII. For tobramycin and sodium stearate up to 1%w/w, the (LW) dispersive components dominate the AB interactions energies. The highest dispersive values were measured for Tobramycin raw material and there is a reduction in the values of LW values with the increase in NaSt content in formulations, even if there is no significant differences between the values.

Table XII: Surface Free Energy Components Obtained via CA Measurements

	Components of surface free energy (mJ m^{-2})					Contact angle (°) with		
	γ_S^{LW}	γ_L^+	γ_L^-	γ_S^{AB}	γ_S	Ethilene Glicole	Diiodomethane	Glycerol
Trm	**39.62±0.53**	1.45±2.28	36.29±31.25	4.35±2.02	43.98±1.70	.23±1.82	51.77±2.71	57.83±3.48
T0	**38.48±0.54**	2.26±2.32	155.25±5.45	37.41±4.87	75.89±4.76	46.90±0.58	42.19±0.64	56.90±0.31
T0.25l	**36.14±0.75**	1.57±2.43	4.20±2.43	4.31±0.33	40.45±0.58	40.03±0.36	46.93±1.13	63.50±0.94
T0.5	**36.13±0.46**	1.84±4.61	3.84±4.61	4.33±2.09	40.46±2.27	36.63±0.87	46.64±0.48	58.64±1.04
T1	**36.83±0.20**	7.16±1.32	21.98±21.98	24.85±8.87	61.68±9.04	31.27±0.36	44.39±0.52	62.99±0.58
T1.5	**35.02±1.97**	9.07±1.65	38.26±10.90	37.16±8.19	72.17±7.55	33.82±0.67	48.62±2.05	65.85±0.42
T2	**33.70±0.09**	14.29±2.67	75.78±29.04	65.57±18.88	99.27±18.82	27.99±0.28	51.02±0.09	65.86±0.83
NaSt	**27.44±0.78**	6.33±1.34	66.58±8.89	41.01±9.89	68.46±8.76	65.06±2.27	62.36±0.97	87.20±0.23

Table XIII: Surface Free Energy Components Obtained via IGC Measurements

	Disp. Surf. En.(mJ/m2):	Corr. Coefficient:	Temp. (K)	Flow (ccm/min)	Mass (g)
Tr.m.	**48.64±0.41**	0.9978±0.0002	308.5	10	0.929
T0	**48.67±0.16**	0.9988±0.0004	303.5	10	0.403
T0.25	**43.01±2.54**	0.9988±0.0011	303.15	10	0.444
T0.5	**40.30±2.49**	0.9989±0.0005	303.15	10	0.479
T1	**39.05±0.56**	0.9991±0.0001	308.15	10	0.908
T1.5	**40.26±0.13**	0.9992±0.0001	303.15	10	0.479
T2	**40.65±0.59**	0.9993±0.0001	303.15	10	0.727

From the dynamic vapour sorption analysis we can see that the raw material is very hygroscopic. The biggest step was between 0 and 10%RH when it went from dry mass to ~4%. The step was even greater when the RH was stepped down. The maximum weight gain at 90%RH was 10% of the dry weight.

Another point to note is that the adsorption and desorption occurred at different rates. In general, the desorption was always much slower than the adsorption across the different

RHs, except between 0 and 10%RH. Tobramycin grabs water molecules quickly with the increase of the RH, but then it "holds" the water molecules so that they come off slower as the RH was decreased.

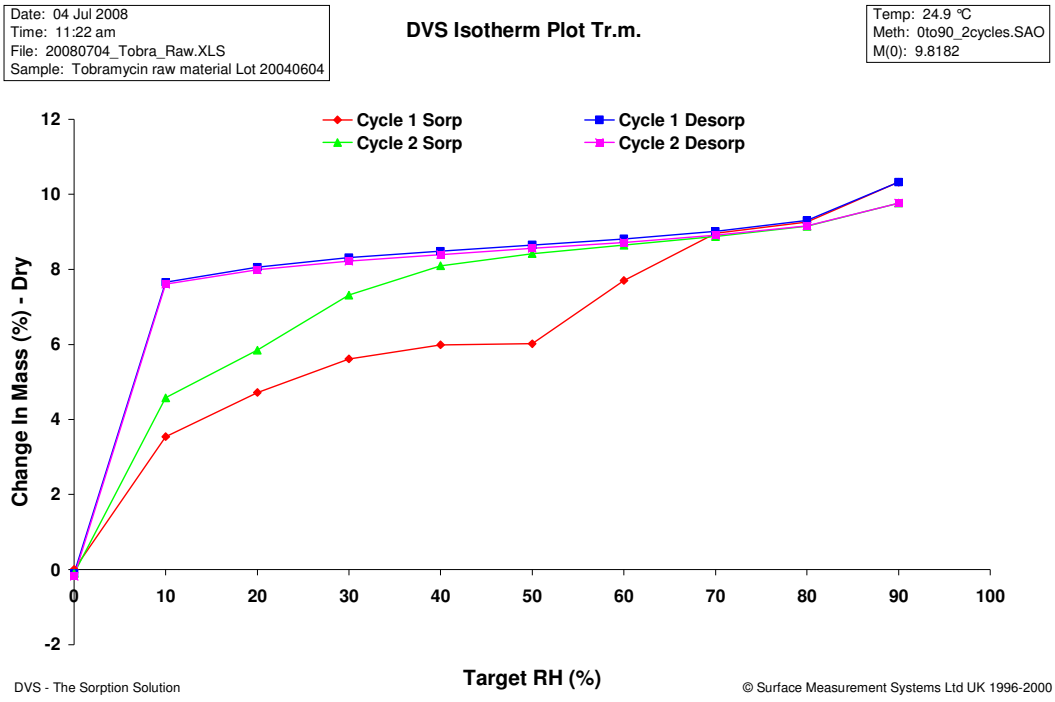

Figure 45: DVS isotherm plot of Tobramycin raw material

The comparison between the DVS isotherm plot confirm the hygroscopic behaviour of the tobramycin powders and SD powders. The highest change in mass was obtained for the T0 formulation, in particular at lowest RH% values. The other formulation analyzed shown the same behaviour of tobramycin raw material. Overall the behaviour is similar for the SD microparticles. From the shape of the graph it also appears they have amorphous contents. However, the moisture uptake at 90% RH decreases with increasing NaSt content.

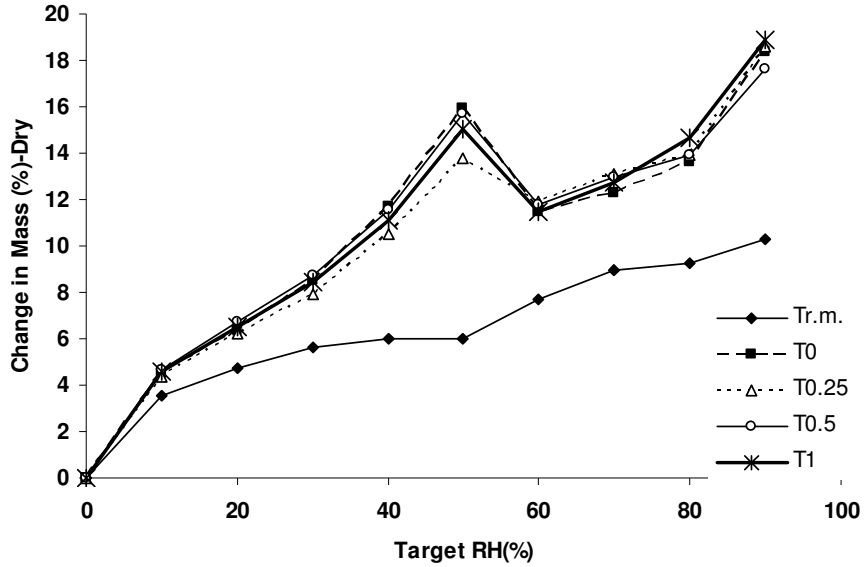

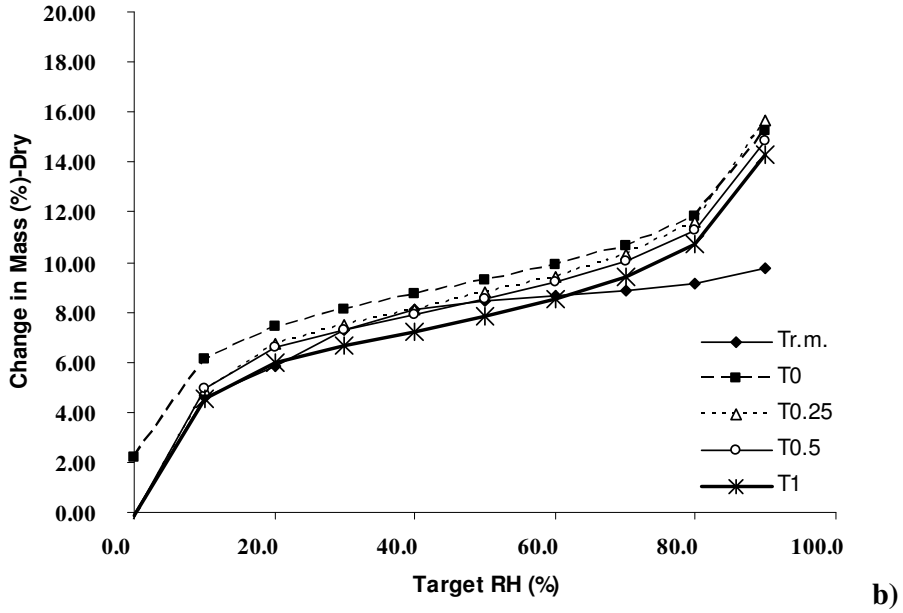

b)

Figure 46: Cycle 1 a) and Cycle 2 b) sorption for Tobramycin raw material, T0, T0.25, T0.5, T1

IV.2 Conclusion

Tobramycin was spray dried in presence of varying amount of sodium stearate used as adjunct to control the aerosolization efficiency in dry powder inhaler. The aerosol performance of the spray-dried powders was related to the percentage of adjunct in the microparticles in the range between 0.25 to 2.0 %w/w. The molecular form of stearate in the spray drying solution and its redistribution during the microparticle growing is considered determinant for the presence of sodium stearate on the surface of the microparticles. In general, particles containing a final adjunct concentration of 1% sodium stearate (w/w) provided the greatest respiration performance (>80% FPF) since the maximum level of sodium stearate was concentrated on the surface of microparticles. In comparison to the literature described inhalation powders, the amount of lipophilic adjunct used for improving the tobramycin powder aerosolization was maintained very low. Preliminary cell toxicity studies have showed that the use of this amount of hydrophilic adjunct has no effect on cell viability over a 24 h period.

IV.3 Part 3 FORMULATION AND CHARACTERIZATION OF SPRAY-DRIED TOBRAMYCIN AND FATTY ACIDS FOR INHALATION.

Fatty acids are carboxylic acids derived from or contained in lipids. They show the general formula: R-COOH, where R is usually a linear carbon chain with a certain number of carbons. Natural fatty acids usually contain 4 up to 28 carbons (most of the fatty acids in complex lipids contain 14 up to 22 carbons, though). The principal fields of application of fatty acids are: biological fuels, components of more complex lipids.

There are multiple classifications of fatty acids. The most widely used, from the biochemical point of view are chemical, due to the presence of double bonds in the carbon chain:

- saturated, with no double bonds;

- unsaturated, with one or more double bonds.

Table XIV: Properties of the fatty acids used in the study (Pharmaceutical Excipients 5)

Systematic name	Trivial name	Shorthand designation	Molecular wt.	Melting point (°C)	Solubility Ethanol 95% (g l^{-1} 20°C)	Solubility Water (g l^{-1} 20°C)
Dodecanoic	lauric	12:0	200.3	43.2-43.8	912	0.055
Tetradecanoic	myristic	14:0	228.4	54.5	189	0.02
Hexadecanoid	palmitic	16:0	256.4	63-64	49.3	0.007
Octadecanoic	stearic	18:0	284.4	≥54	11.3	0.003
Eicosanoic	arachidic	20:0	312.5	75.3	-	-
Docosanoic	behenic	22:0	340.5	79.9	-	-

In Table XIV are show the names (systematic and trivial), the shorthand designation and some features of the fatty acids used for this study.

- **Lauric acid** (12:0) is one of the three most widely distributed saturated fatty acids found in nature (14:0, 16:0, and 18:0). The recent uses of lauric acid are in the manufacture of flavourings, cocoa butter, margarine, alkyd resins, soaps, shampoos and other surface active agents, including special lubricants. Lauric acid as monoglyceride is known to the pharmaceutical industry for its good antimicrobial properties.
- **Myristic acid** (14:0) is found in milk fats (8-12%) and in the head oil of the sperm whale (15%).
- **Palmitic acid** (16:0) is the most common saturated fatty acids in plant and animal lipids.
- **Stearic acid** (18:0) is the highest molecular weight saturated fatty acid occurring abundantly in fats and oils. It is the principal constituent of hydrogenated fats and oils (about 90%).
- **Arachidic acid** (20:0) is found in the depot fat of some animals and in milk fats.
- **Behenic acid** (22:0) this fatty chain does not occur in the principal oils. Large amounts are found in hydrogenated animal and vegetal oils (8-57%). [137-138-139].

All the batches of tobramycin microparticles were produced by spray-drying of tobramycin and fatty acids with different chain length (ratio 99:1). The hydroalcoholic solutions (70:30) were spray-dried on a Mini Spray Dryer Buchi (Buchi, Switzerland) using a inlet temperature of 125°C, feed rate of 3.5 ml min^{-1}, atomization flow 100% and nozzle air flow of 600 ml min^{-1}.

As shown in the Table XV the yield of the processes was in all the cases higher than 55%. The chain length, the only parameter changed, seems not to be correlated with the yield of the process. The powder of tobramycin-palmitic acid showed the lowest yield value. With exception of the palmitic acid, the yield of the powder sinks with incresing chain length of the acid.

Table XV: Yield of SD process, water content, TGA analysis and dimensional analysis of the raw material and SD microparticles.

Fatty Acid (FA)	Yield %	TGA (%)	Water (%)	$d_{v0.1}$	$d_{v0.5}$	$d_{v0.9}$
Tobramycin r.m.		**4.55**	4.55 ± 0.17	0.89±0.02	4.01±0.12	16.02±0.51
Lauric Acid (C12)	68.3	**9.33**	7.24 ± 0.14	0.88 ± 0.00	3.03 ± 0.12	7.20 ± 0.92
Myristic Acid (C14)	66.1	**9.35**	6.54 ± 0.08	0.89 ± 0.01	3.21 ± 0.23	7.02 ± 0.90
Palmitic Acid (C16)	55.0	**11.33**	9.59 ± 0.14	0.93 ± 0.01	3.51 ± 0.25	7.79 ± 0.73
Stearic Acid (C18)	64.8	**10.93**	6.90 ± 0.07	0.98 ± 0.00	3.65 ± 0.19	8.02 ± 0.14
Arachidic Acid(C20)	60.4	**9.73**	9.12 ± 0.16	0.85± 0.00	2.82 ± 0.14	6.90 ± 0.39
Behenic Acid (C22)	57.1	**9.44**	7.84 ± 0.16	0.86 ± 0.01	2.58 ± 0.07	5.87 ± 0.31
Oleic Acid (C18:1)	66.9	**9.27**	-	0.87 ± 0.01	2.56 ± 0.03	5.99 ± 0.01

The particle size analysis was performed for each batch in triplicate and the analysis was repeated nine times. In Table XV you can see the difference between the raw material, non-micronised, and powders produced by spray-drying process. All powders had a d_v 0.5 under 5μm, optimal for lung deposition. The spray-dried powders display a suitable particle size distribution for deposition within the lower airways, because their medium volume diameters are in all cases much lower than 5 μm. These

powders can show useful aerodynamic diameter values, which promise to reach the respiratory area since particles with aerodynamic diameters smaller than 5 µm are respirable and useful for a pulmonary administration. It can also possible to observe that the chain length seems to influence the d_v 50 of the microparticles.

The scanning electron micrographs were effected in order to obtain a visual assessment of the particle size analysis and to investigate the shape and the morphology of the microparticles. The size of the microparticles reflect the data obtained from dimensional analysis, as shown in the micrographs below. They all are micronized and smaller than 4 µm. The particles produced tend to have a spherical shape and are partially corrugated. We can not observe morphological differences attributable to the addition of fatty acids.

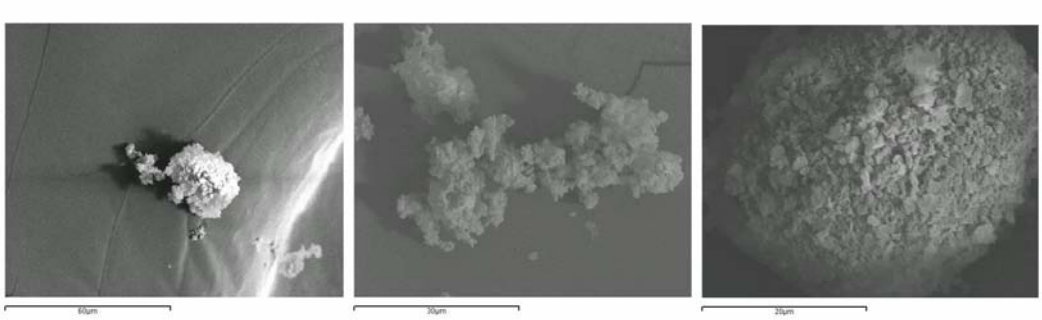

Figure 47: Tobramycin – Raw material at different magnifications

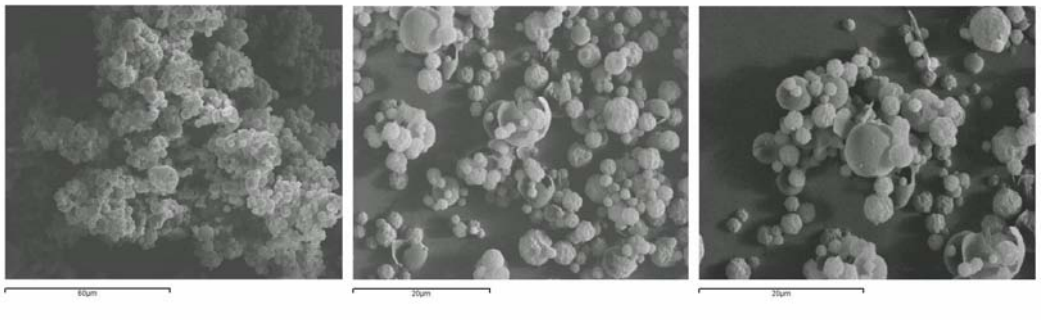

Figure 48: Tobramycin - Lauric acid at different magnifications

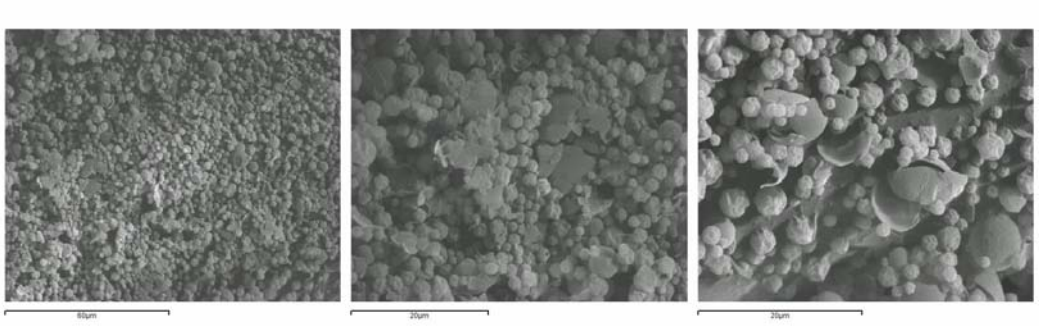

Figure 49: Tobramycin - Myristic acid at different magnifications

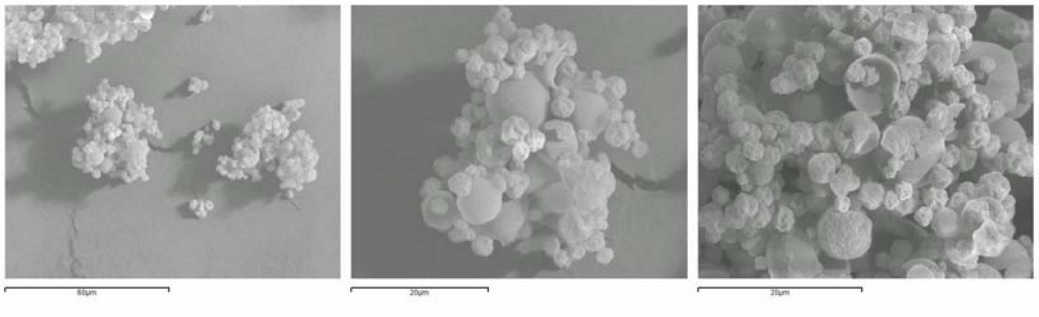

Figure 50: Tobramycin - Palmitic acid

The water content, measured by Karl Fisher titration, is shown in Table XV. Spray-dried powders micronized have a higher water content than the raw material not micronised.

The fatty acids length seems does not influence the quantity of water into the formulations. This data was confirmed also with the TGA. To some extent this loss can be attributed their water content, although at temperatures above 100°C other phenomena could occur. The heating method chosen was 25-110 C, 10K / min. In this case the loss on weight cannot be due totally at the water evaporation around 100°C because the melting point of the fatty acids is below this value. The loss on weight values are the sum of loss on water and acids melt.

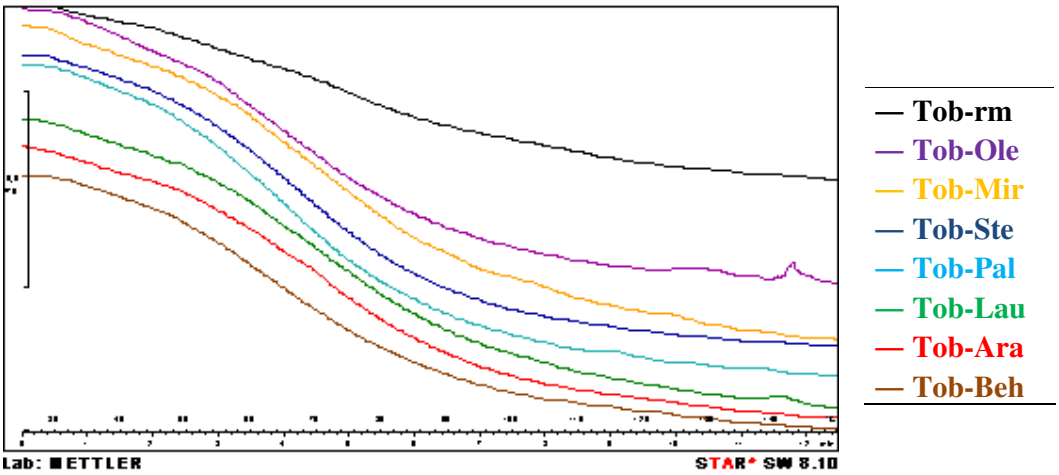

Figure 51: Termogravimetric thermograph of Tobramycin- FA powders.

The calorimetric analysis was effected on the raw material and micronized powders obtained after the process of spray drying.

From the thermograph for all the formulations it's easily seen that the own thermograph shows a board endothermic plateau at 80-100°C, which is characteristic of a water loss. It is possible also to see a board endothermic plateau, partially covered by the water loss, characteristic of the melting point of each fatty acid along with the absence of other termic phenomena, in particular it is evident the absence of the endothermic peak of fusion that characterizes the crystalline raw material (violet).

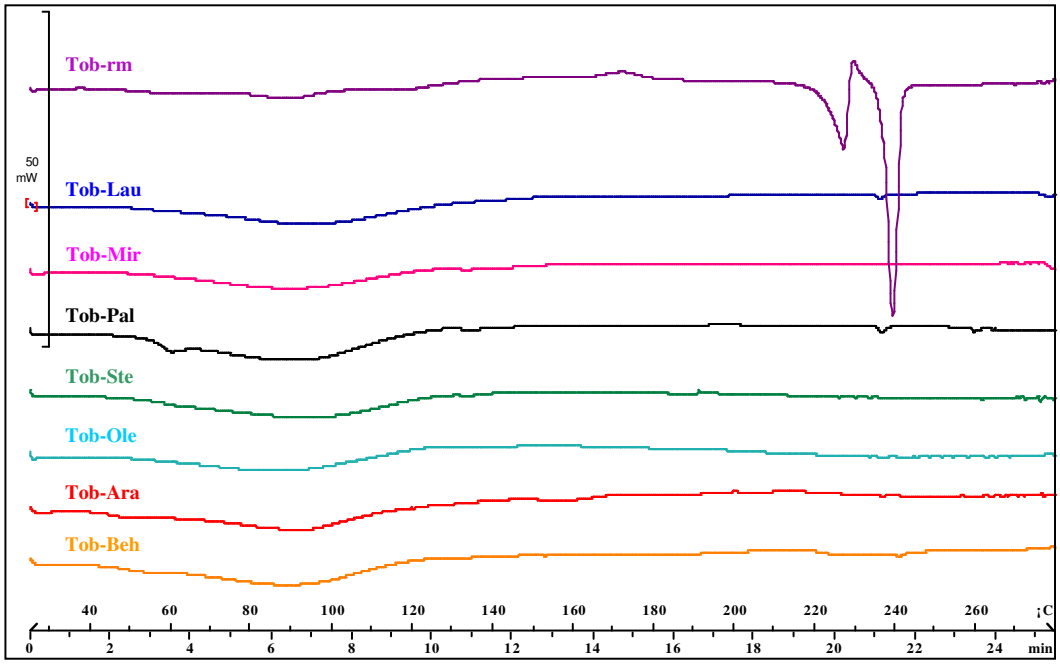

Figure 52: Thermograph of tobramycin-FA microparticles

The amorphous nature of spray-dried powders was further supported by X-ray . Figure 53 shows and compares the X-Ray trace obtained from tobramycin raw material and tobramycin-fatty acids powders. X-Ray powder diffraction analysis of the spray dried samples presented a broad diffuse peak indicative of an amorphous material. Such observations are consistent with the spray drying of many organic materials, specifically those which are composed of binary components[125]. In addition, they are in good agreement with the SEM images which showed particles with smooth spherical structure.

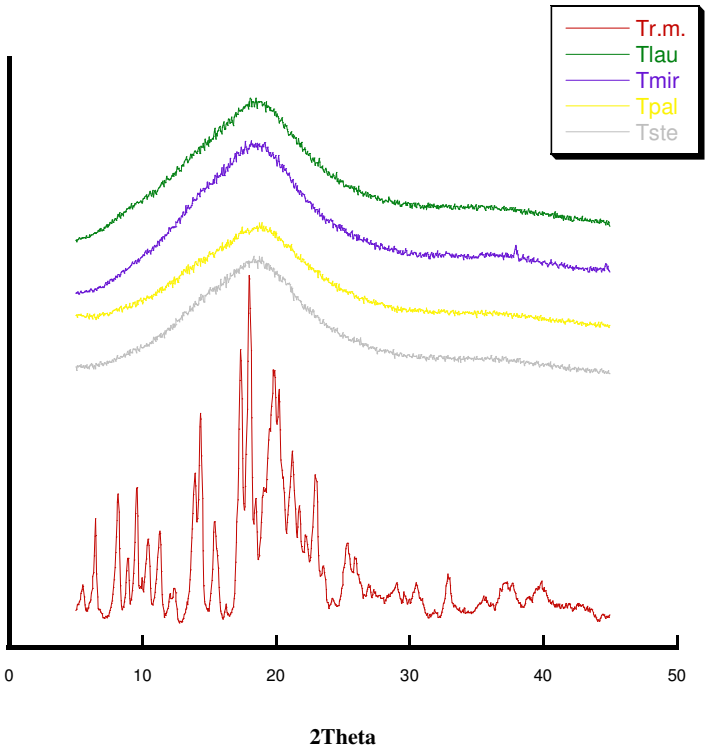

Figure 53: X-Ray powder diffraction patterns of tobramycin raw material and SD powders.

The true, bulk and tapped densities were measured for all the tobramycin-fatty acids powders. Moreover, for each batch the Carr's Index and the Hausner Ratio were calculated, both parameter useful for the evaluation of the flowbility of powder solids. The tapped density of the spray-dried powders was similar for all powders and they ranged between 0.23 and 0.40. The highest values were obtained for tobramycin powder with arachidic acid and behnic acid. Recent studies presented by Bosquillon et al showed that lower power tapped density was associated with better aerosolisation properties. [135].

Table XVI: True and Tapped Density of Tobramycin and fatty acid powders

Batch	True Density (g/ml)	Bulk Density (g/ml)	Tapped density (1250 taps) (g/ml)	Carr's Index (%)	Flowability*	Hausner Ratio
Tob raw material	-	0.22	0.31	29.03	Poor, cohesive	1.40
Tob-Lau	1.56 ± 0.01	0.16	0.23	30.43	Poor, cohesive	1.44
Tob-Mir	1.42 ± 0.01	0.16	0.25	36.00	Very poor	1.56
Tob-Pal	1.49 ± 0.03	0.14	0.23	39.13	Very poor	1.64
Tob-Ste	1.16 ± 0.02	0.15	0.23	34.78	Very poor	1.53
Tob-Ole	1.52 ± 0.01	0.22	0.32	31.25	Poor, cohesive	1.45
Tob-Ara	1.40 ± 0.01	0.25	0.40	37.5	Very poor	1.60
Tob-Beh	1.25 ± 0.11	0.26	0.38	31.57	Poor, cohesive	1.46

The Carr's Index, as previously mentioned, gives an indication of powder flow properties; the values for the spray-dried powders are comprised between 30-39% and indicate cohesive powder characteristic. As shown in Table XVI for all powders both these indexes indicated the very poor flowability properties of the micronized powders.

In Table XVII are reported values of aerodynamic parameters (USP 31), powder distribution in NGI stages and the MMAD values extrapolated from the undersized cumulative percentage versus the aerodynamic diameter of all tobramycin powders. The emitted dose (%) for each batch is higher than 70%; the formulations with the lowerst values were with arachidic and behnic acid (the only lower than 70%) , these formulations had the tendency to form agglomerates during the spray-drying and handling. Moreover, these two powders have worse flowability and confirm that powders with high tapped density show poor aerosolization efficiency. All the formulations shown an MMAD around 3 μm without significant differences. Interestedly, the FPF% values are all around 60% except for the powder with stearic

acid that show a fine particle fraction of 72.6%. This may be related with the properties of the adjunct and it is linked with the aerodynamic properties of the own salt.

Table XVII Deposition parameter (n=3; Mean ± standard deviation) of the different formulation measured by NGI:

Batch	Emitted Dose (mg)	Recovery (%)	MMAD (µm)	FPD <5µm (mg)	FPF <5µm (%)
Tlau	18.8 ± 0.3	94.5 ± 1.2	2.95±0.13	8.4 ± 0.5	60.8 ± 0.6
Tmyr	19.1 ± 0.3	94.5 ± 1.5	2.87±0.11	9.7 ± 0.4	63.5 ± 0.7
Tpal	19.3 ± 1.4	93.0 ± 0.4	3.40±0.25	7.9 ± 0.7	54.8 ± 2.9
Tste	18.7 ± 1.3	88.6 ± 2.3	2.97±0.08	8.4 ± 2.1	72.6 ± 0.92
Tara	14.3 ± 1.6*	94.6 ±2.3	3.04±0.03	9.5 ± 0.5	62.9 ± 5.7
Tbeh	13.2 ± 1.2*	96.5 ± 8.4	3.56±0.50	7.4 ± 0.4	57.3 ± 8.5

***Emitted dose only 65% of Label dose**

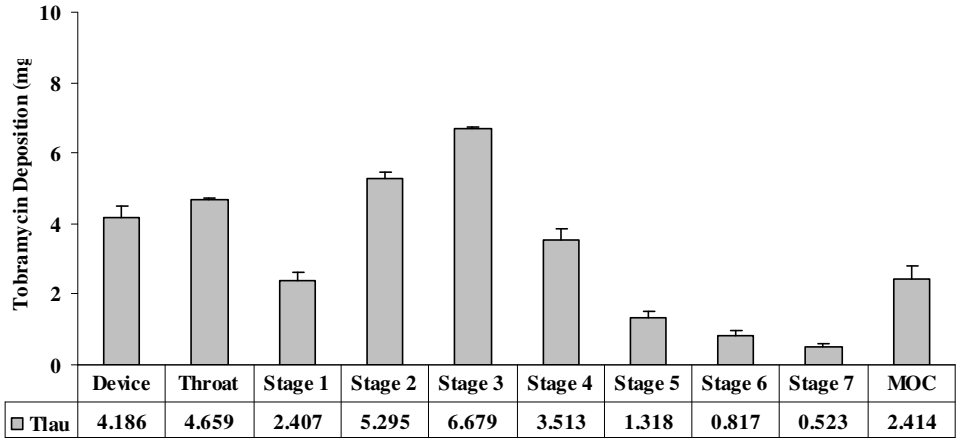

Figure 54: Aerodynamic assessment by NGI of Tobramycin-Lauric acid powder.

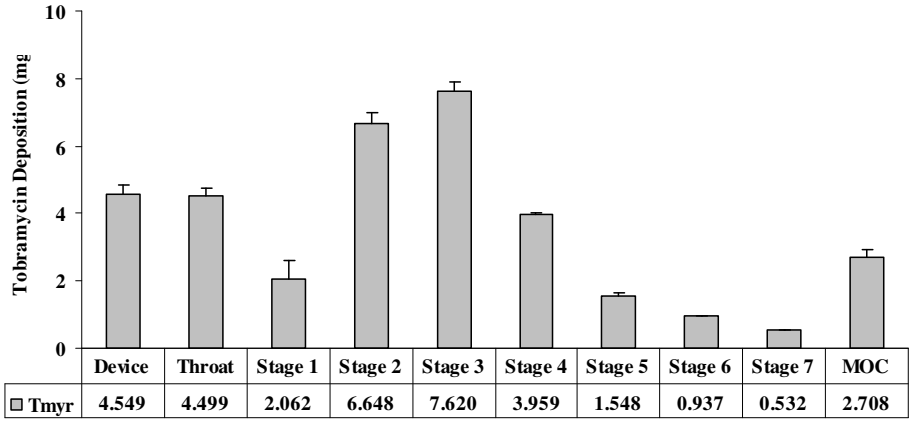

Figure 55: Aerodynamic assessment by NGI of Tobramycin-Myristic acid powder.

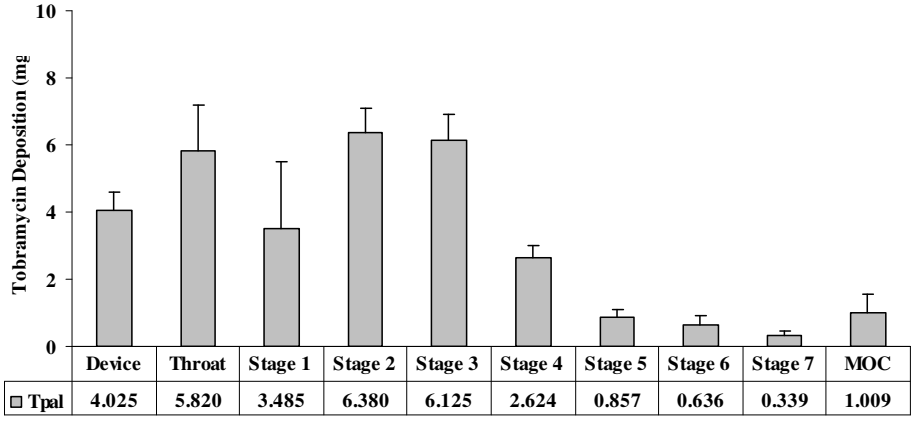

Figure 56: Aerodynamic assessment by NGI of Tobramycin-Palmitic acid powder.

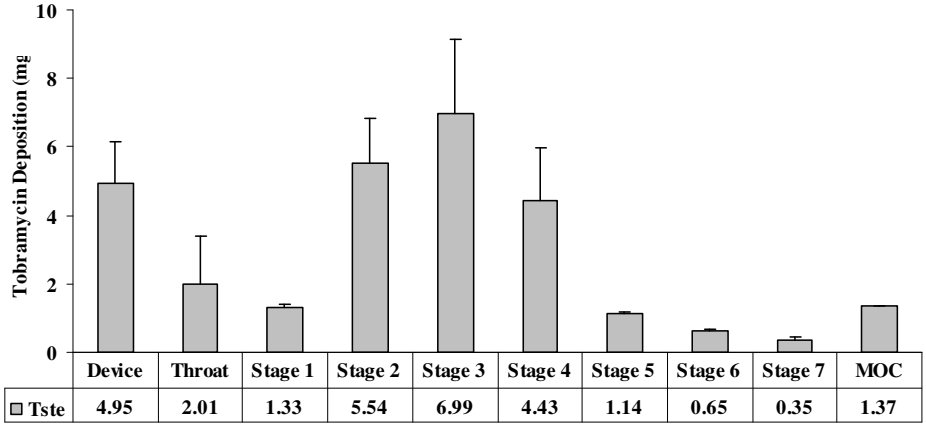

Figure 57: Aerodynamic assessment by NGI of Tobramycin-Stearic acid powder.

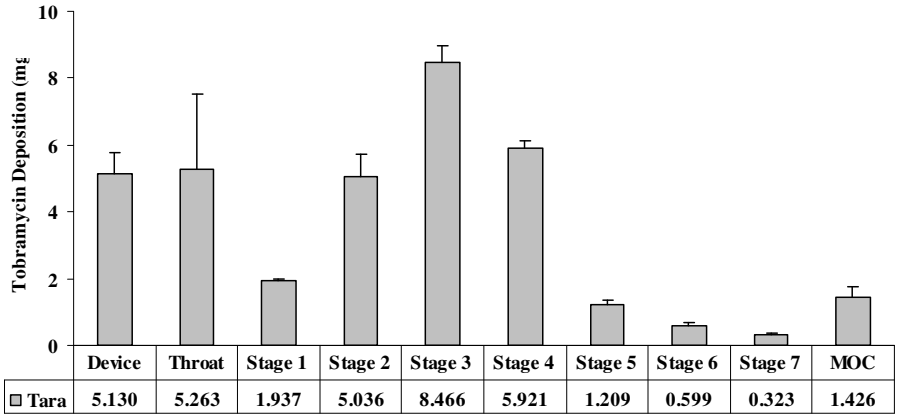

Figure 58: Aerodynamic assessment by NGI of Tobramycin-Arachidic acid powder.

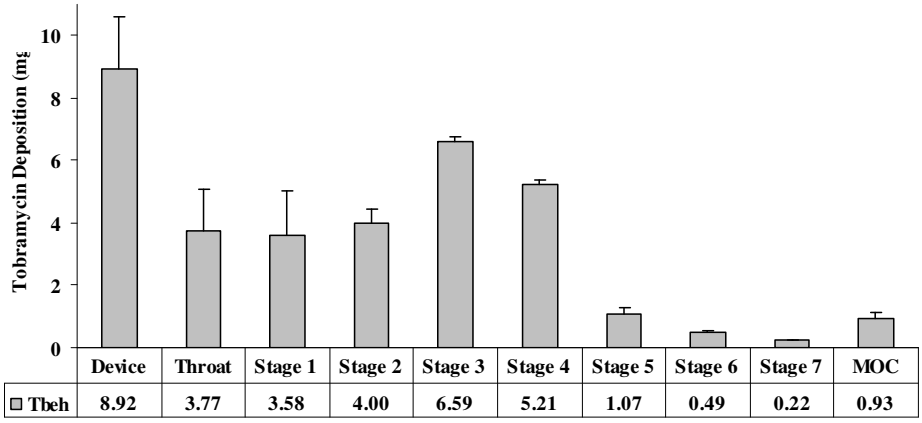

Figure 59: Aerodynamic assessment by NGI of Tobramycin-Behenic acid powder.

The surface energy components and contact angle values with three liquids by Contact Angle method are presented in Table XVIII. The highest dispersive (LW) values were measured for Tpal, even if there were no significant differences from the other values.

Table XVIII: Surface Free Energy Components Obtained via CA Measurements

	Components of surface free energy (mJ m^{-2})					Contact angle (°) with		
	γ_S^{LW}	γ_L^+	γ_L^-	γ_S^{AB}	γ_S	Ethilene Glicole	Diiodomethane	Glycerol
Tlau	33.28±1.53	3.70±2.17	5.43±6.13	6.85±4.74	40.13±3.54	30.23±1.82	51.77±2.71	57.83±3.48
Tmir	33.08±0.56	15.31±0.97	76.01±8.67	68.21±6.04	101.29±5.50	25.17±0.64	52.13±0.99	64.20±0.66
Tpal	34.07±0.47	11.66±1.08	43.62±5.41	45.09±4.89	79.16±4.90	25.27±2.97	50.37±0.85	62.40±0.87
Tste	33.21±0.34	17.70±4.17	132.52±54.40	96.57±31.53	129.77±31.28	33.40±0.56	51.90±0.61	70.10±2.33

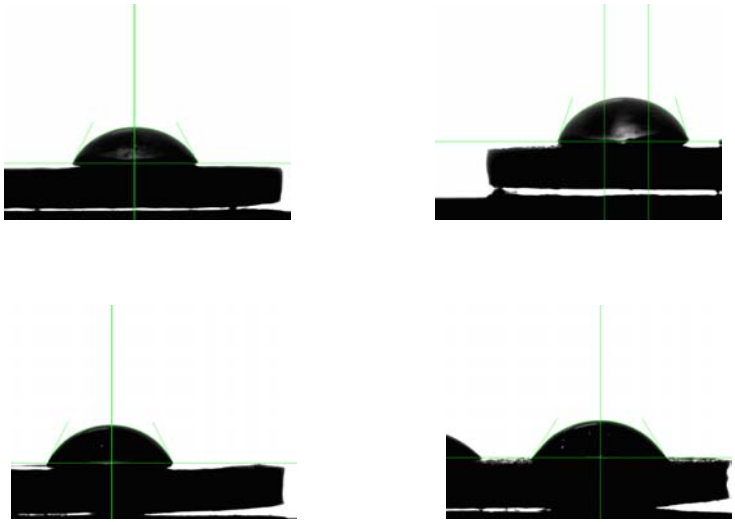

Figure 60: Photographs of different drops on the surface of the powder bed (Gly-Pal, Gly-Ste, Gly-Myr, Gly- Tlau)

When assayed independently, the formulations component did not reduce the viability of A549 cells to the extent of a 75% inhibitory concentration (IC50). The lowest cell viability (compared to the untreated control) was ≈77% for the highest concentration (1mg/ml) of palmitic acid suspension.

The four respirable formulations, which differ only in the fatty acid, had similar effects on the cell viability as those obtained when the fatty acids suspension were assayed alone. The only instances in which cell viability was reduced by >70% (in

particular 66%) were the application of the concentration 0.1 mg/ml of the tobramycin with lauric acid formulation, but were not consistent with the trend obtained from the rest of the data, e.g. the higher concentration of the same formulation. This is in a good correlation with other study declaring that the fatty acids have a very low acute toxicity in animals [140].

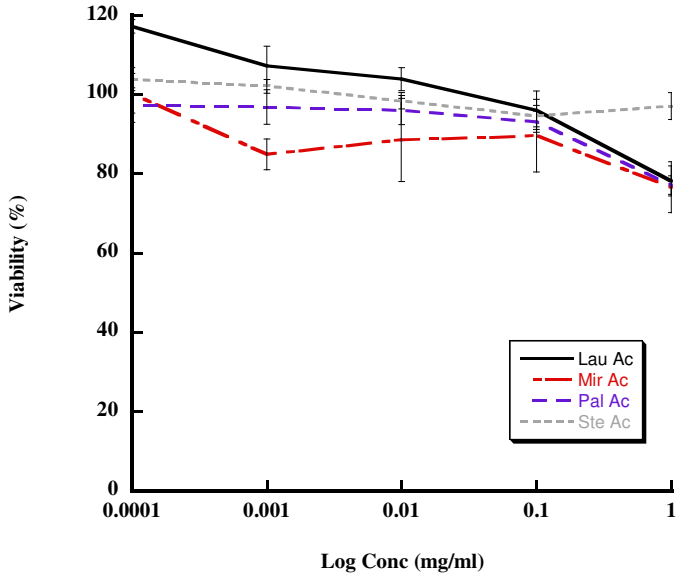

Figure 61: A549 epithelial cell viability measured by MTT cytotoxicity assay after 24 h exposure to different concentrations of formulation (n=5; Mean ± standard deviation).

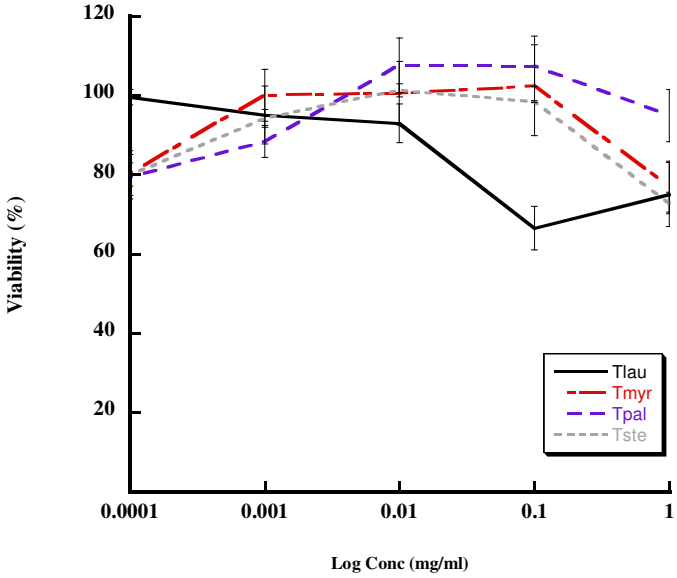

Figure 62: A549 epithelial cell viability measured by MTT cytotoxicity assay after 24 h exposure to different concentrations of formulation (n=5; Mean ± standard deviation).

Moreover, in Table XIX are reported the pH values for the tobramycin raw material and for the spray-dried formulation in DMEM. The formulations shown a basic pH value whilst the fatty acids in DMEM are not able to modify the pH value.

Table XIX: Values of pH for the tobramycin formulations in DMEM at conc. 1mg/ml.

pH values	*Conc. 1mg/ml DMEM*
7.40	DMEM alone
8.40	Tmir
8.40	Tpal
8.40	Tlau
8.40	Tste
7.40	Mir Ac
7.40	Pal Ac
7.40	Lau Ac
7.40	Ste Ac.

IV.3 Conclusion

The formulations of tobramycin as respirable dry powder with a low amount of fatty acid adjunct have great potential for tobramycin delivery as dry powder. In particular this study assessed the influence of the length chain on the chemical-physical properties of tobramycin spray-dried and on their aerodynamic properties.

The spray drying is a feasible method for the production of tobramycin and fatty acids adjunct formulations. All the powders produced with this technique show a volume diameter useful for inhalation. Furthermore, they have amorphous characteristics and a water content higher than 6% for all formulations.

The density measurements, according with the flowability parameters, attest the poor flowing properties of all micropowders. The formulations with long chain fatty acids (C20-C22) have worse density parameters than the formulations with a shorter chain.

Surface energy data obtained with the contact angle method reflect the behaviour of respirability data. There are not significative differences between the formulations in term of total energy.

This study demonstrated that these formulations did not induce any overt toxicity in the alveolar cell line used. These results provide in vitro evidence for an absence of irritancy of the formulations towards the respiratory epithelium. The absence of overt toxicity of these formulations in vitro is an encouraging indicator of the safety of these dry powders as lung delivery system.

IV.4 Part 4 FORMULATION AND CHARACTERIZATION OF SPRAY DRIED AMIKACIN SULPHATE FOR INHALATION

Amikacin sulphate (A) is a potent aminoglycoside antibiotic with a broad-spectrum and limited clinical use owing to nephrotoxicity and ototoxicity and a high dose requirement.

A recent study [141] indicate low doses of Amikacin is able to restore some hCFTR protein expression and function. However, the researchers found that amikacin suppressed a particular premature stop mutation more effectively than gentamicin when administered at clinically relevant doses. Because amikacin is also less toxic than gentamicin, it may represent a superior choice for suppression therapy in patients that carry a premature stop mutation in the CFTR gene. In other words, the amikacin could have significant implications for the therapeutic suppression of premature stop mutations that cause diseases like CF.

Several batches of amikacin microparticles were produced by spray-drying of the drug with different amount of sodium stearate (NaSt) as lipophilic adjunct as shown in Table XX. The solutions were spray dried on a Mini Spray Dryer B-191 (Buchi, Switzerland) using an inlet temperature of 150°C, material feed rate of 3.5 ml min^{-1}, atomization flow 100% and nozzle air flow of 600 ml min^{-1}. The yield of the processes is, for all batches, about 60% and we can say that the process is able to produce amikacin-sodium stearate powders with a good efficiency.

The powders produced were analysed in term of chemical-physical properties and in particular: the particle size analysis was carried out using a Mastersizer laser light diffraction apparatus. The samples were scattered in about 20 ml of ethyl acetate. The tests were performed for each batch in triplicate and analysis was repeated nine times.

In Table XX you can see the difference between the raw material, non-micronised, and powders produced by spray drying process. All had $d_{v0.5}$ under 5μm, optimal for lung deposition. It can also possible to see how the volume diameter of the particle increases with the increasing of the presence of lipid adjunct.

The powders were photographed with a scanning electron microscope to have a visual information about the morphology and the shape of the microparticles constituent the powders. How can see from the photos below the size of microparticles reflect data obtained from laser dimensional. All three are micronized and smaller to 4um. The particles produced tend to have a spherical shape and are partially corrugated. You can not observe morphological differences attributable the addition of sodium stearate. Moreover, in Figure 63-66 are shown microphotographs of the raw material and it is possible to see the change in size and shape caused by spray drying process.

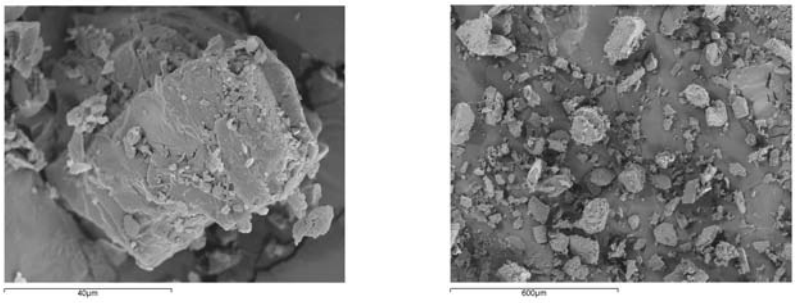

Figure 63 Amikacin Sulphate raw material

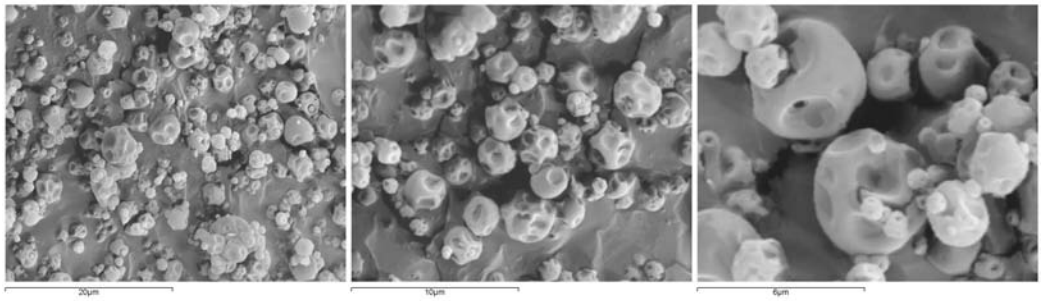

Figure 64 Amikacin spray dried without adjunct (A0).

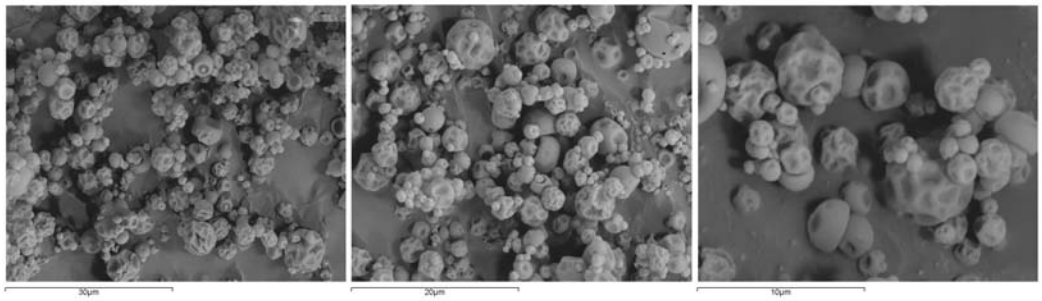

Figure 65 Amikacin spray dried with sodium stearate (A0.25).

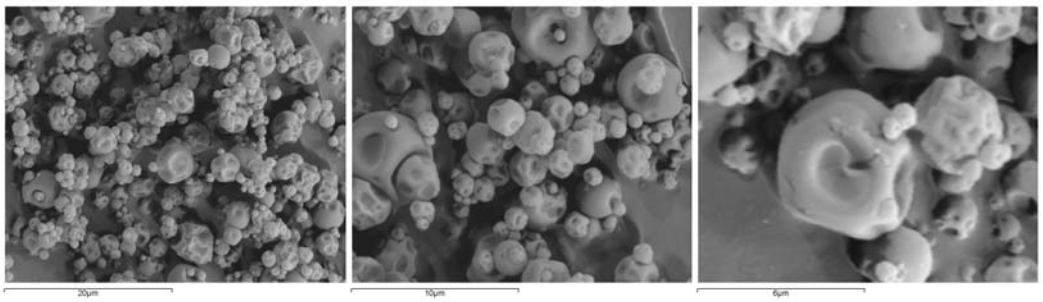

Figure 66: Amikacin sulphate with sodium stearate adjunct (A0.5).

The calorimetric analysis was conducted on the raw material and micronized powders obtained following the process of spray drying.

As you can see from the raw material termograph, there are two peaks showing a first peck of melting of the substance, a subsequent recrystallization and the final melting at around 255 °C. Moreover, the graph of the raw material indicates the presence of water of crystallization that is released at temperatures above 140 °C. This does not happen for micronized powder where you can see the same phenomenon around 100 °C, typical of not linked. The micronized powder does not have a endothermal peak and this indicates the amorphous nature of the product obtained after spray-drying.

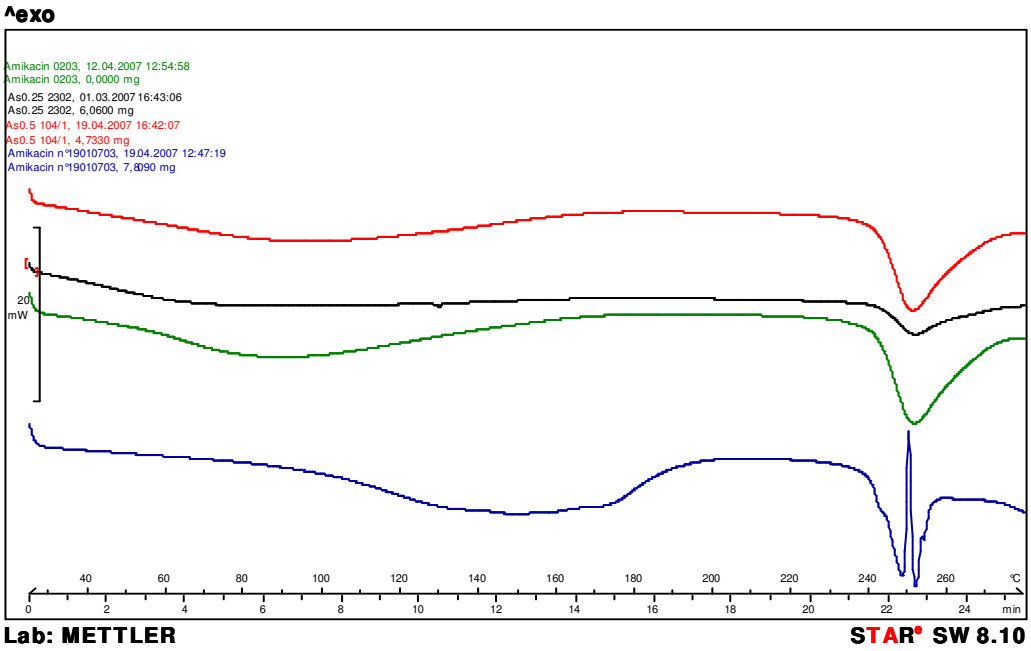

Figure 67: Termograph obtained from: Amikacin raw material (blue), A0 (green), A0.25 (black), A0.5 (red). (From down to the top).

The termogravimetric analysis was conducted to assess the loss in weight of the powders under heating. To some extent the loss in weight can be attributed to water content of the powder itself, although at temperatures above 100 ° C could take over

other phenomena. The heating method is chosen was 25-150 C, 10K / min and the result are shown in Table XX.

Table XX: Yield of SD process, water content, TGA analysis and dimensional analysis of the Raw material and SD microparticles

#	Amikacin (% w/w)	NaSt (% w/w)	Yield (%)	TGA (% w/w)	Particle Size Analysis		
					dv0.1	dv0.5	dv0.9
A r.m.	-	-	-	10.11± 0.1	7.93 ± 1.07	**57.12 ± 2.44**	143.74± 9.46
A 0	100	-	57.6	9.00 ± 0.5	0.92 ± 0.03	**2.50 ± 0.33**	5.27± 0.60
A 0.25	99.75	0.25	58.3	11.45 ± 1.2	0.95 ± 0.01	**3.12 ± 0.05**	8.65 ± 0.72
A 0.5	99.50	0.50	55.4	10.93±0.2	0.91±0.3	**3.28±0.19**	6.82 ±0.16

The true, bulk and tapped densities were measured for all the amikacin-sodium stearate powders. Moreover, for each batch the Carr's Index and the Hausner Ratio were calculated, both parameter useful for the evaluation of the flowability of powder solids.

Table XXI: True and Tapped Density of Tobramycin and fatty acid powders

Batch	True Density (g/ml)	Bulk Density (g/ml)	Tapped density (1250 taps) (g/ml)	Carr's Index (%)	Flowability[135]	Hausner Ratio
A raw material		0.59	0.85	30.06	Poor, cohesive	1.43
A0	1.56 ± 0.01	0.14	0.29	51.15	Extremely poor	2.04
A0.25	1.42 ± 0.01	0.15	0.30	50.00	Extremely poor	2.00
A0.5	1.49 ± 0.03	0.19	0.39	50.87	Extremely poor	2.03

The tapped density of the spray-dried powders was similar for all powders and they ranged between 0.29 and 0.39. The Carr's Index, as previously mentioned, gives an indication of powder flow properties; the values for the spray-dried powders were all around 50% and indicate cohesive powder characteristic and very poor flowability properties. As shown in the Table the low Carr's Index value was achieved for amikacin raw material, a not micronized powder.

In order to increase the handling and the flowability properties of the powders, the agglomerates of chosen size were produced from spray-drying powders.

A procedure for agglomerating microparticles was described [142-143]. In particular the spray-dried powders were put on the top of a stack of two sieves with nominal apertures of 600 μm and 300 μm, respectively (10 cm diameter sieves, Endecotts Ltd, London, UK), which was vibrated for 5 minutes on a laboratory sieve shaker (amplitude 3-4; Analysette 3 Fritz model, Fritsch GMBH, Idar-Oberstein, Germany). Agglomerates between 300 and 600 μm were collected. Reprocessing the non-agglomerated powder and forcing the larger agglomerates through the sieve, the process was repeated five times.

Figure 68: Agglomerates production with sieving.

The fraction of agglomerates on the sieve of 300 μm was collected and characterized with the optical microscope (ausJENA Citoval 2) and scanning electron microscopy (SEM). As you can see from the figures below the size of the agglomerations are between 300 and 600 m and its shape is roughly spherical.

Figure 69: Optical microscope photogaph. a) A0, b)A0.25, c)A0.5.

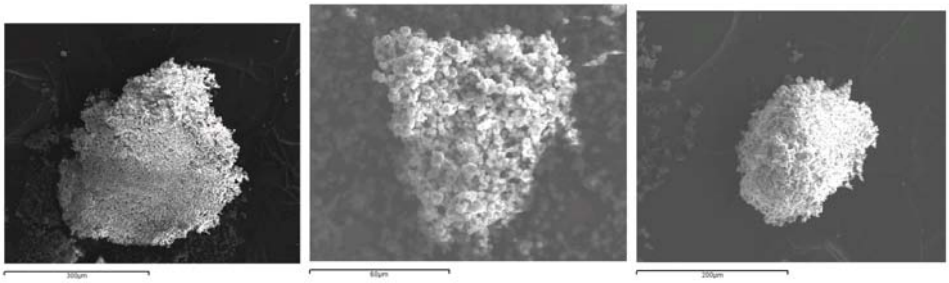

Figure 70: SEM A0, A0.25, A0.5

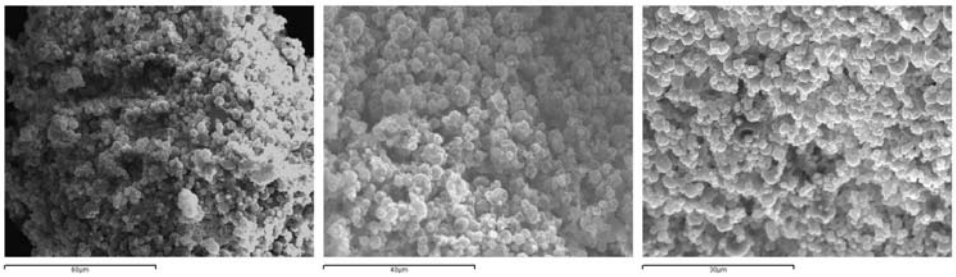

Figure 71: SEM Agglomerates, particular: A0, A0.25, A0.5

The aerodynamic assessment of amikcacin micropowders produced was carried out using the Andersen Cascade Impactor. The Turbospin® was the inhalation device used, who has the optimum at a flow of 60 l / m and get capsule size 2. In these experiments have been used in HPMC capsules.

As you can see from the graph, the powder impacts in the throat for a significant fraction, in all cases more than 20%. The remaining are distributed mainly in the early stages of the impactor and failing to arrive in depth. For all the powders there has been an emitted dose more than 80%, even in those without adjunct. The effect of stearate can be seen observing the FPF% and MMAD values, as shown in the Table XXII.

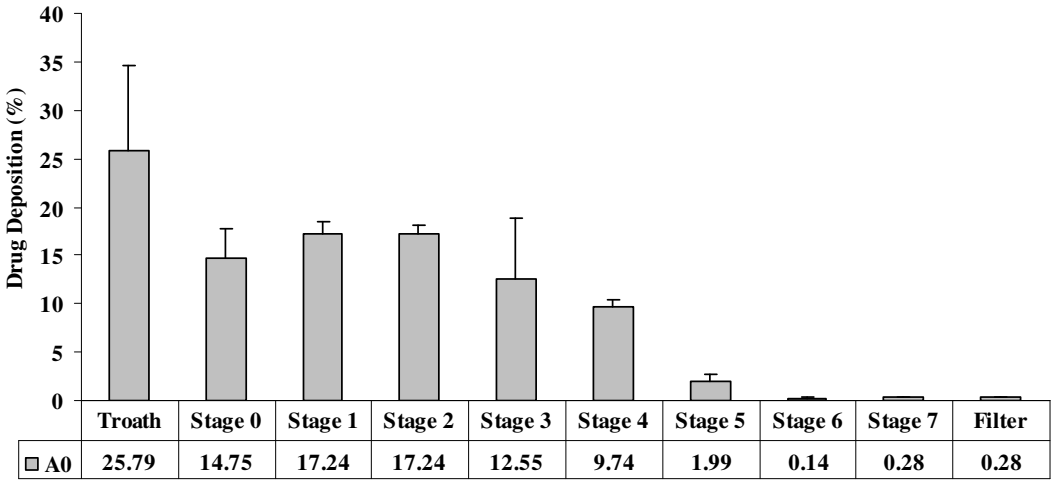

Figure 72: Aerodynamic assessment by ACI of amikacin without sodium stearate powder.

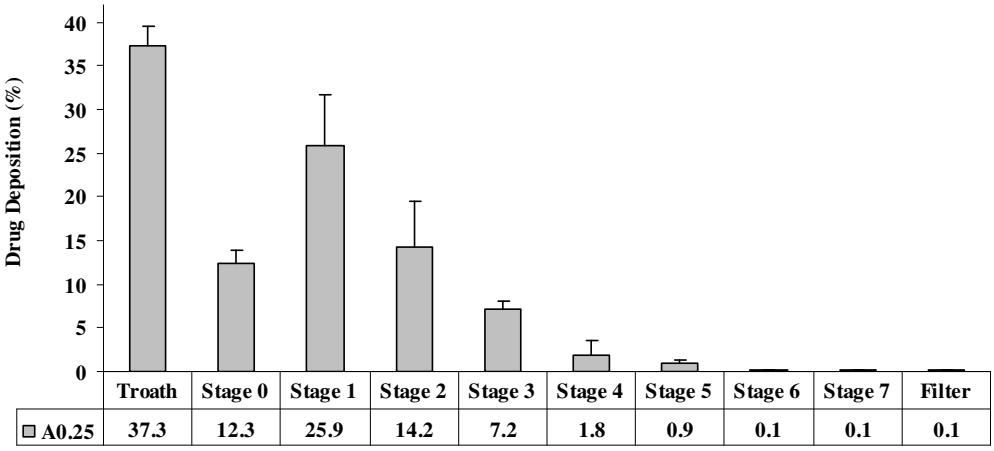

Figure 73: Aerodynamic assessment by ACI of amikacin - 0.25 sodium stearate powder.

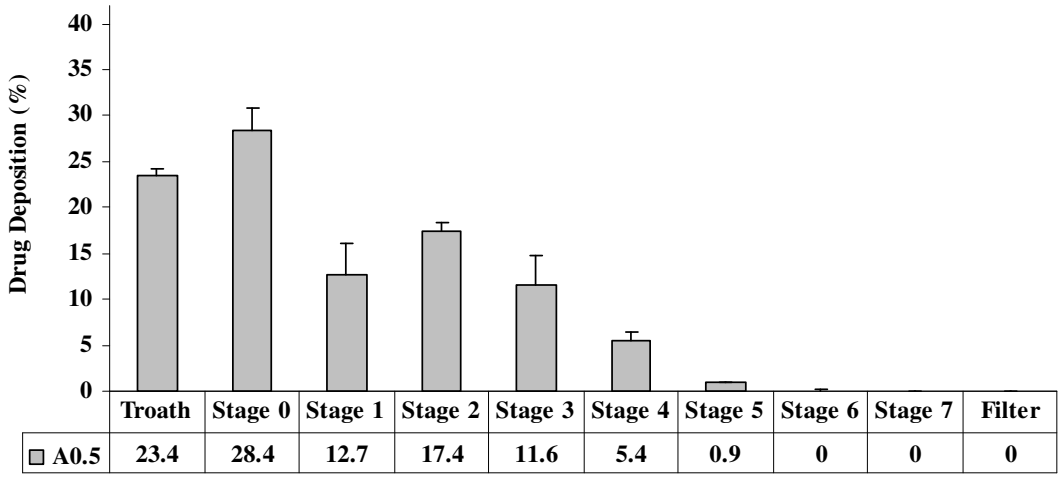

	Troath	Stage 0	Stage 1	Stage 2	Stage 3	Stage 4	Stage 5	Stage 6	Stage 7	Filter
A0.5	23.4	28.4	12.7	17.4	11.6	5.4	0.9	0	0	0

Figure 74: Aerodynamic assessment by ACI of amikacin-0.5 sodium stearate powder.

Table XXII: Deposition parameter (n=3; Mean ± standard deviation) of the different formulation measured by ACI

#	Recovery%	MMAD(µm)	FPD (mg)	FPF (%)
A0	90.83±2.53	3.84±0.15	8.10±1.03	50.20±6.19
Aa0	85,33±1.84	4.76±0.44	7.00±1.81	39.01±3.12
A0.25	94.76±2.33	4.45±0.03	7.09±0.49	38.20±1.37
Aa0.25	94.03±2.58	5.55±0.27	6.38±0.47	34.56±2.13
A 0.5	75.46±4.26	4.72±0.32	5.95±0.67	41.66±3.56
Aa 0.5	80.67±5.79	6.10±0.58	3.92±0.74	28.19±4.33

The respirability tests performed on amikacin agglomerates have shown that the air flow rate (60l / h) was unable to bear the microparticles in initial conditions. In fact the FPF% data were lower than microparticles unaltered. The only advantage seems to be reducing deposition in the throat due to less inertia and to facilitate handling of the formulations during the dosage of the capsules.

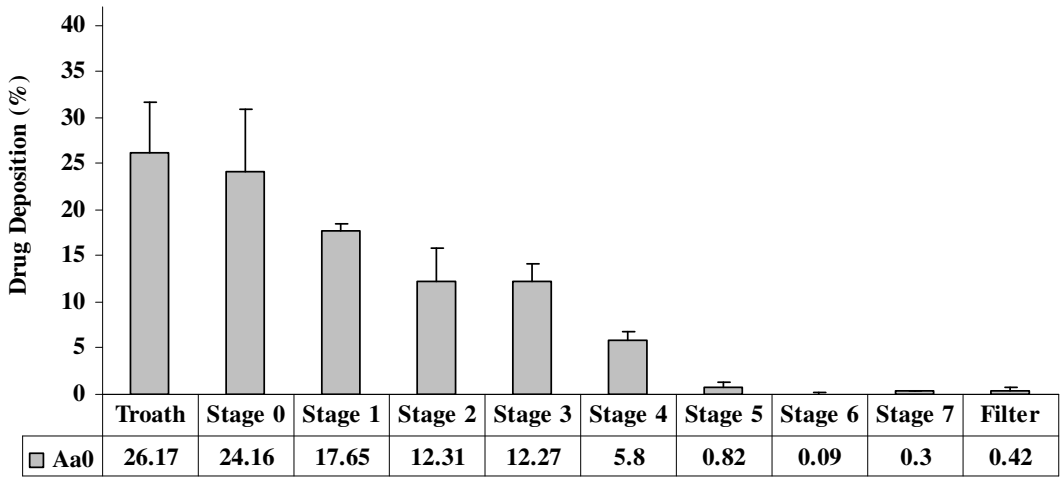

Figure 75: Aerodynamic assessment by ACII of amikacin without sodium stearate agglomerates.

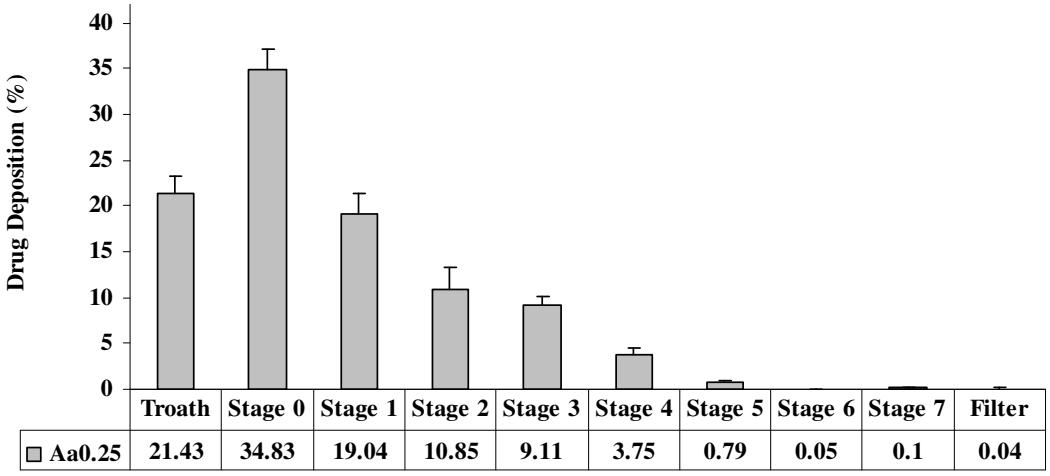

	Troath	Stage 0	Stage 1	Stage 2	Stage 3	Stage 4	Stage 5	Stage 6	Stage 7	Filter
Aa0.25	21.43	34.83	19.04	10.85	9.11	3.75	0.79	0.05	0.1	0.04

Figure 76: Aerodynamic assessment by ACI of amikacin-0.25 sodium stearate agglomerates.

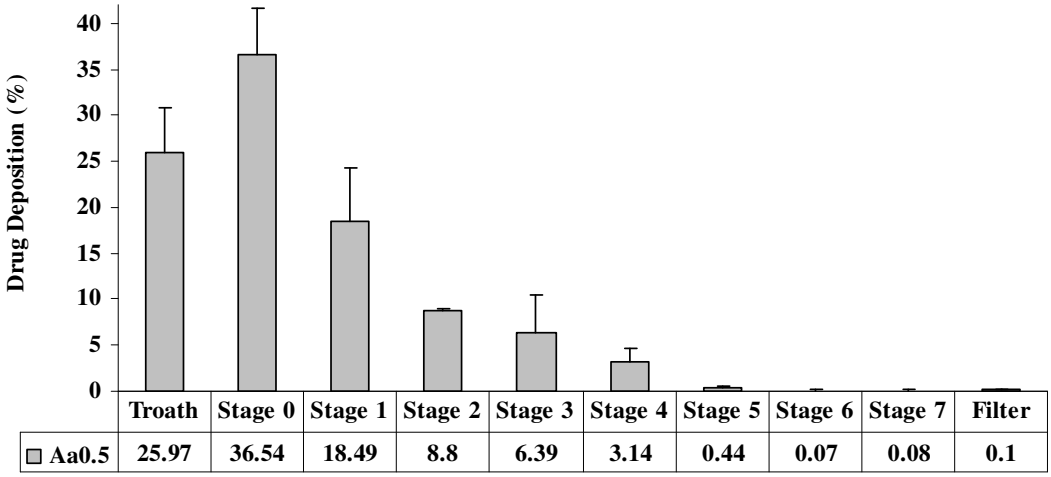

	Troath	Stage 0	Stage 1	Stage 2	Stage 3	Stage 4	Stage 5	Stage 6	Stage 7	Filter
Aa0.5	25.97	36.54	18.49	8.8	6.39	3.14	0.44	0.07	0.08	0.1

Figure 77: Aerodynamic assessment by ACI of amikacin -0.5 sodium stearate aglomerates.

A dissolution test on the powders was carried out in order to assess the effect of the lipophilic adjunct on the dissolution properties of the spray-dried powders.

Amikacin release from the microparticles was monitored in simulated lung fluid (900 ml, pH 7.4, non-sink condition) using the USP paddle method for oral dosage form. Samples of the solution were filtered (0.45 , Millipore, UK) and analysed by HPLC.

The tests were performed for three times on each batch using a dissolution system (), equipped with a paddle system to 75 rotations per minute and such dissolution fluid has been (was) choice a simulated lung fluid (900 ml).

- NaCl 0.68 g l^{-1}
- $NaHCO_3$ 2.27 g l^{-1}
- Gly 0.37 g l^{-1}
- NaH_2PO_4 H_2O 0.16 g l^{-1}
- $CaCl_2$ 0.02 g l^{-1}
- H_2SO_4 5 ml 0.1 M

As you can see from the graph, while finding a difference in the rate of dissolution of this drug can not be considered significant in what happens in a time too short. This could be because the high solubility of the drug, the presence of different amount of sodium stearate does not affect the dissolution profile of the drug. In addiction, as the dissolution system chosen for this study is normally employed for the oral dosage form. 900 ml of fluid in direct contact with formulation is no representative of the lung environment and could mask the little differences between the micronised formulations.

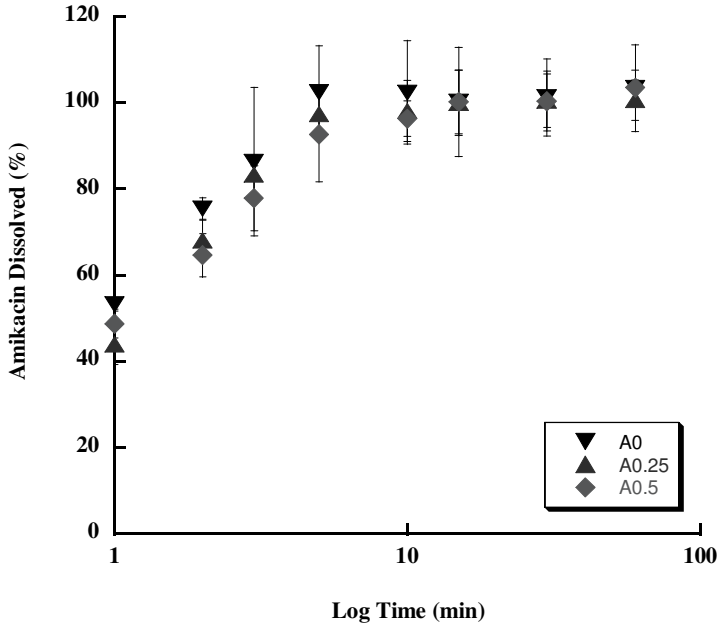

Figure 78: Dissolution profile of amikacin SD formulations.

IV.4 Conclusion

These results demonstrated the ability of spray drying technique to produce high respirable powders of amikacin with or without sodium stearate adjunct suitable for the pulmonary administration. The production of agglomerates on the one hand facilitated the dosage of the formulation in the device, on the other hand decrease the FPF value because the flow through the device is not able to break down the aggregate and reforming the original microparticles.

V CONCLUSIONS

In this work, various approaches to carrier-free formulations were investigated in order to allow the delivery of highly-dosed drugs such as tobramycin. In order to produce particles in an adequate size range for pulmonary delivery, the spray-drying process was chosen.

This study demonstrated the ability of spray drying technique to produce spray-dried powders of tobramycin and with particles dimensions suitable for pulmonary administration (<5µm).

Tobramycin was spray-dried in presence of varying amount of sodium stearate used as adjunct to control the aerosolization efficiency in a dry powder inhaler. The aerosol performance of the spray-dried powders was related to the percentage of adjunct in the microparticles in the range between 0.25 to 2.0 %w/w. Adjunct between 1 and 1.5% w/w showed the best aerosol performance, followed by a significant decrease at 2%. In general, particles containing a final adjunct concentration of 1% w/w sodium stearate, where sodium stearate was concentrated for the majority on the surface of microparticles, provided the greatest aerosol performance (>80% FPF).

The supramolecular form of stearate in the spray drying solutions and its redistribution in the microparticle growing during spray drying was suggested as the determinant for the presence of sodium stearate on the surface of the microparticles. Preliminary cell toxicity studies have showed that the use of this hydrophilic adjunct at the concentrations shown before has no effect on cell viability over a 24 h period. The minimum value of cell viability was higher and non-significantly different from the value exhibited by tobramycin alone (approx 70%).

Interestingly, these new lipid-coated microparticles offered improved deposition of tobramycin in the pulmonary tract. The evaluation of the influence of the coating level showed that the use of only 1% w/w of lipid adjunct was sufficient in order to improve particle dispersion properties during inhalation and thus allows a drastic increase in the fine particle fraction of the powder.

This percentage of lipophilic adjunct has been used to test the aerosolization efficiency of tobramycin spray-dried powders with a series of fatty acids. They have a high respirability and good aerodynamic characteristics. All analyzed spray-dried powders have a MMAD lower than 5 µm and almost all spray-dried powders have an FPF (<5µm) higher than 50%. In particular, tobramycin-stearic acid spray-dried powder among all analyzed powders is the one with highest FPF values (>70%). The use of a lipophilic adjunct clearly has the potential to increase aerosol efficiency. Preliminary cell toxicity studies have showed that the use of this fatty acids at the concentrations shown before has no effect on cell viability over a 24 h period. The lowest value of cell viability was achieved for the formulation with lauric acid (≈65%), non-significantly different from the value of tobramycin alone (≈70%).

This study demonstrated the ability of spray drying technique to produce high respirable powders of amikacin with or without sodium stearate adjunct suitable for the pulmonary administration. The production of agglomerates on the one hand facilitated the dosage of the formulation in the device, on the other hand decrease the FPF value because the flow through the device is not able to break down the aggregate and reforming the original microparticles.

Tests for industrial scaling-up may be performed in order to produce batches of adequate size for production.

These new and orginal carrier-free DPI formulations based on the use of very low excipient levels and presenting very high lung deposition properties offer very important prospects for improving the delivery of drugs to the pulmonary tract. These formulations are more particularly useful for drugs that are active at relatively high doses, such as antibiotics, as they permit the delivery of a high concentration of antibiotic directly to the site of infection while minimizing systemic exposition. Moreover, a reduction in administration time and in systemic side effects allows improved suitability of these formulations for patients.

In conclusion, this approach provides a feasible and attractive alternative to intravenous or nebulisation of antibiotics to treat respiratory infection. These co-spray dried formulations suggested that a powder could be produced that facilitated in vitro drug deposition profiles, compared to deposition patterns from the formulation with the only tobramycin. It is envisaged that this novel tobramycin pulmonary powder could ultimately be used to improve therapeutic outcomes for patients suffering from debilitating respiratory diseases such as Cystic Fibrosis, bronchiectasis and COPD.

BIBLIOGRAPHY

[1] S.W.Clarke, S.P.Newman, Therapeutic aerosol 2 - Drugs available by inhaled route, Torax (1984); 39:1-7.

[2] I.Gonda, The ascent of Pulmonary drug delivery, J.Pham.Sci. (2000); 89(7): 940-945.

[3] A.J.Hickey et al., Inhalation aerosol- Physical and biological basis for therapy, Vol.94, Marced Dekker Ed. NY..

[4] M.J.de J.Valle, F.G.Lopez, A.D. Hurlé, A.S. Navarro, Pulmonary versus systemic delivery of antibiotics: comparison of vancomycin dispositions in the isolated rat lung, Antimic. Agents Chemother(2007); oct: 3771-3774

[5] H.A.Kirst, N.E. Allen, Aminoglycosides antibiotics

[6] Berne R.M., Levy M.L., Fisiologia, Casa Editrice Ambrosiana.

[7] S.P. Newman, S.W. Clarke, Therapeutic aerosol 1 – Physical and practical considerations, Torax (1983); 38:881-886.

[8] G.Azzali, R.D.Lockart, G.F.Hamilton, F.W.Fyfe, Anatomia del corpo umano, CEA

[9] A.Stevens, J.Lowe, Istologia umana, CEA

[10] V.Sauret, P.M.Halson, i.W.Brown, J.S. Fleming, A.G. Bailey, Study of the three-dimensional geometry of the central conducting airways in man using computed tomographic (CT) images, J.Anat. (2002); 200: 123-34.

[11] T.B.B. Martonen, A.E. Barnett, F.J. Miller, Ambient sulfate aerosol deposition in man: modeling the influence of hygroscopicity, Env. Health Persp. (1985); 63:11-24.

[12] H. Fehrenbach, Alveolar epithelial type II cell: defender of the alveolus revisited, Respir Res (2001); 2: 33-46.

[13] M.Griese, Pulmonary surfactant in health and human lung diseases: state of the art, Eur. Respir. J. (1999); 13: 1455-1476.

[14] T.E.Weaver, J.A.Whitsett, Function and regulation of expression of pulmonary surfactant-associated proteins, Biochem. J. (1991); 273: 249-264.

[15] F.Possmayer, K.Nag, K.Rodriguez, R.Qanbar, S.Schurch, Surface activity in vitro: role of surfactant proteins (review), Comp. Biochem. Physiol. Part A (2001); 129: 209-220.

[16] M.Lippmann, Effects of fiber characteristic on lung deposition, retention and disease, Env. Health Persp. (1990); 88:311-217.

[17] B.O.Stuart, Deposition and clearance of inhaled particles, Env.Health Persp. (1984); 55: 369-390.

[18] M.Lippmann, D.B.Yeates, R.E.Albert, Deposition, retention and clearance of inhaled particles, Brit.J. Ind.Med. (1980); 37: 337-362

[19] C.Darquenne, Aerosol deposition in the humen respiratory tract breathing air and 80:20 Heliox, J Aerosol Med (2004); 17(3): 278-285.

[20] H.C.Yeh, R.F.Phalen, O.G.Raabe, Factors influencing the deposition of inhaled particles, Env. Health Persp. (1976); 15: 147-156.

[21] T.R.Gerrity, C.S.Garard, D.B.Yeates, A mathematical model of particle retention in the air-spaces of human lungs, Brit.J.Indust.Med. (1983); 40:121-130.

[22] P.Zanen, L.T.Go, J-W J. Lemmers, Optimal particle size for β_2 agonist and anicholinergic aerosols in patients with severe airflow obstruction, Torax (1996); 51:977-980.

[23] A.J.Hickey, N.M.Concessio, Descriptors of irregular particle morphology and power properties, Adv.Drug Del.Rev, (1997); 26:29-40.

[24] N.R.Labiris, M.B.Dolovich, Pulmonary drug delivery. Part I: Physiological factors affecting therapeutic effectiveness of aerosolized medications,J.Clin.Pharmacol (2003); 56:588-599.

[25] Martonen T, Yang Y. 1996. Deposition mechanics of pharmaceutical particles in human airways. In: Hickey AJ, editor. Inhalation aerosols. New York: Marcel Dekker. pp. 3±27.

[26] A.J.Hickey, T.B. Martonen. Behavior of hygroscopic pharmaceutical aerosol and the influence of hydrophobic additives, Pharm Res 10(1):1-7 (1993)

[27] A.J.Hickey, H.M.Mansour, M.J.Telko, Z.Xu, H.D.C.Smyth, T.Mulder, R.Mclean, J.Langridge, D.Papadopoulos, Physical characterzation of component particles included in dry powder inhalaers. II. Dynamic characteristics, J.Pharm.Sci (2007); 96(5): 1302-1319.

[28] H.Chrystyn, The Diskus™: a review of its position among dry powder inhaler devices, Int.J.Clin.Pract, (2007); 61(6):1022-1036.

[29] P.P.H.Le Brun, A.H.de Boer, H.G.M.Heijerman, H.W.Frijlink, A review of the technical aspects of drug nebulization, Pharm. World Sci. (2000); 22(3): 75-81.

[30] H.Steckel, F.Eskandar, Factors affecting aerosol performance during nebulization with jet and ultrasonic nebulizer, Eu.J. Pharm. Sci. (2003); 19: 443-455.

[31] A.H.de Boer, P.Hagedoorm, H.W.Frijlink, The choice of a compressor for the aerosolisation of tobramycin (TOBI®) with the PARI LC PLUS® reusable nebuliser, Int.J.Pharm (2003); 268: 59-69.

[32] S.P.Newman, Principles of metered-dose inhaler design, Res.Care (2005); 50 (9): 1177-1190.

[33] B.Y.Khassawneh, M.K. Al-Ali, K.H. Alzoubi, M.Z. Batarseh, S.A.Al-Safi, A.M. Sharara, H.M.Alnasr, Handling of inhaled devices in actual pulmonary practice: metered-dose inhaler versus dry powder inhalers, Pespir.Care (2008); 53(3):324-328.

[34] N.R.Labiris, M.B.Dolovich, Pulmonary drug delivery. Part II: The role of inhalant delivery devices and drug formulations in therapeutic effectiveness of aerosolized medications ,J.Clin.Pharmacol (2003); 56:600-612.

[35] http://ozone.unep.org/Publications/MP_Handbook/Section_1.1_The_Montreal_Protocol/

[36] S.P.Newman, S.W.Clarke, Bronchodilator delivery from Gentlehaler, a new low-velocity pressurized aerosol inhaler, Chest (1993); 103: 1442-1446.

[37] D.Prime, P.J.Atkins, A.Slater, B.Sumby, Review of dry powder inhalers, Adv.D.Del.Rev. (1997);26: 51-58.

[38] P.J.Atkins, Dry Powder Inhalers: An overview, Res. Care (2005); 50(10):1304-1312.

[39] H.Steckel, B.W.Muller, In vitro evaluation of dry powder inhalers I: drug deposition of commonly used devices, Int.J.Pharm. (1997); 154: 19-29.

[40] T.Srichana, G.P.Martin, C.Marriott, Dry powder inhaler: the influence of device resistance and power formulation on drug and lactose deposition in vitro, Eu.J.Pharm.Sci. (1998);7: 73-80.

[41] I.Ashurst, A.Malton, D.Prime, B.Sumby, Latest advances in the development of dry powder inhalers, PSTT, (2000); 3(7): 246-256.

[42] S.P.Newman, W.W.Busse, Evolution of dry powder inhaler design, formulation, and performance, Res.Med. (2002); 96:293-304.

[43] N.Islam, E.Gladki, Dry powder inhalers (DPIs), A review of device reliability and innovation, Int.J.Pharm. (2008); 360: 1-11.

[44] D.A.Edwards, C.Dunbar, Bioengineering of therapeutic aerosols, Annu.Rev.Biomed.Eng. (2002),4:93-107.

[45] P-J-Anderson, Delivery options and devices for aerosolized therapeutics, Chest (2001); 120: 89-93.

[46] M.S.Coates, D.F.Fletcher, H.K.Chan, J.A.Raper, The role of capsule on the performance of a dry powder inhaler using computational and experimental analyses, Pharm.Res. (2005); 22(6): 923-932.

[47] P.H.Hirst, G.R.Pitcairn, J.G.Weers, T.E.Tarara, A.R.Clark, L.A.Dellamary, G.Hall, J.Shorr, S.P.Newman, In vivo lung deposition of hollow popous particles from a pressurized metered dose inhaler, Pharm.Res. (2002); 19(3): 258-264.

[48] D.A.Edwards et al., Large porous particles for pulmonary drug delivery, Science (1997); 276: 1868-1871.

[49] A.H.L.Chow, H.H.Y.Tong, P. Chattopadhyay, B.Y.Shekunov, Paticle engineering for pulmonary drug delivery, Pharm.Res. (2007); 24(3):411-437.

[50] R. Veinhard. Pharmaceutical particle engineering via Spray Drying. Pharm Res 25(5):999-1022 (2008).

[51] Zijlstra G.S., Hinrichs W.L.J., de Boer A., Frijlink H.W., The role of particle engineering in relation to formulation and de-agglomeration principle in the development of a dry powder inhalation of cetrorelix, European Journal of Pharmaceutical Science,2004; 23: 139-149.

[52] Robbins and Cotran, Pathologic basis of disease, 7th edition,

[53] J.R.Riordan, J.M.Rommens, B.Kerem, N.Alon, R.Rozmahel, Z.Grzelczak, J.Zielenski, S.Lok, N.Plavsic, J.L.Chou, Identification of the cystic fibrosis gene: cloning and characterization of complementary DNA, Science (1989); 245 (4922): 1066-1073.

[54] G.P.Marelich, C.E.Cross, Cystic fibrosis in adult, WJM (1996); 164(4): 321-334.

[55] Ramsey B.W. Management of pulmonary disease in patients with cystic fibrosis Drug Therapy (1996); 335(3): 179-188.

[56] M.R.Tonelli, M.L.Aitken, New and emerging therapies for pulmonary complications of cystic fibrosis, Drugs (2001); 61(10): 1379-1385.

[57] G.Doring, S.P.Conway, H.G.M.Heijerman, M.E.Hodson, N.Hoiby, A.Smith, D.J.Touw, Antibiotic therapy against Pseudomonas aeruginosa in cystic fibrosis: a European consensus, Eur.Respir.J (2000); 16: 749-767.

[58] D.J.Touw, R.W.Brimicombe, M.E.Hodson, H.G.M.Heijerman, W.Bakker, Inhalation of antibiotics in cystic fibrosis, Eur.Respir.J. (1995); 8: 1594-1604.

[59] D.E.Geller, W.H.Pitlick, P.A.Nardella, W.G.Tracewell, B.W.Ramsey, Pharmacokinetics and bioavailability of aerosolized tobramycin in cystic fibrosis, Chest (2002); 122: 219-226.

[60] C.H.Feng, S.J. Lin, H.L. Wu, S.H. Chen, Trace analysis of tobramycin in human plasma by derivatization and high-performance liquid chromatography with ultraviolet detection, J. Chromatography B (2002); 780: 349-354.

[61] L. Garcia-Contreras, A.J. Hickey. Pharmaceutical and biotechnological aerosols for cystic fibrosis Therapy. Adv Drug D Rev. 54:1491–1504 (2002).

[62] M.E. Drobnic, P. Suñé, J.B. Montoro, A. Ferrer and R. Orriols. Inhaled tobramycin in non–cystic fibrosis patients with bronchiectasis and chronic bronchial infection with pseudomonas aeruginosa. Ann Pharmacother. 39:39-44 (2005).

[63] H. Lode. Tobramycin: a review of therapeutic uses and dosing schedules. C Ther Res. 59:7 (1998).

[64] V.B. Pai and M.C. Nahata. Efficacy and safety of aerosolized tobramycin in cystic fibrosis. Ped Pneumology 32:314-327 (2001).

[65] B.W. Ramsey, M.S. Pepe, J.M. Quan, K.L.Otto, A.B. Montgomery, J. Williams-Warren, M. Vasiljev-K, D. Borowitz, C.M. Bowman, B.C. Marshall, S.Marshall and A.L. Smith. Intermittent administration of inhaled tobramycin in patients with cystic fibrosis. N Engl J Med. 340:23-30 (1999).

[66] G. Döring, S.P. Conway, H.G.M. Heijerman, M.E. Hodson, N. Hùiby, A. Smyth, D.J. Touw. Antibiotic therapy against psedomonas aeruginosa in cystic fibrosis: a European consensus. Eur Respir J 16:749-767 (2000).

[67] R.B. Moss. Administration of aerosolized antibiotics in cystic fibrosis patients. Chest 120:107-113 (2001).

[68] J. Eisenberg, M. Pepe, J. Williams-Warren, M. Vasiliev, A.B. Montgomery, A.L. Smith, B.W. Ramsey. Systems fibrosis using jet and ultrasonic nebulizer concentration in patients with cystic. A comparison of peak sputum tobramycin. Chest 111:955-962 (1997).

[69] D.J. Touw, A.J. Knox, A. Smyth. Population pharmacokinetics of tobramycin administered thrice daily and once daily in children and adults with cystic fibrosis. J of Cystic Fibrosis 6:327-333 (2007).

[70] L. Vidal, A. Gafter-Gvili, S. Borok, A. Fraser, L. Leibovici and M. Paul. Efficacy and safety of aminoglycoside monotherapy: systematic review and meta-analysis of randomized controlled trials. J of Antimicrobial Chemother. 60:247–257 (2007).

[71] S.M. Cheer, J. Waugh and S. Noble. Inhaled Tobramycin (TOBI): a review of its use in the management of Pseudomonas Aeruginosa infections in patients with cystic fibrosis. Adis Drug Evaluation. 63(22):2501-2520 (2003).

[72] M.P. Boyle. Challenge of cystic fibrosis care so many drugs, so little time: the future. Chest 123:3-5 (2003).

[73] P.W. Campbell and L. Saiman. Use of aerosolized antibiotics in patients with cystic fibrosis. Chest 116:775-788 (1999).

[74] G.Pilcer, T.Sebti, K.Amighi. Formulation and characterization of lipid-coated tobramycin particles for dry powder inhalation. Pharm. Res. 23(5):931-940 (2006)

[75] G.Pilcer, F. Vanderbist, K.Amighi. Preparation and characterization of spray-dried tobramycin powder containing nanoparticles for pulmonary delivery. Int .J. Pharm article in press (2008).

[76] M.T.Newhouse, P.H.Hirst, S.P.Duddu, Y.H.Walter, T.E.Tarara, A.R.Clark, J.G.Weers. Inhalation of a dry powder tobramycin pulmosphere formulation in healthy volunteers. 124:360-366 (2003).

[77] K.Masters, Spray dtying handbook 5th ed. (1991), Harlow: Longman Scientific & technical.

[78] K.Mosén, K.Backstrom, K.Thalberg, T.Schaefer, H.G.Kristensen, A.Axelsson, Particle formation and capture during spray drying of inhalable particles (2004) Pharm.Develop.Technol. 9(4): 409-417.

[79] Palmer W, Wangemann K, Kampermann S, and Hosler W, Nuclear Instruments and Methods in Physics Research B (1990) 5134.

[80] S. Edge, A.M. Belu, U.J. Potter, D.F. Steele, P.M. Young, R. Price, J.N. Staniforth; Chemical characterisation of sodium starch glycolate particles,Int.J. Pharm., 240 (2002) 67-78.

[81] F.Lasagni, A.Lasagni, C.Holzapfel, F.Mucklich, H.P.Degischer, Three dimensional characterization of unmodified and Sr-modified Al-Si eutectics by FIB and FIB-EDX tomography, Adv.Engineering Material (2006); 8(8): 719-723.

[82] S.H.Moghdam, R.Dinarvand, L.H.Cartilier, The focused ion beam technique: a useful tool for pharmaceutical characterization, Int.J.Pharm (2006); 321:50-55.

[83] F.A.Stevie, C.B.Vartuli, L.A.Giannuzzi, T.L.Shofner, S.R.Brown, B.Rossie, F.Hillion, R.H.Mills, M.Antonell, R.B.Irwin, B.M. Purcell, Application of focused ion beam lift-out specimen preparation to TEM, SEM, STEM, AES and SIMS analysis, Surf.Interface Anal. (2001); 31: 345-351.

[84] L.A.Giannuzzi, F.A.Stevie, Itroduction to focused ion beam: instrumentation, theory, techniques and practice, Springer, New York NY.

[85] USP 31 Physical tests <699> Density of solids, 265-266.

[86] H.G.Brittain, Physical characterization of pharmaceutical solids, Marcel Dekker, Inc, NY.

[87] C.Reh, S.N.Bhat, S.Berrut, Determination of water content in powdered milk, Food Chemistry (2004); 86: 457-464.

[88] USP General Chapter ^429&, "Light Diffraction Measurement of Particle Size," Pharmacopeial Forum 28 (4), 1293–1298 (2002).

[89] P.Kippas, Appraisal of the laser diffraction particle-sizing technique, Pharm.Tech. (2005); march:88-96.

[90] B.Y.Shekunov, P.Chattopadhyay, H.H.Y.Tong, A.H.L.Chow, Particle size analysis in pharmaceutics: principles, methods and applications, Pharm.Res. (2007); 24(2): 203-227.

[91] USP NF 2006 (= The United States Pharmacopeia 29, The National Formulary 24): 2617-2636.

[92] D.M.Barends, C.L.Zwaan, A.Hulshoff, Micro-determination of tobramycin in serum by high-performance liquid chromatography with ultraviolet detection, J.Chromat. (1981); 225: 417-426.

[93] E.E.Stobberingh, A.W.Houben, C.P.A. van Boven, Comparison of different tobamycin assay, J.Clinical Microbiol. (1982); may: 795-801.

[94] D.A. Stead, J. Chromatogr. B 747 (2000) 69–93.

[95] D.M. Barends, J.S. Blauw, M.H. Smits, A. Hulshoff, J. Chromatogr. 276 (1983) 385–394.

[96] B. Wichert, H. Schreier, H. Derendorf, J. Pharm. Biomed. Anal. 9 (1991) 251–254.

[97] R. Tawa, H. Matsunaga, T. Fujimoto, J. Chromatogr. A 812 (1998) 141–150.

[98] S.Nicoli, P.Santi, assay of amikacin in the skin by high-performance liquid chromatography, J.Pharm.Biomed.An. (2006); 41: 994-997.

[99] L.T. Wong, A.R. Beaubien, A.P. Pakuts, J. Chromatogr. 231 (1982)145–154.

[100] Carmichael J., DeGraff W.G., Gazdar A.F., Evaluation of tetrazolium-based semiautomated colorimetric assay: assessment of radiosensitivity, Cancer Research Vol. 47, 4, 943-946 (1987).

[101] Mosmann, Rapid colorimetric assay for cellular growth and survival: application to proliferation and cytotoxicity assays, Journal of Immunological Methods, 65 (1983) 55-63.

[102] Grenha A., Grainger C.I., Dailey L.A., Seijo B., Martin G.P., Remuñán-López C., Forbes B., Chitosan nanoparticles are compatible with respiratory epithelial cells in vitro, European Journal of Pharmaceutical Science 31 (2007) 73-84.

[103] Dissolution Testing of Immediate Release Solid Oral Dosage Forms, FDA

[104] J.H. Widdicombe, Regulation of the depth and composition of airway surface liquid. J of Anatomy 201 (4) (2002) 313-318.

[105] R. Salama, S. Hoe, H.K. Chan, D. Traini, P.M. Young, Preparation and characterisation of controlled release co-spray dried drug–polymer microparticles for inhalation 1: Influence of polymer concentration on physical and in vitro characteristics, Eu.J. Pharm. Biopharm., 2008 article in press.

[106] T.J. Franz, Percutaneous absorptions. On the relevance of in vitro data, J.of Investigative Dermatology, 64 (1975) 190-195.

[107] F.Lagenbucher, Parametric representation of dissolution-rate curves by the RRSBW distribution, Pharm.Ind. (1974); 5: 472-478.

[108] G.Buckton, H.Gill, The importance of surface energetics of powders for drug delivery and the establishment of inverse gas chromatography, Adv.Drug Del.Rev. (2007); 59: 1474-1479.

[109] F.L. Riddle, F.M. Fowkes, Spectral shifts in acid-base chemistry. I. Van der Walls contributions to acceptor numbers, J. Am. Chem. Soc. 112 (1990) 3259–3264.

[110] M.D.Ticehurst, R.C.Rowe, P.York, Determination of the surface properties of two batches of salbutamol sulphate by inverse gas chromatography, Int.J.Pharm. (1994); 111: 241-249.

[111] D.Traini, P.Rogueda, P.Young, R.Price, Surface energy and interparticle force correlation in model pMDI formulations, Phar.Res. (2005); 22(5): 816-825.

[112] N.M.Ahfat, G.Buckton, R.Burrows, M.D.Ticehurst, Predicting mixing performance using surface energy measurements, Int.J.Pharm. (1997); 156: 89-95.

[113] O.Planonsek, A.Trojak, S.Srcic, The dispersive component of the surface free energy of powders assessed using inverse gas chromatography and contact angle measurements, Int.J.Pharm. (2001); 221: 211-217.

[114] C.J. van Oss, M.K. Chaudhury, R.J.Good, Monopolar surfaces, Adv. In Colloidal and Interface Science (1987); 28: 35-64.

[115] C.J. van Oss, R.J.Good, M.K. Chaudhury, Additive and nonadditive surface tension components and the interpretation of contact angles, Langmuir (1988); 4: 884-891.

[116] C.A.Prestidge, T.J.Barnes, W.Skinner, Time-of-flight secondary-ion mass spectrometry for the surface characterization of solid-state pharmaceuticals, JPP (2007); 59:251-259.

Acknowledgements

This work would not have been possible without the help of many people.

I would like to thank my supervisor, Chiar.mo Prof. Paolo Colombo for having welcomed in his group and giving me the opportunity to take this experience.

Many thanks to Dr. Daniela Traini who supported me with invaluable support and assistance during the research work and who spurred me to improve my knowledge.

I wish to express my sincere thanks to Dr. Paul Young, Dr. Alaina Ammit, Dr. Francesca Buttini, Dr. Alessandra Rossi and Dr. Fabio Sonvico for they kind assistance and Prof. H-K Chan for giving me the opportunity to work with his group.

Dr Philip Kwok, Dr Handoko Adi, Susan Hoe, Tiziana Riccio and Antonio Vitale are very kindly acknowledge for their help in data collection.

And so many thanks to Andrea and Stefania for the careful reading and valuable advices.